行政院國家科學委員會補助專題研究計畫成果報告

※※※※※※※※※※※※※※※※※※※※※※※※※※※※※※※※※※※※※※

※ 土壤之物理及化學不均質性對有機污染復育成效之影響及模擬（Modeling the influence of physical and chemical heterogeneity on the performance of soil remediation for organic contaminants) ※

※※※※※※※※※※※※※※※※※※※※※※※※※※※※※※※※※※※※※※

計畫類別：▒個別型計畫　□整合型計畫

計畫編號：NSC 89-2211-E-002-080、NSC 90-2211-E-002-054 與 NSC 91-2211-E-002-062

執行期間：89 年 8 月 1 日至 92 年 7 月 31 日

計畫主持人：吳先琪 (Shian-chee Wu)

計畫參與人員：林志興 (Jyh-shing Lin)、張美玲(Meei-ling Chang)、施養信(Yang-hsin Shih)、王美雪(Mei-sheue Wang)、梁瑜玲(Yu-ling Liang)、黃鈺雯(Yu-wen Huang)、張嘉芳(Chia-fang Chang)、蕭宏杰(Hung-chieh Hsiao)

本成果報告包括以下應繳交之附件：

出席國際學術會議心得報告及發表之論文各一份

執行單位：國立台灣大學環境工程學研究所

中 華 民 國 九 十 三 年 一 月

摘 要

由於土壤存在物理及化學不均質性，導致在規劃土壤復育工作時，模擬預測污染物行為發生困難。物理的不均質性導致土壤中流體傳輸速度有很大差異而產生流體流動區域及靜止區域。雖然數學的計算能力可以處理不均質的地下水文模式，但是因為地質水文調查的限制，無法提供模式所需要之空間參數，所以必須以統計的方法來處理物理不均質的問題。本研究以對數常態分布的一組質傳係數來描述移動相與靜止相間污染物趨向平衡的速度。模擬的結果與實驗數據相當吻合，顯示當傳輸尺度大於實驗室的土柱時，不平衡的分配或是貫穿曲線脫尾的現象主要是源於污染物在靜止相內受到質傳限制的移動所導致。而此組質傳係數之分布與土壤質地、水分含量及系統之尺度有關，這些性質均是可以很容易測量到的。此外土壤影像擷取系統可以快速及經濟的提供土壤質地之剖面分布，將有助於土壤復育之調查評估及預測工作。

針對土壤化學異質性而言，分別利用重量法與光譜法吾人採用三種不同極性的揮發性有機物作為吸附質，用來研究有機污染物與腐植素之間的作用。腐植素對於高極性有機物丙酮有很高的吸附量，相較於腐植酸更為顯著。由兩腐植質碳 13 核磁共振光譜的比較可知，腐植素之極性較腐植酸為高，所以較高極性之腐植素可吸附較多之丙酮。以吸附動力學而言，丙酮、甲苯與正己烷在腐植素中的外觀礦散係數約在 10^{-8} cm^2/sec 到 10^{-10} cm^2/sec 之間。在脫附實驗中，吾人並未觀測到有甲苯殘餘在腐植素中，但高極性之丙酮與長鏈脂訪族碳氫化合物正己烷則有 35%與 20%的吸附量未完全脫附。

薄膜傅氏紅外光光譜法可偵測在不同相對溼度狀態下，揮發性有機物在薄膜之吸附行為。甲苯在兩相對溼度下吸附於鈣與銅交換之蒙特石之吸附量，可藉由紅外光吸收量來度量。在乾狀態下相較於鈣蒙特石之吸附量，甲苯對銅交換之蒙特石有較大吸附量，可推測甲苯與銅蒙特石有較強之吸附作用關係。在乾狀態下，不論鈣或銅蒙特石皆有部分吸附的甲苯分子以較慢速率脫附，並且可由光譜資料中看出，尚有部分甲苯之特徵峰存在或新波峰出現，所以推測少部分吸附之甲苯分子有吸脫附不可逆現象，甚至有一些轉化作用存在在揮發性有機物與黏土礦物之間。雖然在高溼度狀態下，光譜分析並未發現有甲苯不完全脫附，但在未飽和層中，黏土礦物仍然可能是土壤中慢脫附之限制因子。

含氯化合物三氯乙烯在腐植酸與腐植素圓片中之擴散係數皆在 10^{-8} cm^2/sec 到 10^{-9} cm^2/sec 這個數量級，而且並無觀測到有三氯乙烯殘餘在腐植酸與腐植素中。含氯化合物三氯乙烯在黏土礦物之吸脫附動力在幾分鐘這個時間尺度。所以揮發性有機物在土壤中之傳輸中，各獨立之土壤成分之吸脫附行為並非主要之限制因子。

分子動態模擬方法運用來研究揮發性有機物甲苯在土壤有機物腐植酸中之擴散作用。雖然模擬之擴散係數有些微高估，但對於此複雜的系統已是相當好的模擬結果，而且模擬吸附動力與熱力的結果與實驗的結果有相同的趨勢。吾人相信此方法將是一個很好的輔助工具，不只幫助預測土壤復育所需之化合物參數，應可輔助了解更多的環境問題。

運用上述之評估技術並將土壤物理與化學異質性之影響整合於模式中，將有助於未來土壤污染整治方案及與效益評估。

Abstract

The distributed mass-transfer coefficient approach is used to model the transport of pollutants where there is heterogeneous soil texture and mass-transfer limited partition kinetics. The experimental and simulation results indicate that in a length scale larger than that of a laboratory soil column the phenomenon of non-equilibrium transport or tailing is resulted mainly from the mass-transfer limited migration of the sorbate into the stagnant region inside the immobile phases. The problem of modeling each of these immobile phases due to the lack of geological information can be improved by using a distributed mass-transfer coefficient set, which is related to some of the easily obtained soil properties such as the length scale of the system of concerned, the moisture content and the heterogeneity of the soil texture profile. Also the soil video imaging system can be used to identify and locate the layers with high hydraulic conductivity and layers with low hydraulic conductivity, or say the heterogeneity of the soil column with quite low cost and in short time, which will be a promising tool to help on the characterizing, modeling and remediation of a contaminated site.

Three VOCs were used to study the interaction between humin and organic contaminants. Higher sorbing capacity of humin for more polar VOCs and the C^{13}-NMR data of humin indicate that humin was more hydrophilic than Aldrich humic acid. The apparent diffusivity of acetone, toluene, and hexane in the disks ranged from 10^{-8} to 10^{-10} cm^2/s. The sorbed toluene in humin does not seem persistent to desorption; however, acetone and hexane, either a polar or a linear compound, show persistence against desorption. On the completion of the desorption experiments, there were approximately 35% and 20% sorbate residue for acetone and hexane, respectively.

The sorption kinetics of toluene in dry and humid clay films was investigated by tracking the change of the IR absorbance. Under humid condition, similar toluene sorbed intensities are found on Ca -and Cu– montmorillonites. However, higher intensities of toluene sorbed were found on Cu-form under dry condition, which indicates stronger interaction occurring. On Ca- and Cu-montmorillonite, some portion of toluene is desorbed at an extremely slow rate under dry conditions. Either some original toluene peaks or some new peaks are persistent against desorption from montmorillonites, also suggesting the existence of irreversibly sorbed species. There

may be some transformation of VOCs in clay systems. Although the persistence was not observed under high humidity conditions by spectroscopic method, the clay minerals could be a controlling factor of slow desorption in soil.

The sorption and desorption of trichloroethylene (TCE) in humic acid and humin disks was investigated by microbalance. The apparent diffusivity of TCE in these two humic substances was in the 10^{-8} to 10^{-9} cm^2/s magnitude. There are no residual sorbed TCE observed via a microbalance. The intrinsic sorption/desorption time scale of TCE on two cation exchanged montmorillonites was only few minutes by thin film/FTIR method.

Molecular dynamic simulations were also used to study the sorption of organic contaminants in soil organic matter. The simulation results of the sorption kinetics and thermodynamics of toluene in humic acid are in good agreement with the experimental data. We believe that this technique will become a powerful tool not only to facilitate the solving of the problems of contaminated soil clean-up but also to be applied to a wider range of environmental problems.

After studying soil chemical heterogeneity, we found the intrinsic sorption is fast for VOCs into humin, humic acid, and montmorillonite. So they do not contribute to the sequestration process in soils. The mass transfer of contaminants into soil plays the important role on the slow sorption/desorption in soils.

Table of Contents

Chapter 1 Introduction

1.1 Background

Soil is a heterogeneous matrix which affects the remediation, prediction, and fate of a pollutant in the soil. Many laboratory and field observations found that there was transfer rate-limited transport of organic contaminant. For example, when soil vapor extraction (SVE) approach is used for cleaning up the organic contaminants, it is often found that in a short period of time the concentrations of the organic contaminants in the soil gas are reduced to very low level. However, after a brief pause of the air-extracting operation, the concentrations of the organic contaminants in soil gas are built up again to reach another new concentration plateau. The phenomenon is sometimes called “rebounding”. (Wilson and Lin, 1997) This phenomenon is believed due to that the fluid moving rate is much slower in some mass-transfer-limiting areas in soil. The contaminants previously entered in these areas will take longer time to be released than what in the fast-flowing regions. The existence of the mass-transfer-limiting areas in soils brings difficulties to the soil pollution remediation engineering. To predict the average residual concentration in the exhausted air or groundwater from the contaminated zone, sophiscated mathematical models and powerful computation softwares have been developed and may help greatly. However, the lack of precise and sufficient values of aquifer properties, such as the hydraulic conductivity of each grid point, makes the modeling of the contaminant migration in the heterogeneous matrix fail.

Soil is chemically a heterogeneous matrix with various inorganic and organic constituents. Each component of the soil exhibits a unique sorption behavior toward organic sorbates. The chemical heterogeneity complicates the prediction of the fate of a pollutant in the soil. Recently, the slow sorption of organic contaminants in soil aggregates resulted from the interactions between the sorbates and SOM and micropores was investigated. Humin, a tenaciously rigid SOM, could be a HSOM and constrain the mobility of organic contaminants in its inflexible polymer chains. Smectite, one expanding clay mineral group, has a lot of interlamellar regions providing hydrocarbons more micropore spaces to enter into but hardly to escape from. Moreover, these reactive clay minerals could act as a mediator to transfer electrons

involving chemisorption or as a catalyst to help produce new chemicals. More understanding of these sorption mechanisms can be obtained by way of the computational chemistry. The molecular simulation method has been used to solve the environmental issues recently. To better predict the rates of pollutant migration and attenuation in soil, the sorption rate and the reversibility of the sorption process with each soil component should be further investigated.

1.2 Scope and Objectives

The aim of this report is to better understand the effect of the soil chemical and physical heterogeneity on the transport of organic contaminants in soils. The objectives of the first part of this study were to investigate the relationship between the mass transfer coefficients and the soil characteristics and to establish a pollutant transport model with the distribution of the coefficients capable of reflecting the heterogeneity of the subsurface matrix. Results from laboratory experiments and field test were used to calibrate the distribution of the coefficients and as basis for the discussion of the scale and moisture effect on the soil heterogeneity in terms of pollutant transfer rate.

The other purposes of this study is to improve our understanding of the relationships among soil chemical heterogeneity properties, kinetics and thermodynamics processes for the sorption of VOCs in soil systems via separating and studying individual soil component which could contribute to the slow sorption phenomenon. Delineation of the sorption rate and the reversibility of each soil component are necessary to precisely predict the rates of migration and attenuation of the pollutants in soil. Moreover, humidity or water content plays an important role in the distribution of contaminants in different soil components, so the sorption experiments under different levels of humidity were performed by an innovative thin film/FTIR method. Another goal of the present study is to predict the sorption kinetics and mechanisms of hydrocarbons in a complex humic substance from the computational chemistry.

Chapter 2. The effects of soil heterogeneity on the mass-transfer limited transport of organic tracers in the soil columns and field

The effects of soil heterogeneity on the transport of pollutants in the groundwater can be described by a set of distributed mass-transfer coefficients. A numerical model was developed in which the groundwater aquifer was divided into a mobile phase and several immobile, or stagnant, phases. The movement of pollutants is governed by advection and dispersion in the mobile phase, and by mass transfer between mobile and immobile phases.

A distributed mass-transfer coefficient approach is used to model the transport of pollutants where there is heterogeneous soil texture and mass-transfer limited partition kinetics. The experimental and simulation results indicate that in a length scale larger than that of a laboratory soil column the phenomenon of non-equilibrium transport or tailing is resulted mainly from the mass-transfer limited migration of the sorbate into the stagnant region inside the immobile phases. The problem of modeling each of these immobile phases due to the lack of geological information can be improved by using a distributed mass-transfer coefficient set, which is related to some of the easily obtained soil properties such as the length scale of the system of concerned, the moisture content and the heterogeneity of the soil texture profile. Also the soil video imaging system can be used to identify and locate the layers with high hydraulic conductivity and layers with low hydraulic conductivity, or say the heterogeneity of the soil column with quite low cost and in short time, which will be a promising tool to help on the characterizing, modeling and remediation of a contaminated site.

2.1 Introduction

Contamination of soil by organic chemicals are frequently occurring serious environmental problems in the recent years. The organic contaminants will deteriorate the water quality of the nearby residential wells and threaten the human health. Recent examples in Taiwan were pentachlorophenol contamination of An-shun site in Tainan, PCE and TCE contamination of RCA site in Taoyuan. The

remediation of these site require appropriate techniques and high cost. Often, cleaning-up these site faces the problem of long-lasting clean-up time due to the persistency of residual organic pollutants in the soils and groundwater aquifers.

Understanding the fate and transport of contaminants in soils is essential for selecting correct technologies and designing remediation plans. For example, the speed of that the organic contaminants will be cleaned away is often much slower than that predicted by solely the flow velocity of the carrying fluid, groundwater or air, during the remediation of a site (Pignatello and Xing, 1996; Zhang and Brusseau, 1999). The extent of sorption of contaminants in soil matrixes and its rate are important processes controlling the slagashness of removal of contaminants from the porous media.

The processes of cleaning up the organic contaminants in soil are often characterized by an initially fast recovery followed by an extremely slow recovery of the organic contaminants. Often the cleaning time is tenfold or hundred times longer than the contact time. Where the contact time can be represented by the time for one pore volume of fluid flowing through the whole length of the contaminated porous matrix (Griffioen, 1998；Miller et al., 1998；Lorden et al., 1998)

Many laboratory and field observations found that there was transfer rate-limited transport of organic contaminant. For example, when soil vapor extraction (SVE) approach is used for cleaning up the organic contaminants, it is often found that in a short period of time the concentrations of the organic contaminants in the soil gas are reduced to very low level. However, after a brief pause of the air-extracting operation, the concentrations of the organic contaminants in soil gas are built up again to reach another new concentration plateau. The phenomenon is sometimes called “rebounding”. (Wilson and Lin, 1997) This phenomenon is believed due to that the fluid moving rate is much slower in some mass-transfer-limiting areas in soil. The contaminants previously entered in these areas will take longer time to be released than what in the fast-flowing regions. The existence of the mass-transfer-limiting areas in soils brings difficulties to the soil pollution remediation engineering. To predict the average residual concentration in the exhausted air or groundwater from the contaminated zone, sophiscated mathematical models and powerful computation softwares have been developed and may help

greatly. However, the lack of precise and sufficient values of aquifer properties, such as the hydraulic conductivity of each grid point, makes the modeling of the contaminant migration in the heterogeneous matrix fail.

Soils are spatially heterogeneous in terms of the soil texture and structure, so as the moisture content. The soil spatial heterogeneity results in that in some area the fluid is moving very quick but in some area the fluid is moving very slow or even nearly stagnant. (Wilson and Lin, 1997；Culver et al., 2000). Inside the stagnant area with very low hydraulic conductivity there always retains some amount of immobile water, where the solutes will not easily be removed from or penetrate into the fluid by advection, instead, can only be transferred between the mobile region and the immobile region by diffusion. Then the immobile water behaves as a sink or a source of the solute in different periods of the sorption process.

The key parameters affecting the transferring capability between the mobile and immobile regions are the diffusion coefficients of the solute in the less permeable regions, the dimensions of them, and the hydraulic conductivity contrasts between the regions. The consequence of the solute-storage effect offered by transverse diffusion into low-permeable aggregates is a slower rate of migration of the frontal portion of a contaminant in the permeable regions than the groundwater velocity and a longer tail of solute concentration in the fluid when the peak has passed by.

2.2 Model development

Mathematic models based on the diffusion process in stagnant aggregates has been developed to quantify the sorption behavior of sediment grains in a completely mixed suspension (Rao *et al*., 1980; Wu and Gschwend, 1986; 1988). The mass transfer of solute between the advective area and the nonadvective area is governed by the diffusion in the aggregates (Wu and Gschwend, 1986; 1988 , Brusseau and Rao, 1989). Wu and Gschwend (1988) have used a first-order mass transfer model to approximate the behavior of the sorption in aggregates with a uniform size. The relationship between the first-order transfer coefficient and the aggregate and solute properties has been established in either a closed batch or an open system (Wu and Gschwend, 1988), in which the transfer coefficient is a function of the size of the

aggregate, the solute diffusivity in water, the intra-aggregate porosity and the local partition coefficient. This approach greatly reduces the calculation needs.

In many cases the size of the aggregates is not uniform. The diffusion model is able to take the aggregate size distribution into account and describe the sorption process in a system with uniform sizes or discrete size groups well, however, needs high amount of calculation to perform a simulation or a prediction. Also, in modeling the non-equilibrated transport in soils and groundwater aquifers, there is often lack of information of the size distribution and location of the non-uniform impermeable regions or aggregates.

Rabideau (1991) have modeled the transport of pollutants in groundwater by dividing the soil matrix into a region controlled by advection and another region without any influence of advection. Rabideau and Miller (1994) had been using a single transfer coefficients, into and out of the stagnant regions, to predict the breakthrough curve and found that the clean-up time would be longer than that of advection-diffusion only if there were mass-transfer limiting regions. To reflect the size distribution and the often found two stage sorption kinetics, slow sorption following a fast sorption, Wu and Gschwend (1986) has applied a two-site model to simulate the sorption process in sediment suspensions. Further discretization of the sorbent in terms of the first-order transfer coefficient will help to improve the model prediction and keep the calculation simple.

Culver et. al. (1997) have been separating the soil into many classes. Each class has a specific mass transfer coefficient. The value of these mass transfer coefficients can be fit into a log-normal distribution function or a gamma distribution function with only two characterizing parameters, mean and the deviation. Applying models with specific distributions of mass transfer coefficients or a two-site model to simulate the TCE transfer in groundwater (the saturated soil column) the authors found that the models with distributions of mass transfer coefficients described the experimental results better than the two-site model.

Deitsch et. al. (2000) conducted model simulation for time courses of the sorption and desorption of 1,2-dichlorobenzene to natural soil by using the Γ probability density function to generate the distribution of the first-order rate coefficients. The results of the simulation were consistent with the results by the model adopting an

intra organic matter diffusion mechanism.

All (Most) of the above-referenced studies acquired the first-order rate coefficient(s) or the distributed mass transfer rate coefficients by adjusting the parameters to fit the experimental data. In predicting the transport and fate of pollutants or evaluating the efficiency of a remediation scheme there is often lack of experimental results to support the parameterization of the sorption process of the specific sorbent-sorbate system in the field. Relating the parameters to the soil properties will help to predict their values and obtain insight of the mechanisms that contribute to the mass-transfer limited sorption process. Most of all, the experimental results and subsequent transfer coefficients obtained in laboratory scale may not properly reflect the sorbing behavior of the subsurface continuum in the field sites.

2.3. Materials and Methods

2.3.1. Model Formulation

Soils often exhibit a variety of small-scale heterogeneities such as cracks, macropores and voids, which permeate and separate the matrix or inter-aggregate pore regions. A consequence of the wide variations in fluid velocity generated by heterogeneous void space within an averaging volume is that the transport processes in some soils and geologic formations cannot be successfully described using the advective–dispersive equation (ADE). (Schwartz et al., 2000) That is, the common assumption of equilibrium sorption cannot accurately describe many laboratory and field observations. (Griffioen, 1998; Culver et al., 2000)

When two comparable subsurface regions with significant different hydraulic conductivities, K, (e. g. one is one hundred times of another) co-exist in parallel, the fraction of flow, proportional to the K, through the lower permeable region may be negligible. On the other hand, we may divide the subsurface continuum into two phases, mobile and immobile phases, according to the relative hydraulic conductivity. The regions having K higher than some specific value and allowing ninety percent of the flow to pass can be classified as the mobile phase and the other regions as the immobile phase. In the mobile phase, the contaminants are

transported relatively fast by advection. However, in the immobile phases the fluid is stationary, the contaminant migration is dominated by molecular diffusion. The volume fractions of the mobile phase and the sum of the immobile phases are f_m and f_s, respectively, where $f_m + f_s = 1$, where $f_s = \Sigma\ f_{sj}$ j = 1 to N.

When the contaminant transport in vadose zone, that the fluid only can be pass the gaseous phase in the mobile phase. The contaminant in the gaseous phase in the immobile phase is stationary, because the gas in the immobile phase exists in the inter-aggregate pore regions is immobile. The solid phase in vadose zone is immobile, so the contaminant in solid phase is stationary and transport in the gaseous phase by mass transfer effective. The contaminant in the liquid phase is stationary, because the liquid in vadose zone always sorption on the soil pellet surface and permeate into the inter-aggregate pore regions, so the liquid phase in vadose zone is immobile .

For one-dimensional, incompressible flow with negligible density effects due to concentration gradients, the contaminant transport in each region can be described using the ADE :

$$\frac{\partial C_T}{\partial t} = \frac{\partial}{\partial x}(flux) = D_{mg}\frac{\partial^2 C_{mg}}{\partial X^2} - U_{mg}\frac{\partial C_{mg}}{\partial X}$$

The uptake and release of organic tracers in and out of an immobile region can be described by a first-order mass transfer model with a specific mass-transfer coefficient. For a good number of immobile regions in heterogeneous subsurface soil matrix or groundwater aquifers the distribution of the size of the immobile regions is a distribution function, $F(\alpha)$, where α is the mass-transfer coefficient.

$F(\alpha)$ = the total fraction of the immobile regions with the coefficients lower than α.

$F(0) = 0$

$F(\infty) = 1$

As mentioned previously, α is believed to be a function of the tracer and the soil properties. Wu and Gschwend (1986) has established correlation between the first-order rate constant and the molecular diffusivity, the aggregate radius, the soil-water partition coefficient, intra-aggregate porosity and bulk density. When

there is only one sorbate to be considered and constant soil porosity and organic matter content can be assumed, the most important soil property is the dimension of the aggregate, or the dimension of the immobile region in the soil column. It is also reported in the literature that the sizes of the natural particles are often in a lognormal distribution, that is, the distribution of the amount of particles is a normal distribution in according to the logarithmic scale of particle size. There is little information about the dimension of the immobile phase in the soil so far, but lognormal distribution will be a starting point for $F(\alpha)$. Let

$y = \log(\alpha)$

μ = the average of $\log(\alpha)$

$y = \mu + Z \times SD$

F(z) = probability of (total volume of immobile regions with) $y \geq \mu$ with standard deviation SD

Adopting a numerical approach we separate the distribution of the immobile regions into N groups, with the coefficient α_j and the fraction (probability intensity) f_{sj} for the jth group. The volume fractions of the mobile phase and the sum of the immobile phases are f_m and f_s, respectively, where $f_m + f_s = 1$, where

$\Sigma \ f_{sj} = 1 \qquad j = 1 \text{ to } N$

There are gas, liquid and solid phases in mobile phases and immobile phases. When the organic compounds have gotten into soil then the organic compounds will be distributed to all phases.

The average concentration of the organic compound, C_T, is

$C_T = F_m \times C_m + F_s \times C_s$,

where C_T is the average concentration of the organic compound (mg/ soil cm^3), C_m is the average concentration in mobile phase (mg/ soil cm^3), C_s is the average concentration in immobile phases (mg/ soil cm^3), F_m is the volume fraction of the mobile phases, F_s is the volume fraction of the immobile phases.

There are solid, liquid and gaseous phases in each phase. The averaged

concentration in the mobile phases, C_m, is the weighted sum of the concentrations in the solid, liquid and gaseous phases.

$$C_m = \rho_m \times C_{ms} + \theta_m \times C_{ml} + a_m \times C_{mg},$$

where C_{ms}, $C_{ml,}$ and C_{mg} are the concentrations in solid, liquid and gaseous phases respectively. Similarly, the averaged concentration in the immobile phase, C_s, is also the weighted sum of the concentrations in the solid, liquid and gaseous phases.

Far many immobile phases existing in the soil column simultaneously the average concentration in all the stationary phases, C_s, is

$$C_s = \Sigma (f_{sj} \times C_{sj}) \; ; \; j=1,2,.....N,$$

in which, N is the number of the immobile phases with difference sizes and mass-transfer coefficients, f_{sj} is the volume fraction of the jth immobile phase with the concentration of C_{sj}. C_{sj} is defined as

$$C_{sj} = \rho_{sj} \times C_{ssj} + \theta_{sj} \times C_{slj} + a_{sj} \times C_{sgj} \; ; \; j=1,2,.....N,$$

where C_{ssj}, $C_{slj,}$ and C_{sgj} are the concentrations in solid, liquid and gaseous phases respectively. The total averaged concentration in the stationary phase is

$$C_s = \Sigma (f_{sj} \times C_{sj}) = \Sigma (f_{sj} \times (\rho_{sj} \times C_{ssj} + \theta_{sj} \times C_{slj} + a_{sj} \times C_{sgj})) \; ; \; j=1,2,.....N$$

The averaged concentration, C_T, in the column soil is then

$$C_T = F_m \times C_m + F_s \times C_s = F_m \times (\rho_m \times C_{ms} + \theta_m \times C_{ml} + a_m \times C_{mg}) + F_s \times (\Sigma (f_{sj} \times (\rho_{sj} \times C_{ssj} + \theta_{sj} \times C_{slj} + a_{sj} \times C_{sgj}))); \; j=1,2,.....N$$

Where C_{ms} is the concentration in the solid phase in the mobile phase (mg/g), C_{ml} is the concentration in the liquid phase in the mobile phase (mg/ cm^3), C_{mg} is the concentration in the gaseous phase in the mobile phase (mg/cm^3), ρ_m is the bulk density of the mobile phase (g/cm^3), θ_m is the liquid content in the mobile phase (cm^3/cm^3), a_m is the gas content in the mobile phase (cm^3/cm^3), C_{ssj} is the concentration in the solid phase in the jth immobile phase (mg/g), C_{slj} is the concentration in the liquid phase in the jth immobile phase (mg/ cm^3), C_{sgj} is the concentration in the gaseous phase in the jth immobile phase (mg/cm^3), ρ_{sj} is the bulk density of the jth immobile phase (g/cm^3), θ_{sj} is the liquid content in the jth

immobile phase (cm^3/cm^3), a_{sj} is the gas content in the jth immobile phase (cm^3/cm^3).

If the tracer is moving with a uniform flow through an isotropic aquifer in only one dimension and the concentration is averaged over the cross-sectional plane, the concentration variation by time is equal to the spatial derivative of the sum of the advection and diffusion fluxes,

$$\frac{\partial C_T}{\partial t} = \frac{\partial}{\partial X}(flux) \qquad [\text{ Eq. 1 }]$$

When the contaminant transport in the vadose zone is of concern, the movement of the liquid is often negligible. The mass flux of contaminants is mainly contributed by the flow in the gaseous phase. The solid phase in mobile zone is immobile too, since the contaminant in solid phase is stationary and transferred among solid, liquid and gaseous phases by diffusive mass transfer only. The contaminant in the liquid phase is stationary, because the liquid in vadose zone always sorption on the soil pellet surface and permeate into the inter-aggregate pore regions, so the liquid phase in vadose zone is immobile . The contaminant in the gaseous phases in the immobile phase is stationary, because the gas in the immobile phase existing in the inter-aggregate pore regions is immobile.

For one-dimensional, incompressible flow with negligible density effects due to concentration gradients, the contaminant transport in each region can be described using the ADE :

$$\frac{\partial C_T}{\partial t} = \frac{\partial}{\partial x}(flux) \qquad [\text{Eq. 1}]$$

$$\frac{\partial}{\partial x}(flux) = D_{mg}\frac{\partial^2 C_{mg}}{\partial X^2} - U_{mg}\frac{\partial C_{mg}}{\partial X}$$

where D_{mg} is the dispersion coefficients of the gas flows in the mobile phase, U_{mg} is the linear flow velocity of the gas flows in the mobile phase, and X is the longitudinal dimension. The left hand side of Eq. 1 is the change of the summation of the concentrations in all phases with time.

$$\frac{\partial C_T}{\partial t} = \frac{\partial}{\partial t}[F_m\times(\rho_m\times C_{ms} + \theta_m\times C_{ml} + a_m\times C_{mg}) + F_s\times(\Sigma(f_{sj}\times(\rho_{sj}\times C_{ssj} + \theta_{sj}\times C_{slj} + a_{sj}\times C_{sgj})))] \quad , \quad j=1,2,\ldots..N_\circ$$

In a time scale longer than hours or days, in the length scale as small as a grain, it can be assumed that the concentrations of an organic tracer in the gas, liquid and solid phases of mobile phase and each immobile phase are in equilibrium. The concentrations in immobile liquid and solid phases can be related to the mobile phase with a linear partitioning relationship, that are $C_{ms}=K_{md}\times C_{mg}$, $C_{mg}=K_{mh}\times C_{ml}$ in each immobile phases and are $C_{ssj}=K_{sdj}\times C_{sgj}$, $C_{sgj}=K_{shj}\times C_{slj}$ in immobile phases。 K_{md} is partition coefficient between the solid phase and the gaseous phase; K_{mh} is the partition coefficient between the liquid and the gaseous phase (the reciprocal of the Henry's Law constant); K_{sdj} is the partition coefficient between the solid phase and the gaseous phase in jth stationary phase; K_{shj} is the partition coefficient between the liquid and the gaseous phase in the jth stationary phase. Then, the transport governing equation can be expressed as

$$\frac{\partial C_T}{\partial t} = \frac{\partial}{\partial t}[f_m\times(\rho_m\times C_{ms}+\theta_m\times C_{ml}+a_m\times C_{mg}) + f_s\times(\Sigma(f_{sj}\times(\rho_{sj}\times C_{ssj}+\theta_{sj}\times C_{slj}+a_{sj}\times C_{sgj})))] \quad ; j=1,2,.....N$$

$$= \frac{\partial}{\partial t}[f_m\times(\rho_m\times K_{md}\times C_{mg}+(\theta_m/K_{mh})\times C_{mg}+a_m\times C_{mg}) + f_s\times(\Sigma(f_{sj}\times(\rho_{sj}\times K_{sdj}\times C_{sgj}+(\theta_{sj}/K_{shj})\times C_{sgj}+a_{sj}\times C_{sgj})))] \quad ; j=1,2,.....N$$

$$= \frac{\partial}{\partial t}[f_m\times(\rho_m\times K_{md}+\theta_m/K_{mh}+a_m)C_{mg}]+ + f_s\times(\Sigma(f_{sj}\times(\rho_{sj}\times K_{sdj}+\theta_{sj}/K_{shj}+a_{sj})C_{sgj})))] \quad ; j=1,2,.....N$$

Since f_s、 f_{sj} are all constant system parameters, we may let $f_s\times f_{sj}=f_j$；j=1,2,.....N, and express the left-hand-side of the governing equation as

$$\frac{\partial C_T}{\partial t} = \frac{\partial}{\partial t}[f_m\times(\rho_m\times K_{md}+\theta_m/K_{mh}+a_m)C_{mg}] + \Sigma(f_j\times(\rho_{sj}\times K_{sdj}+\theta_{sj}/K_{shj}+a_{sj})C_{sgj})] \quad ; j=1,2,.....N$$

$$= f_m\times a_m\times\frac{\partial C_{mg}}{\partial t}+[f_m\times\rho_m\times K_{md}+(f_m\times\theta_m)/K_{mh}]\frac{\partial C_{mg}}{\partial t} + \Sigma(f_j\times(\rho_{sj}\times K_{sdj}+\theta_{sj}/K_{shj}+a_{sj})\frac{\partial C_{sgj}}{\partial t}) \quad ; j=1,2,.....N$$

By combining the left-hand side, $\frac{\partial C_T}{\partial t}$, and the right-hand side, $\frac{\partial}{\partial X}(flux)$, we obtained

$$D_{mg}\frac{\partial^2 C_{mg}}{\partial X^2}-U_{mg}\frac{\partial C_{mg}}{\partial X}$$
$$= f_m \times a_m \times \frac{\partial C_{mg}}{\partial t} + [f_m \times \rho_m \times K_{md} + (f_m \times \theta_m)/K_{mh}]\ \frac{\partial C_{mg}}{\partial t}$$
$$+ \ \Sigma\left(f_j \times (\rho_{sj} \times K_{sdj} + \theta_{sj}/K_{shj} + a_{sj})\ \frac{\partial C_{sgj}}{\partial t}\right) \ ; j=1,2,.....N$$

From the above discussion, we recognized that due to the mass-transfer limitation the concentrations between the gaseous phases and the liquid or solid phases, or between the mobile phases and the immobile phases will not reach equilibrium. That is, for example, the concentration change of the gaseous concentration in the immobile phase with time is proportional to the difference between the gaseous concentration of the immobile phase and the gaseous concentration of the mobile phase.

$$\frac{\partial C_{sgj}}{\partial t} = \alpha_{sj} \times (C_{mg} - C_{sgj}) / FSC$$

in which α_{sj} is the mass-transfer coefficient of the jth immobile phase, FSC is the total fraction of the immobile phases. The transport governing equation is finally:

$$D_{mg}\frac{\partial^2 C_{mg}}{\partial X^2}-U_{mg}\frac{\partial C_{mg}}{\partial X}$$
$$= f_m \times a_m \times \frac{\partial C_{mg}}{\partial t} + [f_m \times \rho_m \times K_{md} + (f_m \times \theta_m)/K_{mh}]\ \frac{\partial C_{mg}}{\partial t}$$
$$+ \Sigma\left(f_j \times (\rho_{sj} \times K_{sdj} + \theta_{sj}/K_{shj} + a_{sj})\ \frac{\partial C_{sgj}}{\partial t}\right) - \frac{\partial C_{sgj}}{\partial t} \ ; j=1,2,.....N$$

$$\frac{\partial C_{sgj}}{\partial t} = \alpha_{sj} \times (C_{mg} - C_{sgj}) / FSC$$

2.3.2. Column experiments

For the column experiments, soil material was obtained from the alluvial soil near the Shindian river in Taipei, Taiwan. The particle size distribution was generated by dry sieving. Any particles smaller than the 0.12mm were collected and packed into a glass column apparatus. The soil is composed of 2.8% of clay, 36,1% of silt, and 61.1% of sand. The natural organic-matter content is 1.87%, and its specific gravity is 2.73 g/cm^3.

The column experiments include two glass columns under different conditions. Column A was conditioned with moisturized air under a flow rate of 6.5ml/min let for 72 hours. The water content of the soil in Column A was 1.6%. The bottom of Column B was dipped in a reservoir of water for 24 hours before the experiment. The soil was moisturized by capillary suction of water from the bottom up. The water content of the soil in Column B varied from the bottom at 24.15% to the top of the column at 14.06%. The schematic diagram of the column experiment apparatus is given in Figure 2.1. Experimental parameters are given in Table 2.1.

Before extracting the column with air each column was added a layer of soil spiked with pure toluene. Each column was extracted with air under different flow rate. Gaseous samples were taken at different time and locations of columns, and analyzed with a gas chromatograph equipped with a flame ionization detector.

Table 2.1. Some experimental parameters and properties of soil columns

	column A(2)	column B(3)
soil describe	air-dried soil	moisturized soil
column diameter (cm)	4.8	4.8
column length (cm)	101	30
whole bulk density (g/cm^3)	1.378	1.378
water contain (%)	1.6	14.09(top)-24.15(bottom)
total porosity	0.4952	0.4949
air-extracting flow rate (cm^3/min)	7.23	5.53
total mass of added toluene (mg)	772	380

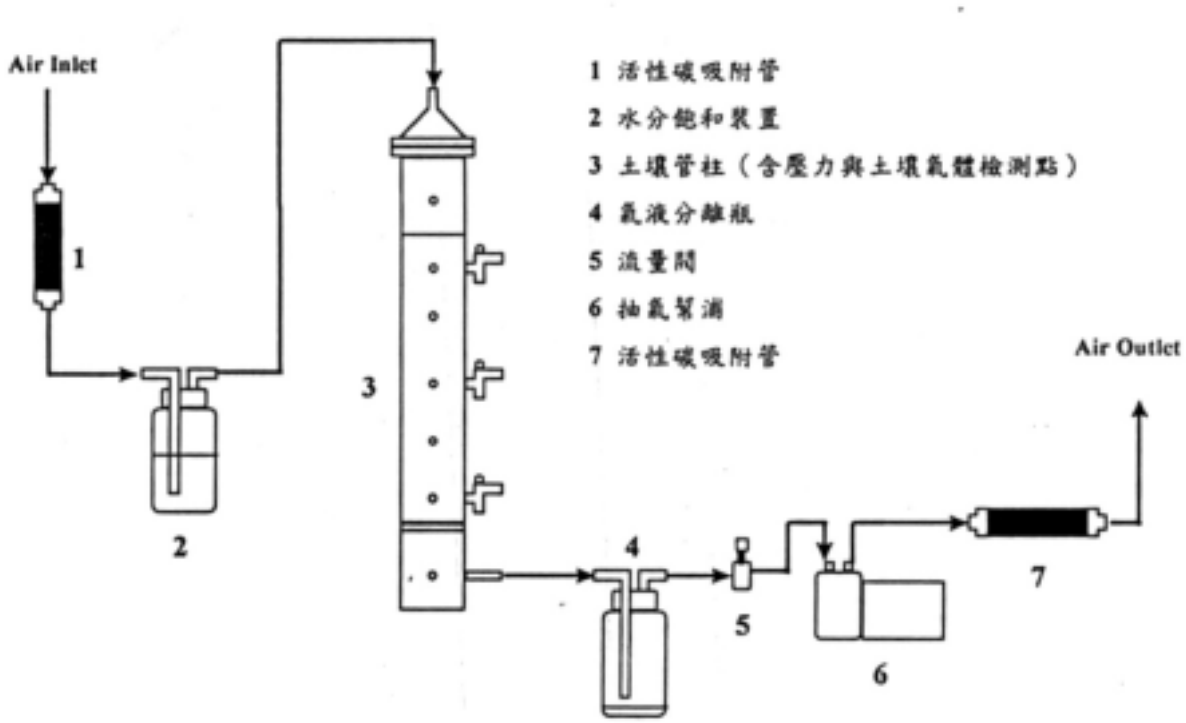

Figure 2.1 The schematic diagram of the column experiment apparatus

2.3.3. Model simulation for column experimental results

A finite difference scheme written in Fortran computer program was use to solve the concentration distribution at different time and place for the transport .of toluene in a soil column. The initial conditions, boundary conditions and model parameters were input according to the real experimental setting.

C_T=Co for t = 0, X = 0~3 cm

$C_{go}= C_T/(\rho_m \times K_{md} + \theta_m/K_{mh} + a_m)$

$C_g= C_{go}$

$C_{sgj}= C_{go}$

Otherwise C_g=0，C_{sgj}=0，

At the boundaries:

C_g=0 at X＝-30 cm,

$$\left.\frac{\partial C_g}{\partial X}\right|_{(X=H)} = \left.\frac{\partial C_g}{\partial X}\right|_{(X=H-\Delta X)} \quad \text{at X＝H.}$$

Adopting a numerical approach we separate the distribution of the immobile regions into N groups. The jth group has a coefficient α_{sj} and a fraction (probability

intensity) f_{sj}., where

$$\Sigma \ f_{sj} = 1, \quad j = 1 \text{ to } N$$

f_{sj} is a normal distribution density function in the respect of y, that is

$$f_{sj} = f_{sj}(y_j) = F(y_{j+1/2}) - F(y_{j-1/2}), \quad j=1 \text{ to } N$$

where $y_j = \log(\alpha_{sj})$, $y_{j+1/2} = y_j + 0.5 \Delta y$, $y_{j-1/2} = y_j - 0.5 \Delta y$ and Δy is the segment width. The distribution function has a mean μ and a standard deviation SD which are fitting parameters during the simulation of the column experiments.

2.3.4. Tracer field test and model simulation

The field test for soil vapor extraction was conducted in the experimental farm of National Taiwan University in Hsin-tein. The SVE site had a radius of 2.7 meters and covered with 15-cm bentonite layer to avoid air leaking into the sucking well. Around the suction well there were 10 monitoring well in a quarter of a circle shown in Figure 2.2.

The diameter of the suction well was 6 inches. The screen opened between thedepth of 1 meter to 4 meter with total opening length of 3 meters. The monitoring wells were distributed in a quarter circle with depth around 1 meter to 1.8 meter depth which were installed by applying a direct push-in probe to drill a 2-inch hole, putting one or more Teflon tubes with screened aluminum heads at the desired positions then stuffing the surrounding of the head with quartz sands and sealing the hole with bentonite.

Samples were taken from the Teflon tubes with a hand pump. The suction wellwas connected to a demister and a vacuum pump at a suction head of 50 inches of water and a flow rate at 80 cfm. Sulfur hexafluoride, SF_6, gas was used as the tracer, which has little affinity with soils , no toxicity, high persistency in soils and high sensitivity for detection.

Before the tracer test was conducted the site had been condition for one day by suction at the previously described operational conditions. Fifty cubic centimeters of SF_6 were injected in each of the six injection wells while the sucking pump was temporarily stopped. Suction was started immediately after the tracer being injected. Samples were taken at different times and analyzed with GC-ECD for the gaseous

concentration of SF_6.

The geology of the site is shown in Table 2.2.

The governing equation of the transport of a tracer in a cylindrical coordinate system is

$$\frac{\partial(C_g)}{\partial t} = D_g\left[\frac{\partial^2 C_g}{\partial r^2} + \frac{1}{r}\frac{\partial C_g}{\partial r}\right] - \frac{\partial(vC_g)}{\partial r}$$

$$D_g = D_{gf} + D_{gm}$$

$$D_{gm} = \xi \cdot v$$

$$v = \frac{Q}{\pi \cdot R^2 \cdot H}$$

ξ is the dispersivity (cm), Q is the flow rate (cm^3/min), H is the length of the screen (cm), R is the radius of the well (cm), D_{gf} is the molecular diffusion coefficient (cm^2/min). The only fitting parameters above is dispersivity. All other parameters can be measured on site. Q is 565.2 cm^3/min, the length of the screen is 300 cm, molecular diffusion coefficient is 3.66 cm^2/min。

Assuming that the injected tracer at 250 cm from the center is evenly distributed in a 2 cm by 300 cm layer of soils. The outer boundary was set at 300 cm from the center. The boundary conditions are

$C_g = 0$ r = 300 cm

$\frac{\partial C_g}{\partial r} = 0$ r = 0 cm

The initial condition at t = 0 is

$C_g = C_0$ at r = 249 - 251 cm

$C_g = 0$ otherwise

Table 2.2 The geology of the SVE sits

depth (m)	description	Soil particle size distribution (%)				Water content (%)	Bulk density (g/cm^3)
		gravel	sand	silt	caly		
0~0.5	Grayish dark silt with sands	0	47.5	44.2	8.3	17.7	1.41
0.5~1.5	Yellow brown sandy soil	3.3	42.1	47.1	7.5	16.8	1.65
1.5~3	Yellow brown sandy soil with gravels						
3~4.5	Yellow brown sandy soil						
4.5~5.5	Grayish caly						

2.3.5. Soil heterogeneity characterization

Traditional methods have been used to characterized the heterogeneity of the subsurface soil layer. Mechanical soil texture analysis of segments of a soil sample core will give the vertical distribution of the soil texture along the depth. Profile of the hydraulic conductivity of the soil layer is obtained by measuring the permeation of core segment by a permeameter. The soil moisture content also shows the porosity and heterogeneity of the soil column.

A new technique, Geo VIS, that can avoid the tedious sampling and analyses in the laboratory and uncover the profile the soil texture and some properties has been developed (Fig. 2.3). A frill rod is equipped with a video camera in side the belly and project to the surrounding soil stratum through a quartz window. Video signals are transmit to a monitor or a video recorder. The resolution of the camera is finer than 0.01 mm, which is fine enough to distinguish between clayey and sandy soils. Also, the equipment can be used to explore any NAPL in the aquifers. In this study, the technique was used to identify and locate the layers with high hydraulic conductivity and layers with low hydraulic conductivity, or say the heterogeneity of the soil column.

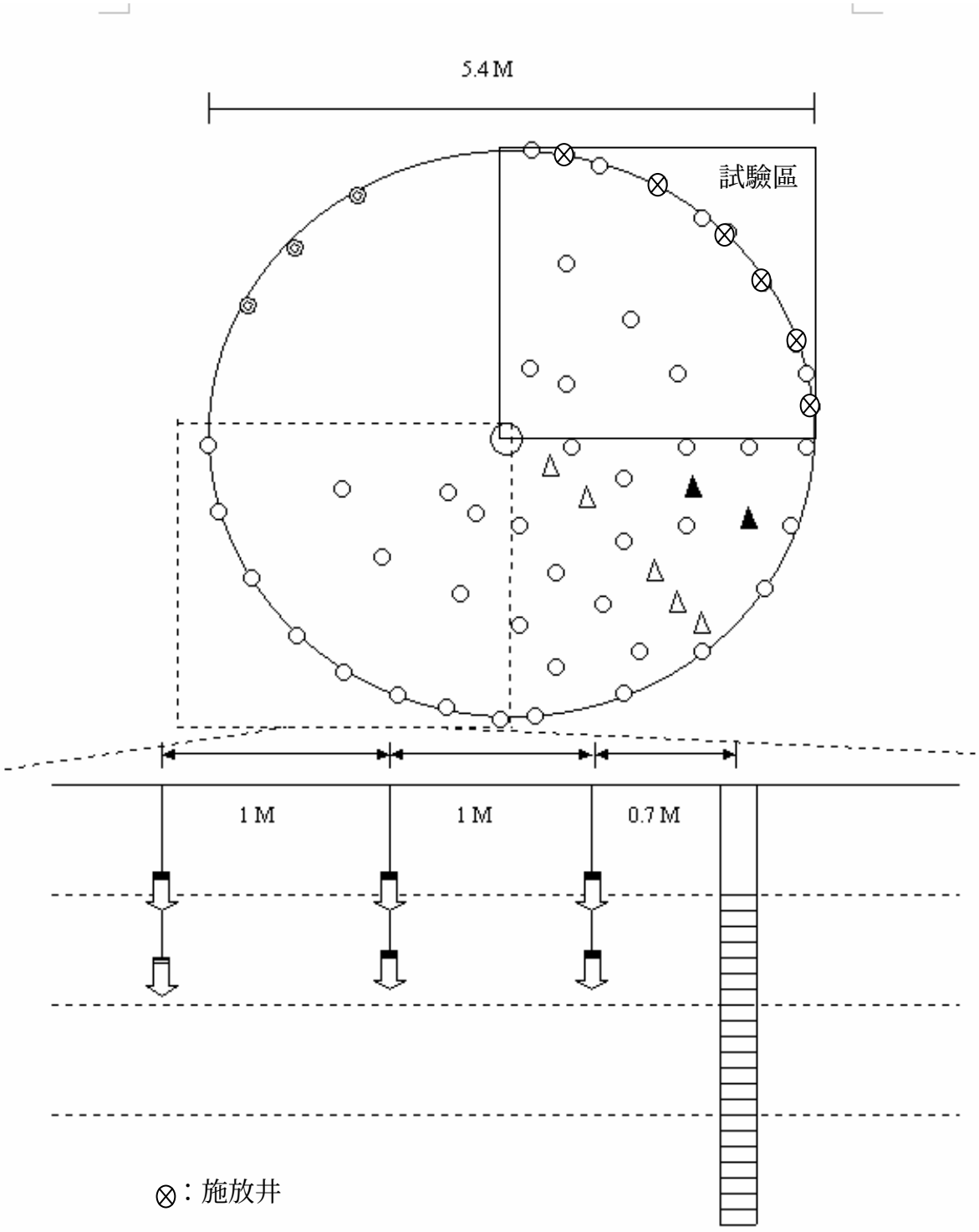

Figure 2.2 The locations of the suction well, injection wells and sampling wells on the SVE experimental site

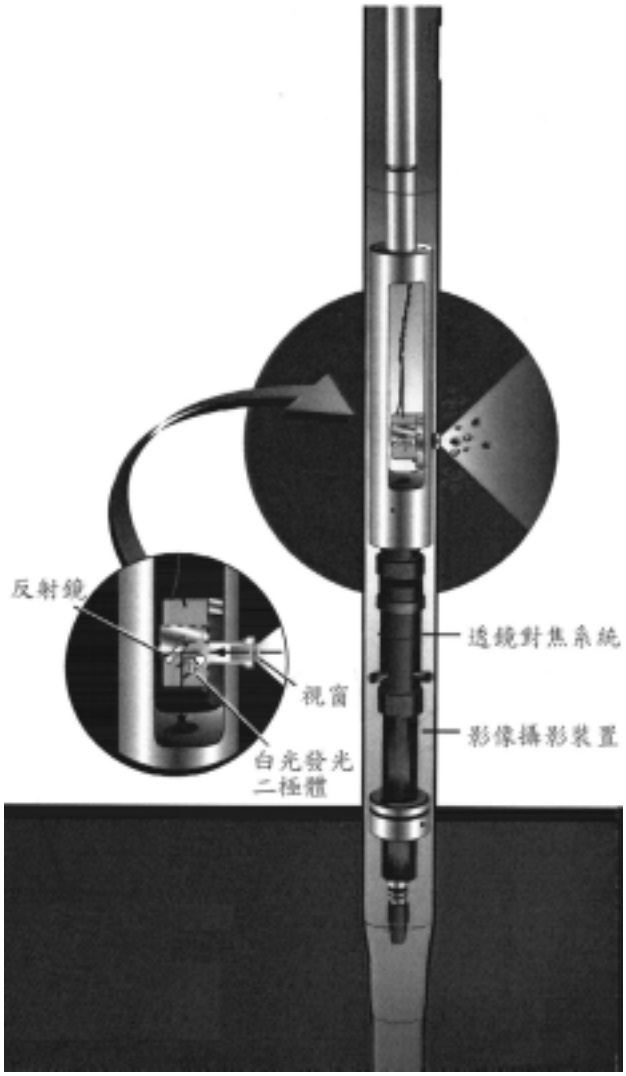

Figure 2.3 The schematic diagram of the In-situ video geo-probe (Geo VIS)

2.4. Results and discussion

2.4.1. Column experimental results

We have been using the advection-diffusion governing equation to simulate the transport of tracer in soil column with the consideration of immediate equilibration between the mobile phases and immobile phases, or only first-order sorption kinetics, or two-stage first-order (two-box) sorption kinetics, or a distribution of mass-transfer limiting immobile regions. We found that the equilibration assumption or the first-order sorption kinetics approaches were not able to satisfactorily describe the experiment results.

Adopting a numerical approach we separate the distribution of the immobile regions into 10 groups. The jth group has a coefficient α_{sj} and a fraction (probability density) f_{sj}., where

$$\Sigma \ f_{sj} = 1, \quad j = 1 \text{ to } 10$$

f_s is a normal distribution density function in the respect of y, that is

$$f_{sj} = f_{sj}(y_j) = F(y_{j+1/2}) - F(y_{j-1/2}), \quad j=1 \text{ to } 10$$

where $F(z) = Pr(Z \leqq z)$ is a normal distribution function.

$$y_j = \log(\alpha_{sj}),$$

$$\alpha_{sj} = 10^{Yi},$$

$$y_{j+1/2} = y_j + 0.5 \Delta y,$$

$$y_{j-1/2} = y_j - 0.5 \Delta y$$

and Δy is the segment width. The distribution function has a mean μ and a standard deviation SD. Also

$$y_j = \mu + z*SD, \quad -2.5 < z < 2.5$$

The breakthrough curve of soil column A shows slightly tailing and a retardation factor of 23.3, while soil column A shows significant tailing and much small retardation factor of 3.4 (Fig. 2.4 and Fig. 2.5). Moisturizing the soil would greatly reduce the sorption capacity of the soil, facilitate the removal of the contaminant, however, likely to increase the heterogeneity of the porous matrix (with more significant tailing).

The best-fitting values of model parameters are shown in Table 2.3. The total fraction of the mobile phases.

Table 2.3 The modeling parameters and the results of model simulation

model parameters	column A	column B
dispersivity (cm)	3	4
water content (%)	1.6	14.09(top)-24.15(bottom)
gas volume fraction	0.4952	0.354(top)-0.2534(bottom)
diffusion coefficient in air (cm^2/min)	4.824	4.824
Henry's law constant (C_{mg}/C_{ml})	0.28	0.28
Simulation results and the best fitting values		
f_m	0.7	0.4
fs	0.3	0.6
retardation factor	23.3	3.4
$K_p=C_s/C_g$	8	0.7
Mass transfer coefficient		
$\mu = \log \alpha_s$	-0.5	-2.0
averaged α_s	0.3162	0.01
standard deviation of α_s, SD	0.5	1.5

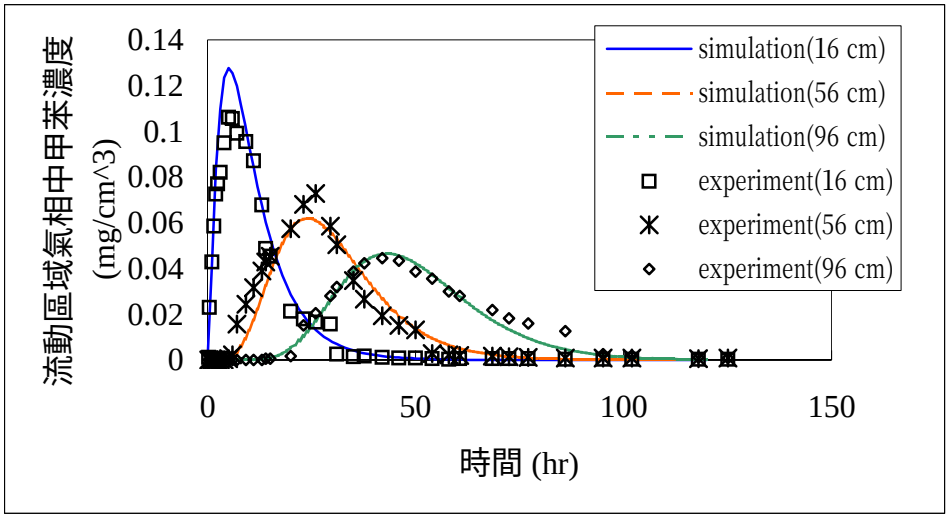

Figure 2.4 The concentration of toluene at the locations of 16 cm, 56 cm, and 96 cm from the top of the soil column, respectively, in column A packed with dry soils (symbols) and the model simulation results (lines). A log-normal distribution of the mass-transferring coefficients is adopted with the mean at 0.32 and standard deviation at 0.5.

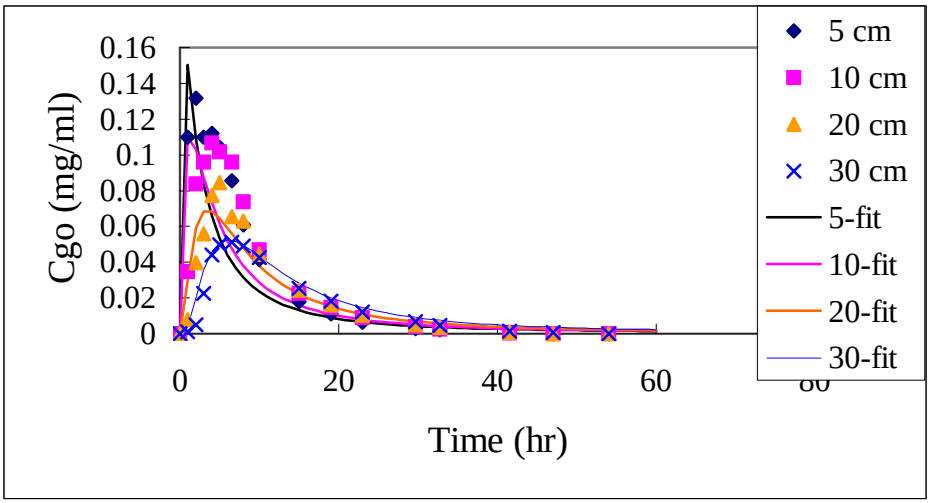

Figure 2.5 The concentration of toluene at the locations of 5 cm, 10 cm, and 20 cm from the top of the soil column, respectively, in column B packed with water-soaked soils (symbols) and the model simulation results (lines). A log-normal distribution of the mass-transferring coefficients is adopted with the mean at 0.01 and standard deviation at 1.5.

The distributed mass-transfer coefficient approach is obviously able to simulate the transport of pollutants where there is heterogeneous soil texture and mass-transfer limited partition kinetics. The tailing of the breakthrough curve can be described quite well. Comparing the best-fitting parameters, we found that the mean of the mass-transfer coefficients of the moisturized soil column was much lower (by a factor of 30) than that of the dry soil column. It indicates that the transfer of the tracer between the mobile phases and the immobile phases in the moisturized is much slower. The reason of the slower equilibration is believably due the larger sizes of the immobile phases, which are the result of blockage of the gas channels by capillary water. Also, due to the uneven distribution of water in the soil column, the variation of the size of stagnant aggregates is high, which is reflected by the larger standard deviation of the fitting mass-transfer coefficient.

2.4.2. Tracer test on a soil-vapor-extraction field site

The concentrations of SF_6 at the suction well, 70 cm from the well and 150 cm from the well at different time are shown in Figure 2.6 to Figure 2.8. The peak of the concentration passed through the suction well 34 minutes after the beginning.

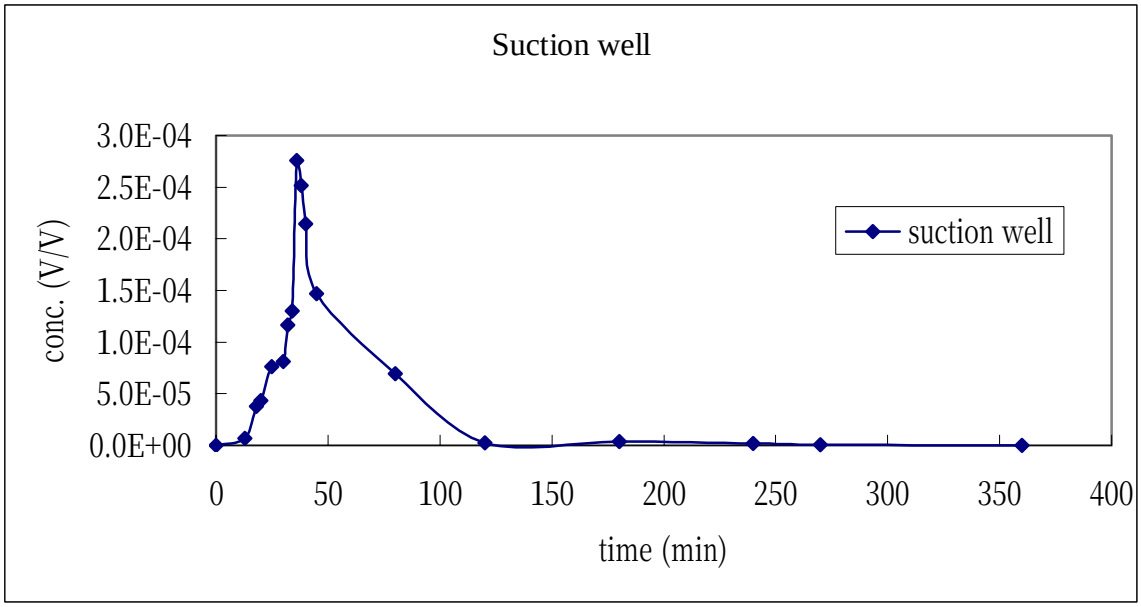

Figure2.6 The breakthrough curve of tracer at the suction well

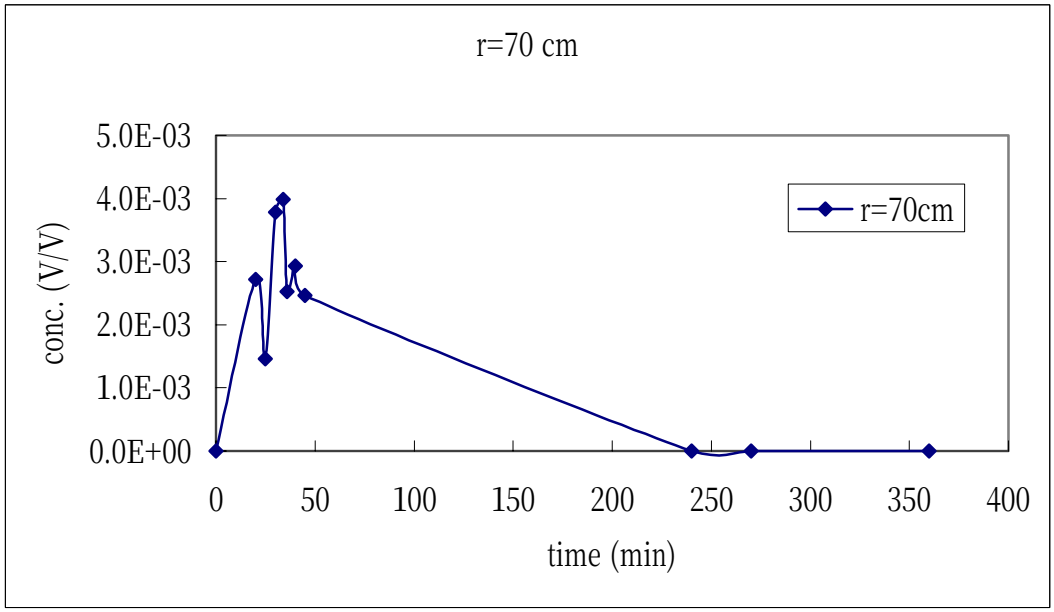

Figure 2.7 The breakthrough curve of tracer at the sampling well 70 cm from the center

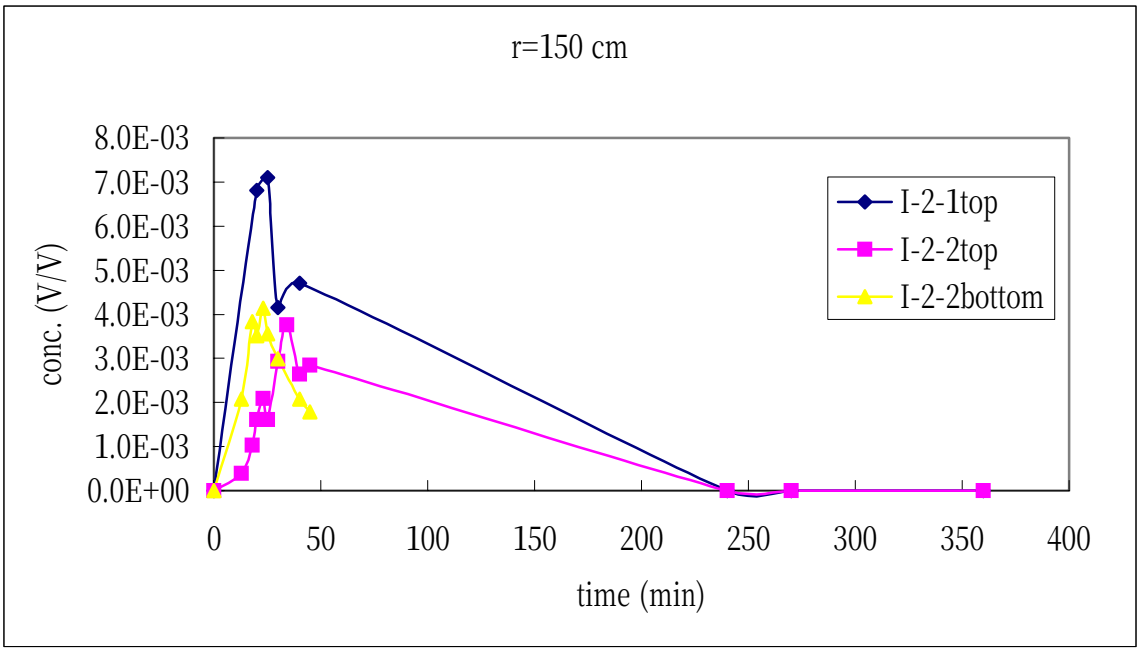

Figure 2.8 The breakthrough curve of tracer at the sampling well 150 cm from the center

2.4.3. Application of soil video imaging system to in-situ soil monitoring

The soil video imaging system was fabricated that utilize a micro imaging device in internal part of a drill rod. The soil video imaging system is an on-line image monitoring system that can be applied to capture the continuous images of soil profile through a digital camera to perform the soil texture distribution investigation while drilling into the subsurface soil layer (see Fig. 2.9). Due to the limitation of budget, we were not able to apply any hydraulic pressurizing driller. Therefore, only images from shallow soil column were obtained (Fig. 2.10).

One snap shot is shown as Fig. 2.11 , the resolution of this photo is around 10 um, and the diameters of the observed soil aggregates were in the range of 10 um and 100 um. The continuously on-line images were converted to the mpeg files. Apparently different soil texture distributions were observed from soil core samples at different depth. At a deeper location, the image indicates a finer and more uniform soil texture than that at the depth of 80 cm (Fig. 2.11). With a continuous image of the soil profile, we will be able to identify soil layers with relatively high permeability or layers with relatively low permeability.

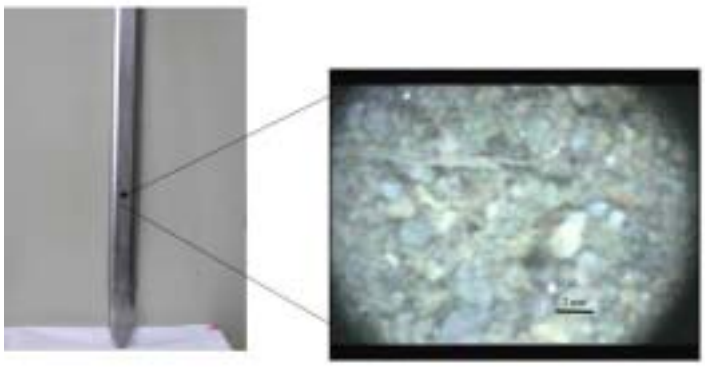

Figure 2.9 Soil video imaging system. The drilling rod.

Figure 2.10 The image of the texture of soil at depth of 80 cm.

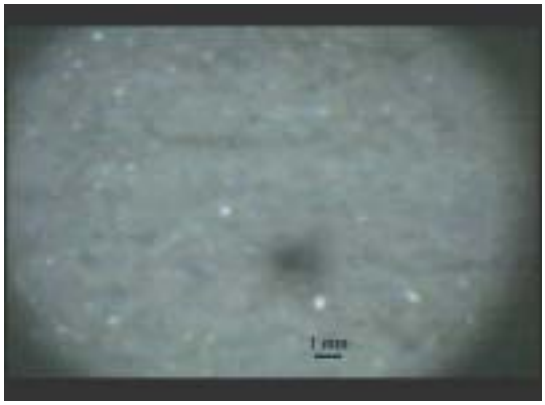

Figure 2.11 The image of the texture of soil at a depth larger than 80 cm.

The results show that using this technique to distinguish between clayey and sandy soils. Also, the equipment can be used to identify and locate the layers with high hydraulic conductivity and layers with low hydraulic conductivity, or say the heterogeneity of the soil column.

2.5. Conclusions

The distributed mass-transfer coefficient approach is able to model the transport of pollutants where there is heterogeneous soil texture and mass-transfer limited partition kinetics. The experimental and simulation results also indicate that in a

length scale larger than that of a laboratory soil column the phenomenon of non-equilibrium transport or tailing is resulted mainly from the mass-transfer limited migration of the sorbate into the stagnant region inside the immobile phases. The problem of modeling each of these immobile phases due to the lack of geological information can be improved by using a distributed mass-transfer coefficient set, which is related to some of the easily obtained soil properties such as the length scale of the system of concerned, the moisture content and the heterogeneity of the soil texture profile. Also the soil video imaging system can be used to identify and locate the layers with high hydraulic conductivity and layers with low hydraulic conductivity, or say the heterogeneity of the soil column with quite low cost and in short time, which will be a promising tool to help on the characterizing, modeling and remediation of a contaminated site.

Chapter 3 Sorption Kinetics of Toluene in Humin under Two Different Levels of Relative Humidity

3.1 Introduction

The rate of sorption/desorption of volatile organic compounds (VOCs) plays an important role in pollutant fate modeling and contaminated soil remediation. Irreversible VOC sorption to or slow VOC desorption from soils in laboratory studies or field scales has been reported (Aochi and Farmer, 1995; Pingatello and Xing, 1996). It is found that a portion of VOCs desorbs very slowly from soil particles and a certain fraction of it is retained strongly by the particles (Steinberg et al., 1987; Pingatello, 1990). The retention of VOCs by soil components affects the fate of pollutants in the environment and the effectiveness of contaminated soil and aquifer remediation. Delineation of the sorption rate and of the reversibility of the sorption process with essential soil components is necessary to better predict the rates of pollutant migration and attenuation in soil.

Soil, a chemically heterogeneous matrix, contains various inorganic and organic components that each exhibits unique sorption behavior for pollutants (Chiou, 1998). The chemical heterogeneity complicates the prediction of the sorption or desorption rates of pollutants in the soil. Recent studies reveal the existence of a slow sorption/desorption of some organic compounds with soils (Luthy et al., 1997; Pignatello and Xing, 1996). This phenomenon has been attributed in part to a slow diffusion of the compounds through the micropores of soil particles (Farrell and Reinhard, 1994; Lin et al., 1994) and in part to their slow migration through soil organic matter (SOM) (Brusseau et al., 1991; Fu et al., 1994).

Sorption to humic substances is contended to contribute to the irreversible retention of xenobiotic compounds by soil (Cheshire, 1979). However, the sorption of toluene to humic acid, an integral member of soil humic substance, is found to be reversible and diffusion-controlled (Chang et al., 1997). Since humin represents a highly stable, recalcitrant, and high-molecular-weight fraction of SOM (Almendros et al., 1996; Hatcher et al., 1985), it may behave differently than the humic acid in the kinetics of sorption. Due to its cross-linked structure, humin may be capable of retaining VOCs for a significantly longer time and thus contribute to the slow or apparent irreversible sorption.

Although, the sorption of nonpolar solutes by humin shows a slightly nonlinear

effect, due to the existence of a small amount of high-surface-area carbonaceous material (Chiou et al., 2000), the soil organic matter, including humin, behaves by and large like a partition medium for VOCs (Boyd et al., 1988; Chiou, 1988; Chiou et al., 1990; Chiou and Kile, 1994; Chiou, 1998). The amorphous humic structure provides a "solvent-like" medium that organic molecules can enter into or escape from it according to the thermodynamic gradient.

Humin is defined as the portion of humic materials that is insoluble in an aqueous solution at any pH. To be separated from the inorganic minerals in soils, humin is obtained by extensive digestion of soils with a mixture of concentrated HF and HCl (Stevenson, 1982). The HF/HCl extraction method has been widely applied for humin preparation (Chefetz et al., 2000; Grasset and Ambles, 1998; Guthrie et al., 1999; Lichtfouse et al., 1998a; Lichtfouse et al., 1998b), while the MIBK (methyl isobutyl ketone) method, as suggested by Rice and MacCarthy (1990), has also been applied for extraction of humin. In the MIBK method, humic substances are allowed to partition between water and MIBK as a function of the pH in water phase. Humin is then isolated from fulvic acid and humic acid. However, this method is so selective that some humin component could not be retrieved by MIBK. To meet the purpose of our experiment on the sorption/desorption rate of toluene with near natural humin, the solvent extraction was not adopted in order to prevent a significant alteration of the humic composition.

A spectroscopic approach has been adopted to address the interaction between VOCs and humic substances by Aochi and Farmer (1997). The authors investigated the sorption/desorption behavior of 1,2-dicholoethane on humic acid and fulvic acid under dry conditions. They found that an absorbance band increases continuously after days of desorption and the sorbed chemical was strongly retained. However, the sorption kinetics of VOCs on humin in a system resembling the natural level of humidity on a short time scale (say, minutes) has not been investigated. In this study, toluene, a model nonpolar, mononuclear hydrocarbon, was used as the sorbate to delineate the sorption behavior of VOCs with humin. Humin disks were prepared and used to study the rate of transport of toluene in humin matrix with artificially exaggerated mass transfer distance. Thin humin films were also used to mimic natural humin in a near-natural soil environment.

3.2 Materials and Methods

3.2.1 Soil Sample

Approximately ten kilograms of Yamingshan soil, classified as medial, thermic, Pachic Melanudands according to the definition by USDA (USDA-NRCS, 1993), were

air-dried, freed of large plant debris, and screened through a 20-mesh (0.84 mm) sieve. Small plant debris was further removed by flotation using ethanol. Then, soil sample was mixed well.

3.2.2 Humin

Humin was extracted according to the procedure developed by Rigol et al. (1998) and Russell et al. (1983) except that an ethanol/hexane mixture (1:1 v/v) was used to remove fats and waxes to avoid the interference from toluene, which is the target VOC to be studied. In short, soil was refluxed to remove fats and waxes and extracted by sodium hydroxide to remove humic acids and fulvic acids. The solid residue was separated by centrifugation, neutralized with 6 M HCl, washed with 0.1 M HCl and deionized water, and finally freeze-dried. The humin fraction was isolated from the solid residue by sequentially removing the mineral matter with a three-step digestion procedure: first, suspension in a 1:1 mixture of 0.2 M HF and 0.2 M HCl (20 ml/g) for 64 hours; subsequently, digestion in a 1:1 HF (5.5 M) and HCl (1.1 M) mixture for 1 hour three times; and, finally, digestion in 5.5 M HF four times for 16 hours each time. After centrifuging and washing with 0.1 M HCl and water three times, the final residue designated as humin was freeze-dried and ready for use.

A previous investigation by IR spectroscopy (Rigol et al., 1998) suggested that the treatment of soils with HF decreases the structural mineral matter content with relatively little influence on the nature of humin. Despite the challenges presented by modification, humin obtained by HF-extraction procedure were used for some sorption experiments (Chefetz et al., 2000; Gurthrie et al., 1999; Rigol et al., 1998). The ^{13}C-NMR spectrum (not presented) of the solid residue after removal of waxes, humic and fulvic acids, and treatment by weak acids before severe HF/HCl extraction, is the same as that of the humin product after the severe HF/HCl treatment. The severe treatment procedure removed most of soil inorganic components while the humin components were preserved.

3.2.3 Sample Characterization

Element Analysis. Elements such as C, H, and N of humin were quantified in triplicate samples using an Element Analyzer (EA) (Perkin-Elmer CHN-2400). Inorganic carbon was removed according to Ball et al. (1990). To determine the contents of major elements such as Fe, Al, Si, and Ca, samples were pretreated by fusion with $LiBO_2$ at 1000^{o}C for 30 min. The product was dissolved in 0.9 M HNO_3 and diluted to 0.3 M HNO_3. The major elements in the solution were quantified in

triplicates by inductively coupled plasma optical emission spectroscopy (ICP-OES) (Ingamells, 1970; Rigol et al., 1998).

Solid-State ^{13}C-NMR Spectrometry. The cross polarization/magic angle spinning (CP/MAS) ^{13}C spectra of samples were measured on a Bruker DSX400WB NMR Spectrometer with a 7-mm diameter probe. The spinning rate was 7000 Hz. The acquisition parameters included contact time of 1 ms, pulse delay of 1 s, and pulse width of 4.2 μs.

The ^{13}C-NMR spectra were analyzed according to the chemical-shift assignments made by Perminova et al. (1999) and Chefetz et al. (2000): 5-50 ppm, aliphatic H and C-substituted C atoms; 50-108 ppm, aliphatic O-substituted C atoms; 108-145 ppm, aromatic H and C-substituted C atoms; 145-163 ppm, aromatic O-substituted atoms; 163-190 ppm, C atoms of carboxylic, esteric, and amide groups. The distribution of C in each structural group was calculated as the percentage to the total carbon. The region between 5 to 108 ppm was calculated as aliphatic C and 108 to 163 ppm as aromatic C. The total aromaticity was calculated by expressing the aromatic C as a percentage of the sum of aliphatic and aromatic C; the total aliphaticity was calculated as the percentage of aliphatic C to the sum of aliphatic and aromatic C (Hatcher et al., 1981; Hatcher et al., 1983). The regions 50-108 ppm and 145-190 ppm were calculated as O- or N-substituted C atoms. The polarity was assigned based on the percentage of the sum of O- and N- substituted C atoms.

3.2.4 Preparation of Humin Disks

Humin disks were prepared by pressing the humin powder under a pressure of 12.7 N/m^2 for 1.5 min (Chang et al., 1997). Four disks, all being 12.45 mm in diameter, were 0.34 mm, 0.44 mm, 0.61mm, and 0.64 mm in thickness, and weighed 61.5 mg, 72.8 mg, 100.2 mg, and 102.5 mg, respectively. Their bulk densities were 1.49 g/cm^3, 1.36 g/cm^3, 1.35 g/cm^3, and 1.32 g/cm^3, respectively. The disks were oven-dried (105 ^{o}C) overnight and stored in a desiccator before use.

The scanning electron microscopy (SEM) photographs were taken with a Hitachi S-800 SEM. Figure 3-1 shows the SEM photographs of one of the disks prepared by the above-mentioned procedure. The surface morphology (Fig. 3-1a) and the exposed inner surface of a broken edge with only a few pores and cracks display the homogeneity of the disk.

3.2.5 Sorption/Desorption Experiment

Gravimetric Method. The apparatus was shown in Fig. 3-2 and the procedure used

for sorption have been described elsewhere (Chang et al., 1997). Briefly, the experimental apparatus was maintained in a thermostatic room at 15±0.1°C, 25±0.1°C, or 35±0.1°C. The set temperature was closely monitored for at least one day to ensure its stability before initiation of the experiment. The disk was hung on the sample side of a Cahn 200 electric microbalance enclosed in a glass chamber. The toluene mass flux to the disk was significantly larger than the maximum toluene removal rate, which keeps the vapor concentrations inside the chamber at virtually fixed levels. The experiment was terminated when the change of weight could not be distinguished from the base noise of the microbalance, which was about 2 μg/5hr. The concentration of the toluene was determined with GC/FID (Hewlett-Packard 5890II).

Sorption/Desorption Experiments Traced by FTIR. A drop of the humin suspension in water was placed on the inner surface of a ZnSe window of a gas cell and dried in a desiccator. The absorbance spectra of IR beam passing through the gas cell windows were recorded on an IR spectrometer (BIO-Rad FTS 40) by averaging 200 scans at 2 cm^{-1} resolutions. The sample cell was purged with nitrogen gas carrying a constant toluene vapor concentration and relative humidity (RH below 1% for dry conditions and above 95% for humid conditions) during sorption experiments and purged with nitrogen gas without toluene during desorption experiments (Fig. 3-3).

3.2.6 Estimating Diffusivity

The diffusion model and its incorporation into the gravimetric method has been described in detail by Chang et al. (1997). The model development is briefly summarized here. The one-dimensional mass conservation equation is

$$\frac{\partial q}{\partial t} = D\frac{\partial^2 q}{\partial x^2} \tag{3-1}$$

$$M(t) = S\int_{-l}^{l} q(x,t)dx \tag{3-2}$$

where q (mg/cm^3) is the sorbate concentration in the disk at a distance x from the center plane of the disk and at time t; D is the apparent diffusivity of the sorbate inside the disk; l is the half-thickness of the disk; $M(t)$ is the total sorbed mass of sorbate in the disk; and S is the surface area of the disk.

Given the initial and boundary conditions,

$$q(x,0) = 0 \tag{3-3}$$

$$q(\pm l,t) = q_e \tag{3-4}$$

$$\frac{\partial q}{\partial x}(0,t) = 0 \qquad (3\text{-}5)$$

The analytical solution for the fraction of equilibration is available in Crank and Park (Equations 36 and 37 in Chapter 1, 1968) and can be expressed as

$$M_t / M_e = f(t) \qquad (3\text{-}6)$$

where M_t is the sorbed mass and *f(t)* is the dimensionless solution that is zero at t=0 and unity when t approaches infinity.

For the desorption process, the initial and boundary conditions are

$$q(x,0) = q_e \qquad (3\text{-}7)$$

$$q(\pm l,t) = 0 \qquad (3\text{-}8)$$

and Eq. 5. The analytical solution during desorption is

$$M_t / M_e = 1 - f(t) \qquad (3\text{-}9)$$

The diffusivity can be estimated by the best fit of the experimental results using the least-squares method.

3.3 Result and Discussion

3.3.1 Characteristics of Humin

The humin fraction contributes to 6.84% of the weight of the original soil and 15.9% of the weight of the total organic fraction (Table 3-1). The contents of the major elements, such as C, H, O, and N, in humin are shown in Table 3-2. The low atomic H/C ratio (1.08) indicates that a large fraction of the organic matter contains aromatic carbons. However, there is still a significant amount of aliphatic carbons according to the ^{13}C-NMR results (Fig. 3-4).

Table 3-2 shows the amounts of Si, Al, and Fe in the humin fractions determined by ICP-OES. No noticeable amount of crystalline minerals can be detected through XRD (X-ray diffraction) observation. A small amount of these metals must be in amorphous form. The low inorganic content of the humin plus its low sorbing power for toluene did not significantly affect the sorption experiments.

The ^{13}C-NMR spectrum of humin (Fig. 3-4) revealed the following composition: 50.2 % aliphatic moieties (32 ppm), 32.5 % carbohydrates (73 and 103 ppm), 14.4 % nonpolar aromatic compounds (128 ppm), and 2.9 % amide or carboxylic compounds (172 ppm) similar to the observation made by Chefetz et al. (2000). The total aromaticity of humin, 15.1 %, close to 8.8 % reported by Chefetz et al. (2000), is different from that of Aldrich humic acid (66.7 %) (Perminova et al., 1999). The major

peaks and distribution of C-containing contents were similar to those determined from the reported humin spectrum of Chefetz et al. (2000) but different from those for humic acid (Perminova et al., 1999).

3.3.2 Sorption Experiments

The experimental conditions and the results of seven sorption experiments, including two sets of duplicates of the same disks (A1 and A2, B1 and B2, respectively), are shown in Table 3-3. The sorption of toluene on the humin disk took about 50 hours to reach steady state under 15°C (Fig. 3-5a). However, it took about twice that time for complete desorption (Fig. 3-5a). Similar slower desorption processes were observed at 25°C and 35°C as well (Fig. 3-5b and 3-5c, respectively). The sorption process seemed reversible. There was no observable residual toluene remaining in the humin disks after desorption.

We define the SOM-gas distribution coefficient [K_d, (mg/g)/(mg/L-gas)] between the solid phase and the gaseous phase as

$$K_d = \frac{q_e / \rho}{C_g} \tag{3-10}$$

where C_g is the VOC concentration (mg/L) in the gaseous phase and ρ is the bulk density of the disk (g/cm^3). The observed K_d decreases with the temperature in the partial pressure (P/P_0) range from 0.029 to 0.054 (Table 3-3).

Whether the toluene sorption to humin is a physical or a chemical process can be elucidated via the measured enthalpy change (ΔH). Applying the van't Hoff equation, the relationship between the change of enthalpy and K_d can be quantified as

$$\frac{d \ln K_d}{dT} = \frac{\Delta H}{RT^2} \tag{3-11}$$

where R is the ideal gas constant, T is the absolute temperature (K), and K_d is the equilibrium SOM-gas distribution coefficient.

The plot of ln K_d versus $1/T$ is shown in Fig. 3-6. Assuming that ΔH is constant over the studied temperature range, a relatively low negative value of enthalpy change, -9.0 kcal/mole, is obtained, which implies that the sorption process is a physical, exothermic process. The enthalpy change from the subcooled VOC to the sorbed VOC is calculated to be 1.5 kcal/mole by subtracting the enthalpy of condensation (-10.5 kcal/mole). This small and positive net enthalpy is illustrative of a partition process. There appears to be no chemical bond formed or broken during sorption and desorption.

We may also estimate the value of K_d by using the following equation:

$$K_d = \frac{K_{oc} \times f_{oc}}{K_H} \qquad (3\text{-}12)$$

where K_{oc} is the soil organic carbon-water partition coefficient, and f_{oc} is the organic carbon fraction, and K_H is the Henry's Law constant. Estimates of K_{oc} were obtained from the relationships between log K_{oc} and log K_{ow} established by Karickhoff et al. (1979) and Chiou et al. (1983). K_d at other temperatures can be calculated by correcting the temperature effect according to Schwarzenbach et al. (1993). The values of the experimental K_ds fall between those predicted by Karichoff's and Chiou's methods (i.e., 0.38 and 0.098 (mg/g)/(mg/L-gas) at 25°C, respectively) in all temperature ranges. The results indicate that the sorption of toluene in humin is a partition process and the distribution coefficient can be estimated from the Henry's Law constant and the organic carbon-water partition coefficient.

3.3.3 Diffusion inside Humin Disks

The rate of the penetration of VOC is quantified by the diffusivity in the humin matrix. Figure 3-5 shows the time courses of sorption and desorption and the simulation of the weight changes by using a diffusion model. The average of the three best-fitting diffusivities of toluene at 25°C is 7.0×10^{-9} cm^2/sec. The value is on the same order of the diffusivity of toluene in humic acid (Chang et al., 1997; Piatt and Brusseau, 1998) but lower than the diffusivity of the compound in water by a factor of 1000. According to the ^{13}C-NMR spectra, humin is not the same as humic acid. However, toluene molecules in the cross-linked network of humin have a diffusivity similar to that in humic acid. Diffusivity is 7.25×10^{-9} cm^2/s and 3.71×10^{-9} cm^2/s for propane into two different olefinic matrix ionomers at 25°C (Del Nobile et al., 1995). However, the diffusivity is only 1.8×10^{-7} cm^2/s for toluene in butyl rubber at 30°C (Schneider et al., 1994), and 5.2×10^{-7} cm^2/s and 1.7×10^{-7} cm^2/s for benzene and o-xylene in natural rubber at 25°C (Guo et al., 1995). Thus, the value of the diffusion coefficient in the humin disks is closer to that of VOC in polymers rather than that of VOC in a liquid.

The value of the diffusivity in humin is far less than that in the air. Pore diffusion has been suggested by researchers to be the rate-controlling mechanism of sorption in soil aggregates. If pore diffusion is the major mechanism of the transport of VOC in humin, then the diffusivity of gases in porous medium will be reduced by sorption and matrix tortuosity. The expression of the effective intra-aggregate diffusivity in gaseous phase is similar to the effective diffusivity in water (Schwarzenbach et al., 1993), which is

$$D = \frac{\phi f D_a}{K_d(1-\phi)\rho_s + \phi} \cong \frac{f D_a}{R} \qquad (3\text{-}13)$$

where ψ is the porosity, f is tortuosity, and ρ_s is true density of solid sorbent, D_a is the diffusivity of the sorbate in air, R is the retardation factor, and K_d is the distribution coefficient of the sorbate in the sorbent. Based on the observation of SEM photos of the humin disk, we could not identify any porosity and therefore ignored the porosity term. The diffusion coefficient of toluene in air is 0.086 cm^2/s (Gilliand, 1934) and retardation factor ($R=K_d(1-\psi)\rho_s+\psi$) of humin is 420. The diffusivity of toluene molecules in this presumably porous organic matter is 2.07×10^{-4} cm^2/s. The experimental diffusivity is lower than this estimate by five orders of magnitude. Therefore, diffusion in humin is more likely associated with a polymeric network than with a porous solid matrix. If a tortuosity factor were introduced to quantify the extra length that the sorbate molecules have to travel through, the tortuosity would be 3.38×10^{-5}, which also indicates that the migration path of the sorbate is far less a straight path but is rather like narrow curving interstices through tightly woven fiber.

3.3.4 Thermodynamics of Diffusion

The sorption and desorption diffusivities of toluene in humin increase with temperature (Table 3-3). There were two sets of diffusivity results during desorption lost due to accidental power failure. A higher temperature raises the rate of diffusion because it provides more energy to facilitate the vibration of polymer segments and helps to mobilize VOC molecules. Hence, toluene molecules can surmount the activation energy barrier more easily when they are squeezing through the macromolecular matrix.

This effect of temperature on diffusivity can be described by the Arrhenius equation (Crank and Park, Chapter 2, 1968):

$$D = D_0 \exp(-\frac{E}{RT}) \qquad (14)$$

where D_0 is the diffusivity of the reference state and E is the activation energy of diffusion. By plotting lnD versus 1/T (Fig. 3-6), the activation energy for sorption and desorption are found to be 19.4 and 22.2 kcal/mole, respectively. The values are slightly higher but at the same order of magnitude when compared with the activation energy of toluene for sorption (10.1 kcal/mole) and for desorption (15.7 kcal/mole) into humic acid at temperatures ranging from 25°C to 45°C (Chang et al., 1997). The diffusion activation energy is 11.1 kcal/mole for propane into rubber at 23-45°C (Michaels and Bixler, 1991) and 4.8 kcal/mole for toluene into butyl rubber (Vahdat,

1991). Certain level of activation energy is needed to form an interstitial space or free volume for penetrants (Rogers, 1985) and involves intermolecular and intramolecular interactive forces, which depend on the dimensions of the penetrant and the structure of the polymer molecules (Crank and Park, 1968). This result indicates that humin has tighter cross-linkage or is more rigid than some polymers and humic acid.

Sorption in humin seems to be reversible. However, the desorption rate is slower than the sorption rate by a factor of 2. The activation energy of toluene desorption is slightly higher than that of sorption. The higher activation energy of desorption suggests that a new stable toluene/humin structure may have been formed during the sorption/equilibration period.

3.3.5 Sorption/Desorption traced by FTIR

During the triplicated thin-film sorption experiments, the thickness of the sorbent film was only roughly 5 μm. In fact, the film was composed of very small humin aggregates, whose median size was 12 μm, as measured by laser granulometer (Clias model 715). The mass transfer distance through sorbent layer was significantly reduced. The change in intensity of IR absorbance at 729 cm^{-1} showed that the sorption process for the thin-film system under dry conditions (RH<1%) had a time scale of a few minutes and was reversible (Fig. 3-7). The observation of the reversibility was consistent with the aforementioned gravimetric experimental results. The ^{13}C-NMR spectra of Guthrie et al. (1999) suggested non-colvalent interaction between aromatic compound (pyrene) and humin. These data support our hypothesis that there is no observable molecular bonding between toluene and humin.

Sorption of toluene by thin humin film under humid conditions (RH>95%) showed similar results to those for dry humin. However, the sorption and desorption of toluene were slightly slower under humid conditions than dry conditions. The reason might be the hindrance of the hydrated humin network to the vapor movement. Saturating the humic acid with water is known to lower the partitioning capacity of the humic acid for nonpolar organic compounds, indicating that the overall polarity of the hydrated humic acid is increased (Chiou et al., 1988). The polarity of humin estimated by the integration of the characteristic response of ^{13}C-NMR is 35.4%. As a result of the humin hydration, the humin molecular network might become more cross-linked due to the hydrogen-bond formation between polar functional groups and water molecules. As a consequence, the migration of toluene within the hydrated humin film was retarded. The IR spectra of toluene sorbed to the thin humin film under either dry or humid condition were similar to those of liquid toluene, suggesting that there is no specific binding formed for toluene with either dry or hydrated humin.

Long and Thompson (1954) studied water induced acceleration of the diffusion of organic vapors in polymers. They found that the sorption rates for nonpolar compound in hydrophobic polymer are slower under humid condition than dry condition in a water-benzene-polystyrene system. Quite evidently water has no appreciable effect on the diffusion rate of organic vapors in polyolefins (Crank and Park, Chapter 8, 1968). Chang (1982) studied the diffusion coefficients of toluene in polymer films under different humid conditions. The diffusion coefficients in humid conditions are less than in dry conditions. Our observation is consistent with this result.

Piatt and Brusseau (1998) have estimated that the intraorganic matter diffusion coefficient in aqueous phase for toluene in a soil predominated humic acid is 3.8×10^{-9} cm^2/sec. This value is also slightly lower than what Chang et al. (1997) have measured in a dry condition. This result for humic acid is consistent with our observation of toluene in humin by FTIR method. They also concluded that diffusion is highly restricted within the SOM matrix and the mass transfer coefficients are not significantly different for different SOMs. The similarity of the diffusivities of toluene in humic acid and humin in our study agrees with their conclusion (Piatt and Brusseau, 1998).

3.4 Conclusion

The results indicate that the sorption of toluene to humin could be a slow process (in time scale of hours) because of constrained mass transfer through humin molecular structures only if the humin mass is as thick as about a half-millimeter. There seems to be no strong interaction between toluene and humin molecules according to the IR spectra of the sorbed toluene in humin. Partitioning is believed to be the major sorption mechanism. Based on the results above and results presented in other literature (Chang et al., 1997), it may be concluded that the sorption kinetics with time scale of few minutes to days for toluene on natural humic substances is controlled primarily by mass transfer in polymeric humic structures.

Table 3-1. Relative amount of soil components

Fats and waxes† (%)	Plant residues† (%)	Humic acid and fulvic acid ‡ (%)	Humin † (%)	Mineral matter§ (%)	Total (%)
0.90	0.07	36.10	6.84	55.48	99.39

† Calculated from the weight of this component.

‡ Calculated from the weight lost after NaOH extractions.

§ Calculated from the weight lost after HCl/HF extractions.

Table 3-2. Relative content of the major elements in humin

C (%)	H (%)	O† (%)	N (%)	Atomic H/C	Si (%)	Al (%)	Fe (%)	Ca (%)
35.81	3.23	55.04	0.84	1.08	0.68	2.94	0.97	0.49

† by difference.

Table 3-3. Conditions and results of sorption and desorption experiments by the gravimetric method

	Experimental runs						
	A1	A2	B1	B2	B3	C1	C2
Weight (mg)	61.5	61.5	61.5	61.5	72.8	100.2	102.5
Thickness (mm)	0.34	0.34	0.34	0.34	0.44	0.61	0.64
Density (g/cm^3)	1.49	1.49	1.49	1.49	1.36	1.35	1.32
Temperature (^oC)	15	15	25	25	25	35	35
VOC concentration (mg/L)	2.98	4.46	5.59	4.29	4.29	6.45	6.67
VOC pressure (P/P_o)	0.036	0.054	0.039	0.030	0.030	0.029	0.030
Maximum sorbed mass (μg)	82.7	114	96	94	91	96.5	112
K_d ((mg/g)/(mg/L))	0.45	0.42	0.28	0.36	0.29	0.15	0.16
$D_s x10^9$ (cm^2/sec)‡	2.8	3.2	7.0	6.9	7.1	30	25
$D_d x10^9$ (cm^2/sec)§	1.5	1.2	4.0	N.A.†	5.5	17	N.A.†

† not available.

‡ diffusivity during sorption.

§ diffusivity during desorption.

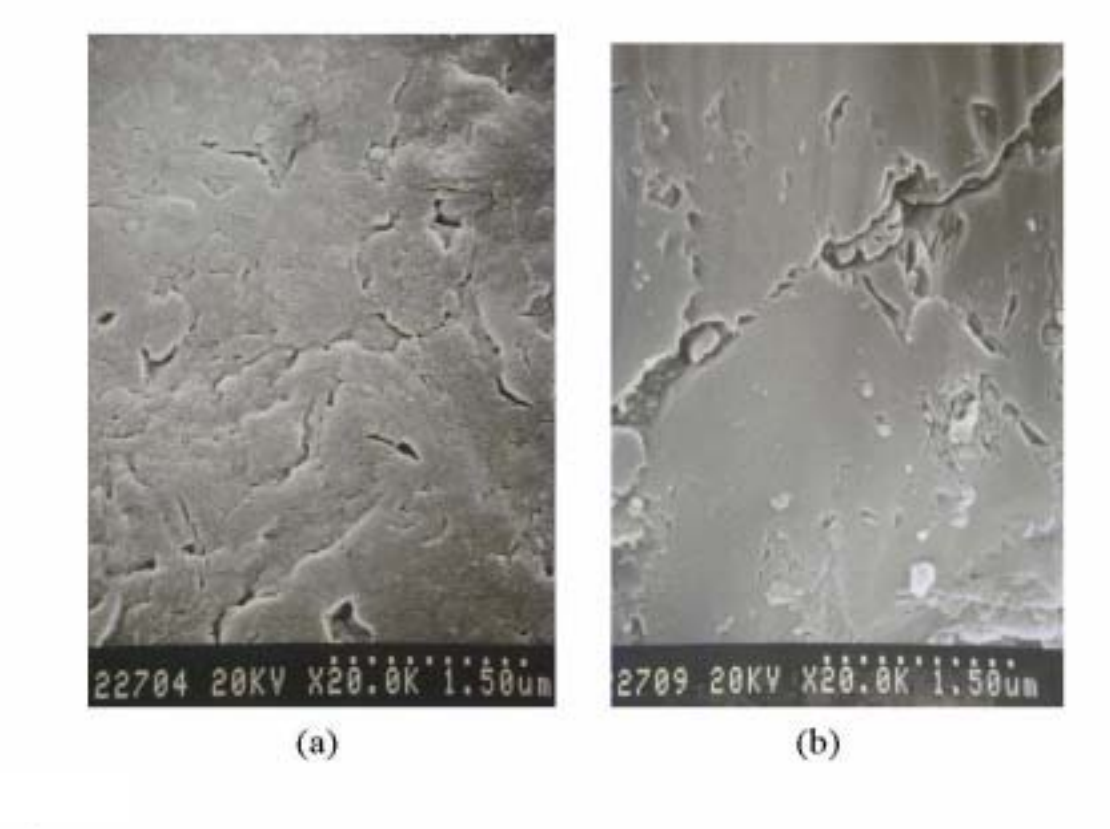

Fig. 3-1. (a) Surface and (b) cross-section of a broken edge of a humin disk observed by SEM.

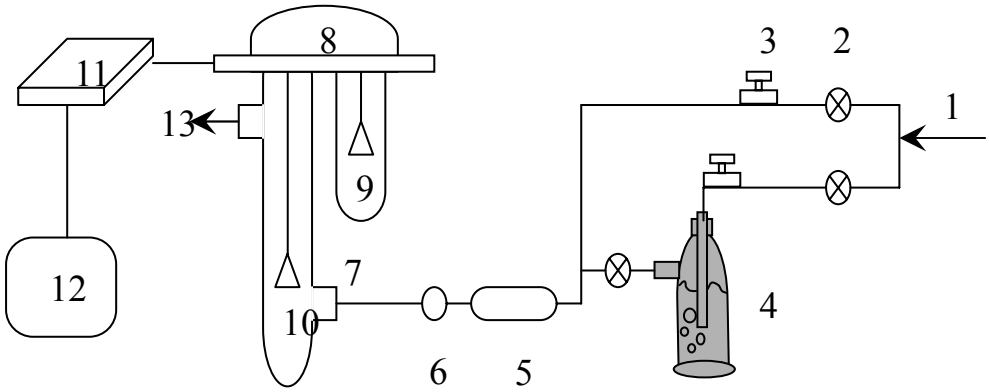

1. HC-free N_2 gas
2. On-off valve
3. Mass flow controller
4. Liquid toluene in a sparge bottle
5. Mixing chamber
6. GC sampling port
7. Inlet port of the gas chamber
8. Microbalance
9. Tare side
10. Sample side
11. Microbalance controller
12. Data processor
13. Vent

Fig. 3-2. Schematic diagram of the experimental setup for the sorption and desorption experiments by the gravimetric method.

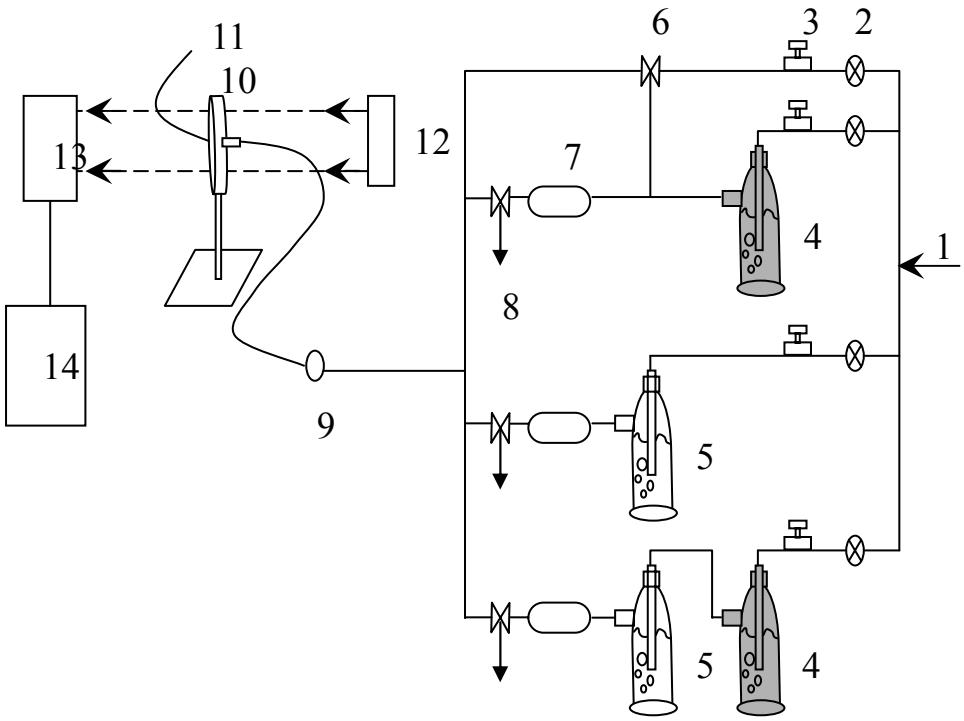

1. HC-free N_2 gas
2. On-off valve
3. Mass flow controller
4. Liquid toluene in a sparge bottle
5. Water in a sparge bottle
6. Three-way valve
7. Mixing chamber
8. Vent
9. Gas sampling port
10. Soil sample on ZnSe window
11. Gas vent
12. IR source
13. MCT Detector
14. Data processor

Figure 3-3. Schematic diagram of the experimental setup for the sorption and desorption experiments by the infrared spectroscopic method.

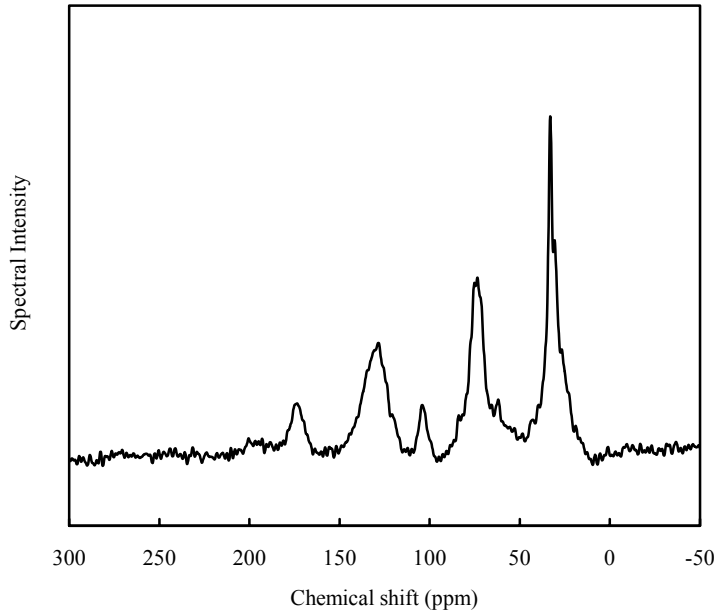

Fig. 3-4. Solid-state ^{13}C-NMR spectrum of humin.

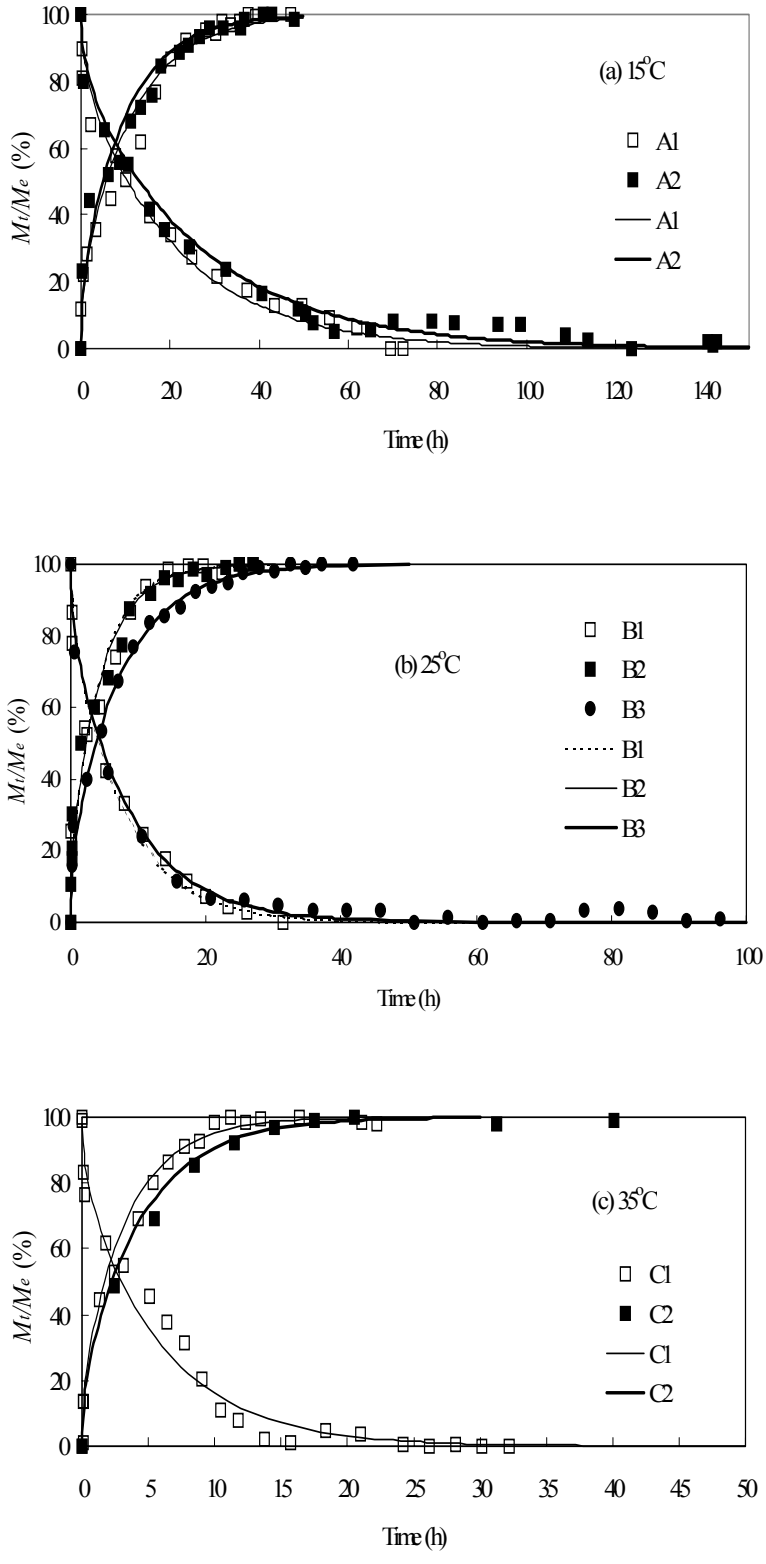

Fig. 3-5. Experimental results (squares and circles) and model best fittings (solid lines) of toluene sorption and desorption at different temperatures: (a) sorption and desorption at 15°C for disk A, (b) sorption and desorption at 25°C for disk B, and (c) sorption desorption at 35°C for disk C. A1 and A2, B1 and B2, respectively, are the results of duplicated experiments only with different VOC concentrations.

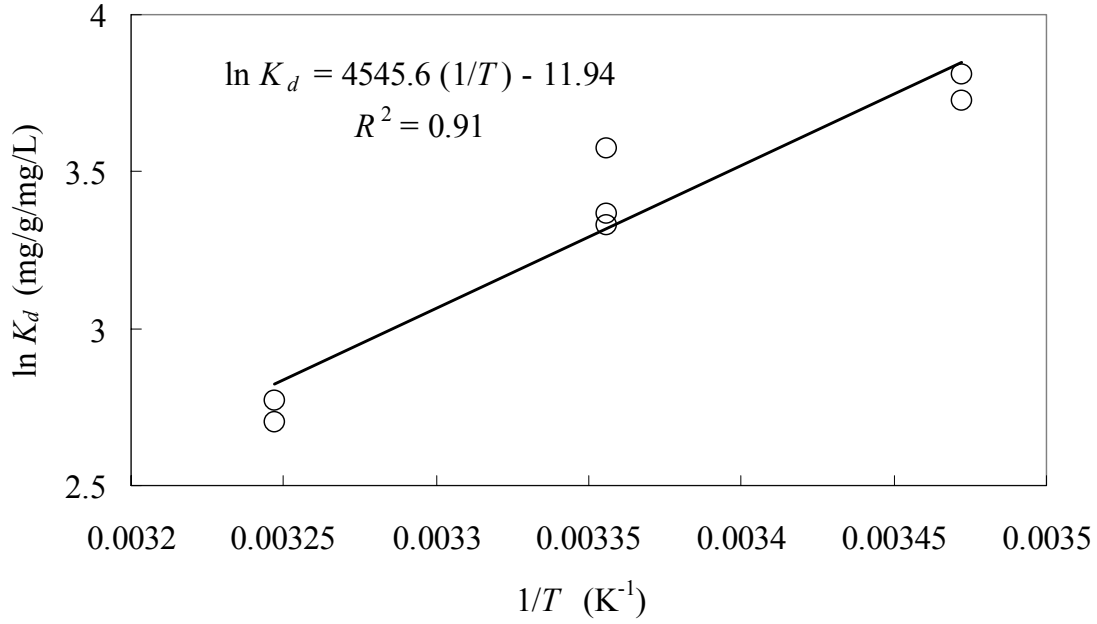

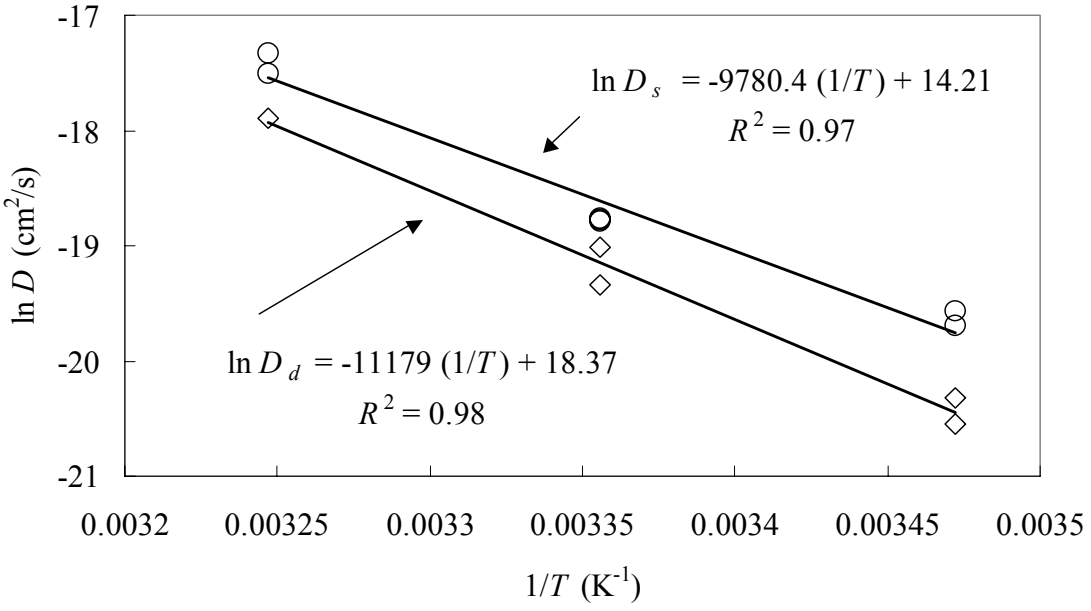

Fig. 3-6. (a, top) Plot of ln K_d versus 1/T (K^{-1}) for toluene sorption, and (b, bottom) plot of ln D_s and ln D_d versus 1/T (K^{-1}) for toluene sorption and desorption at temperatures ranging from 15°C to 35°C.

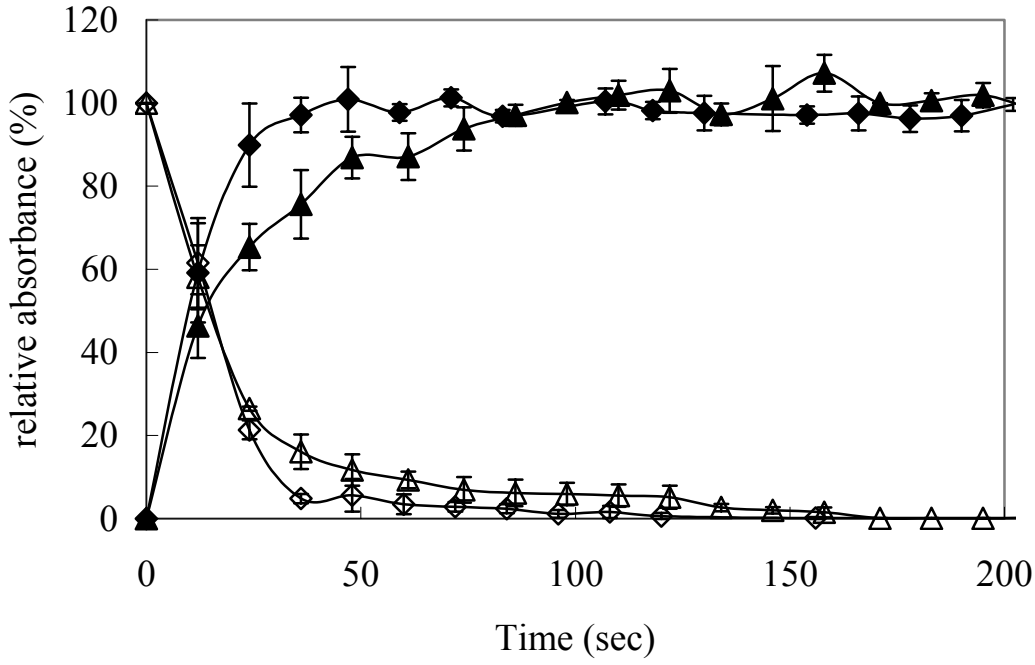

Fig. 3-7. Relative absorbance intensity of sorbed toluene on humin varying with time for sorption (solid symbols) and desorption (empty symbols) at 729cm^{-1} by FTIR under dry (diamond) and humid (triangle) conditions.

Chapter 4 Sorption Kinetics of Selected VOCs in Humin

4.1 Introduction

Sorption plays an important role in the transport, fate, and remediation of organic contaminants in soil. Irreversible sorption or slow desorption of VOCs in the laboratory or the field has been reported. A portion of sorbed VOCs is released slowly from soil particles and some fraction is retained in the particles (Pignatello and Xing, 1996; Aochi and Farmer, 1995; Steinberg et al., 1987). Recent reviewing papers have summarized the findings of the slow sorption/desorption of organic compounds in natural particles (Pignatello and Xing, 1996; Luthy et al., 1997). The retaining mechanisms affect the fate of pollutants in the environment and the effectiveness of remediation of contaminated soils and groundwater aquifers.

This phenomenon of slow equilibration has been attributed to the slow diffusion through micropores of soil particles (Lin et al, 1994) or the slow migration in soil organic matter (SOM) (Farrell and Reinhard, 1994; Fu et al., 1994). In fact, soil is chemically a heterogeneous matrix with various inorganic and organic constituents. The chemical heterogeneity complicates the prediction of the fate of a pollutant in the soil due to the different sorbing behaviors for different chemical components.

Humic substance is known to contribute to retention of xenobiotic compounds (Cheshire, 1979). Delineation of the mechanisms controlling the rate and the reversibility of sorption on humic substances are necessary to precisely predict the rates of the spreading and attenuation of the pollutants in the subsurface environment. However, Chang et al (1997) had investigated the diffusive mass transfer hindrance in soil humic acid, however, were not able to fine the real location where the slow or irreversible sorption happened. Humin, characterized by its high molecular weight, low solubility and cross-linked chemical structure (Hatcher et al, 1985), might become an environment into and out of which organic molecules can hardly move (White et al., 1999; Hu et al., 2000; Achtnich et al., 1999).

Therefore, this articel seeks to illustrate the sorption and desorption kinetics of VOCs in humin films made of humin powders to elucidate whether a strong association exists between VOCs and humin and to identify the properties of humin which correlate to the irreversibility, if any, of VOC sorption.

4.2 Materials and Methods

4.2.1 Reagents

Acetone (purity> 99.9%), toluene (purity> 99.9%), and *n*-hexane (purity> 99%), the three tested VOCs, were gas chromatographic analytical grade and purchased from Merck, Darmstadt, Germany. Sodium hydroxide (purity> 99%), and hydrochloric acid (HCl) (purity> 37%) were guaranteed reagents for trace element grade and also purchased from Merck. Hydrofluoric acid (HF) (purity> 49%) was Traceselectultra grade and purchased from Riedel-de Haën, Seelze, Germany. Aldrich humic acid was purchased from Aldrich Chemical, Milwakee, WI, USA. Montmorillonite (STx-1), mainly sodium saturated, was obtained from the Source Clay Mineral Repository of the Clay Minerals Society. Copper (II) chloride and silver nitrate were guaranteed reagents for trace element grade and purchased from Acros Organics. Hydrogen peroxide and calcium chloride were also guaranteed reagents for trace element grade and obtained from Merck. The deionized water was further purified with the milli-Q reagent water system, by Millipore, Bedford, MA, USA

4.2.2 Humin

Humin was extracted from Yamingshan soil, classified as medial, thermic, Pachic Melanudands according to the definition by USDA (USDA-NRCS, 1993), were air-dried, freed of large plant debris, and screened through a 20-mesh (0.84 mm) sieve. Small plant debris was further removed by flotation using ethanol. Then, soil sample was mixed well.

The humin extraction method is according to the procedure developed by Rigol et al. (1998) and Russell et al. (1983) except that an ethanol/hexane mixture (1:1 v/v) was used to remove fats and waxes to avoid the interference from toluene, which is the target VOC to be studied. In short, soil was refluxed to remove fats and waxes and extracted by sodium hydroxide to remove humic acids and fulvic acids. The solid residue was separated by centrifugation, neutralized with 6 M HCl, washed with 0.1 M HCl and deionized water, and finally freeze-dried. The humin fraction was isolated from the solid residue by sequentially removing the mineral matter with a three-step digestion procedure: first, suspension in a 1:1 mixture of 0.2 M HF and 0.2 M HCl (20 ml/g) for 64 hours; subsequently, digestion in a 1:1 HF (5.5 M) and HCl (1.1 M) mixture for 1 hour three times; and, finally, digestion in 5.5 M HF four times for 16 hours each time. After centrifuging and washing with 0.1 M HCl and water three times, the final residue designated as humin was freeze-dried and ready for use.

The characterization of humin via element analysis, ^{13}C-NMR spectrometry, and FTIR spectrometry was presented in our previous report. The preparation of humin disks also can be referenced to our previous report.

4.2.3 Sorption/Desorption Experiment of Soil Compartments

Gravimetric Method. The apparatus used for sorption was shown in Fig. 3-2 and the procedure has been described elsewhere (Chang et al., 1997). Briefly, the experimental apparatus was maintained in a thermostatic room at 25±0.1^{o}C. The set temperature was closely monitored for at least one day to ensure its stability before the initiation of the experiments. The disk was hung on the sample side of a Cahn 200 electric microbalance enclosed in a glass chamber. The VOC mass flux to the disk was significantly larger than the maximum VOC removal rate, which keeps the vapor concentrations inside the chamber at virtually fixed levels. The experiment was terminated when the change of weight could not be distinguished from the base noise of the microbalance, which was about ± 0.2 μg. The concentration of the VOC was determined with GC/FID (Hewlett-Packard 5890II).

4.2.4 Estimating Diffusivity via a Microbalance

The diffusion model has been described in detail by Chang et al. (1997). While an edge effect is negligible, the variation of VOC concentration in a humin disk with a thickness of 2×l can be described by a one-dimensional mass conservation equation:

$$\frac{\partial q}{\partial t} = D\frac{\partial^2 q}{\partial x^2} \qquad (4\text{-}1)$$

$$M(t) = S\int_{-l}^{l} q(x,t)dx \qquad (4\text{-}2)$$

where q (mg/cm^3) is the sorbate concentration in the disk at a distance x from the center plane of the disk and at time t; D is the apparent diffusivity of the sorbate inside the disk; l is the half-thickness of the disk; $M(t)$ is the total sorbed mass of sorbate in the disk; and S is the surface area of one flat side of the disk.

The initial condition inside the disk at the beginning of a sorption experiment is

$$q(x,0) = 0 \qquad (4\text{-}3)$$

The boundary condition at the disk surface ($x = \pm l$), where the sorbate concentration q_e is always in equilibrium with the concentration in the gaseous phase, is

$$q(\pm l,t) = q_e \qquad (4\text{-}4)$$

q_e can be estimated from the ultimate sorbed mass M_e divided by the disk volume:

$$q_e = M_e \big/ 2Sl \qquad (4\text{-}5)$$

There is no concentration gradient at the mid-plane of the disk (x=0):

$$\frac{\partial q}{\partial x}(0,t) = 0 \qquad (4\text{-}6)$$

The analytical solution of Equations 1, 2, 3, 4, and 6 is available in Crank and Park (Equations 36 and 37 in Chapter 1, Crank and Park (1968)) and the fraction of equilibration can be expressed as

$$M_t / M_e = f(t) \qquad (4\text{-}7)$$

where M_t is the sorbed mass and *f(t)* is a dimensionless expression that is zero at t=0 and is unity when t approaches infinity.

For the desorption process, the humin disk, after being equilibrated with a VOC for an infinite length of time, is placed in the clean nitrogen gas. The initial condition then is

$$q(x,0) = q_e \qquad (4\text{-}8)$$

and the boundary conditions are

$$q(\pm l,t) = 0 \qquad (4\text{-}9)$$

and Eq. 6. The analytical solution of Equation 1, 2, 6, 8 and 9 during desorption is

$$M_t / M_e = 1 - f(t) \qquad (4\text{-}10)$$

The diffusivity was then estimated by the best fitting of the experimental results.

The experimental parameters of the humin disks are shown in Table 4-1. Seven disks with 12.45 mm in diameter and various thickness ranging from 0.21 to 0.61 mm weighed from 40.8 to 100.5 mg. Their average density was 1.49 g/cm^3.

The experimental conditions and some results of the sorption and desorption experiments are shown in Table 4-2 and Figures 4-1~4-6. Three different volatile organic compounds (acetone, n-hexane, and toluene) were used to probe the properties of humin. The polarity of these three organic compounds increases in the order of : n-hexane< toluene< acetone. The gas-phase VOC concentrations ranged from 4.29 mg/L (P/P_0 = 0.030) for toluene to 39.9 mg/L (P/P_0 = 0.051) for acetone.

4.3 Result and Discussion

4.3.1 Distribution coefficients

The SOM-VOC distribution coefficient [K_d, (mg/g)/(mg/L)] between the solid phase and the gaseous phase is therefore defined in equation (1) of this chapter. The value of the distribution coefficient of acetone is the highest among those of all sorbates (Table 4-3). Although the molecular weight and the K_{ow} value are the lowest among the three sorbates, acetone seems to have the strongest affinity to humin due to its higher polarity. This result indicates that humin might be rich in polar function groups and create a more attractive environment for polar compounds. This result is consistent with the NMR result mentioned above. The values of the distribution coefficients of n-hexane are lower than those of toluene. The difference between the uptake capacities of hexane and toluene in humin may be attributed to slightly higher polarity for toluene.

The distribution coefficient of toluene in humin from this study is lower than that in Aldrich humic acid referred to by Chang et al. (1997). The average distribution coefficients of toluene in humin and humic acid are 0.29 ((mg/g)/(mg/L)) and 4.1 ((mg/g)/(mg/L)), respectively. Aldrich humic acid has a higher sorption capacity compared with humin.

The same result has been reported by Tell and Uchrin (1991) where the humin was mixed with sand and clay. Their results show that the affinity of toluene with humin is lower than with both humic acid and natural organic matter. It has been

reported that SOM containing a higher aromatic content has higher K_{oc} for aromatic contaminants (Hatcher et al., 1981; Chiou et al., 1998). Based on the assignments of ^{13}C-NMR spectra (Perminova et al., 1997; Chiou et al., 1998; Senesi and Loffredo, 1998), the humin used in this study has a total aromaticity of 15.1%, which is lower than that in the Aldrich humic acid used by Chang et al. (1997). Furthermore, the polar group content of 33.4% in humin is higher than that of 3.66% in humic acid. The relative amount of the main structural fragments may explain the lower K_d for toluene in humin. The reason for the distribution coefficient of humin being less than that of humic acid might be the higher lipophilicity as well as the higher aromaticity of humic acid.

4.3.2 Estimation of K_d from K_{ow}

The estimated distribution coefficients were calculated from the organic carbon-water partition coefficients (K_{oc}) of the contaminants multiplied by their organic carbon fractions and divided by the Henry's Law constant (Table 4-3). The estimates of K_{oc} can be derived from the relationships between K_{oc} and the octanol-water partition coefficient (K_{ow}) (Karickoff et al., 1979; Chiou et al., 1983). The organic carbon fractions of humic acid and humin used in this study are 0.39 and 0.35, respectively, determined with the Heraeus CHN-OS element analyzer. The estimated distribution coefficients, K_d, of toluene in humic acid and humin are 0.42 ((mg/g)/(mg/L)) and 0.38 ((mg/g)/(mg/L)) from Karickhoff's equation; and 0.11 ((mg/g)/(mg/L)) and 0.098 ((mg/g)/(mg/L)) from Chiou's equation, respectively. The higher observed distribution coefficients for toluene in Aldrich humic acid could be due to the selective effect of extracting natural humic acid by organic solvents which excluded some polar constituents of humic acid. Notwithstanding that the Aldrich Chemical Co. pronounced that Aldrich humic acid was mined from the earth in Germany and washed with deionized water and nothing else, several reports have suggested that such commercial products are not considered to be appropriate for use as analogues of true soil humic substances. Malcolm and MacCarthy (1986) have used ^{13}C NMR spectroscopy to show clear differences between commercial materials and noncommercial soil-derived humic materials, and as such, the use of commercial preparations, where provenance is unknown, in soil and water investigations was discouraged. It was concluded by Malcolm and MacCarthy that commercial humic acids such as Aldrich humic acid are similar to humic acids extracted from coals (leonardite and dopplerite). By the way, Graber and Borisover (1998) indicated that Aldrich humic acid is a poor model for soil organic matter. The observed

distribution coefficients for toluene in humin shown in Table 4-3 are similar to the estimated values from Karickhoff's equation and slightly larger than those of Chiou's equation.

From the selected compounds that the correlations were based on, Karickhoff's equation is appropriate for mostly aromatic compounds and Chiou's for chlorinated hydrocarbons. For the estimation of the distribution coefficient of toluene, a monoaromatic chemical, toluene, the Karickhoff's regression equation has better predictability. These two equations underestimate distribution coefficients of acetone and hexane in humin due to neglecting the contribution of the polar-polar interaction between acetone and humin and the extremely aliphaticity of hexane.

4.3.3 Two-stage sorption

There was a period, about 3 hours, of lag for sorption of hexane followed by a rapid sorption period on duplicated disks, B1 and B2 (Figure 4-2). There was no obvious two-stage sorption for acetone and toluene sorption experiments. The fact that Disks B1 and B2 were slightly denser than other disks may partially explain the observation that the penetration into humin was more constrained than with others. The other reasons could be the long linear molecular structure of hexane which makes hexane difficult to get into the humin matrix, and the large polarity difference between n-hexane and humin. A certain level of energy is needed to loosen the polymer molecular linkage to form an interstitial space or free volume for penetrants against the intermolecular and intramolecular interactive forces, which depend on the dimensions of the penetrant and the structure of the polymer molecules (Crank and Park, 1968). Therefore, time was required for hexane to solvate the target surface before the molecular diffusion in the matrix occurred.

The conceptual model of VOC sorption and diffusion into solid SOM was proposed and the concentration effect of solvation was mentioned in Chang et al. (1997). Compared to B1 and B2 in Figure 4-2, the higher gas concentration seemed to accelerate the first stage and initiated the early onset of the second stage. After repeated toluene sorption/desorption experiments, the diffusion of hexane in Disk B3 seemed easier, with the diffusivity larger than the other two disks. The lag time was lessened to 1.8 hours. That could result from the loosening of the humin matrix by the frequent penetration of toluene molecules.

4.3.4 Diffusion Coefficients

Figures 4-1 to 4-6 show the time courses of sorption and desorption and the simulation of the weight changes by using the diffusion model. The rate of penetration of VOCs was quantified by the diffusivity of VOC molecules in the humin matrix. The average of the best-fitting sorption diffusivities are 3×10^{-10} for acetone, 6.0×10^{-9} cm^2/sec for hexane, and 7.0×10^{-9} cm^2/sec for toluene at 25°C which are lower than those of the same compounds in water by a factor of 1000, indicating highly constrained diffusion within the humin matrix. The complex and networking properties of humin may cause great constraint to the diffusive flux. Furthermore, the diffusivities of acetone were the lowest among the three VOCs probably due to the strong interaction between the polar moieties of acetone and those of humin.

The diffusivities for these three VOCs in humin were around 1×10^{-9} cm^2/s (Table 4-2), which is similar to the volatile organic compounds (benzene, toluene, chlorobenzene, dichlorobenzene, and trichloroethene) in humic acid and fulvic acid estimated by Piatt and Brusseau (1998). Piatt and Brusseau (1998) studied the diffusion coefficients of several compounds in soils coated with humic acid and fulvic acid. They found that the diffusivities for given solutes were approximately five orders of magnitude smaller than their corresponding aqueous diffusion coefficients and spanned a range of more than 3 orders of magnitude for different solutes. They also pointed out that diffusion was highly restricted within the SOM matrix and was very dependent on the size and shape of the solute, which was also found in this study.

4.3.5 Desorption Process

The desorption diffusivities of these three VOCs are shown in Table 4-2 and Figures 4-2, 4-4, and 4-6. The slowest diffusive was found for acetone probably due to its highest affinity with the humin matrix. With disk B1 and B2 the desorption diffusivities of hexane were also slightly lower than those of toluene, just as the sorption diffusivities were. However, disk B3, which had previously been used for toluene sorption, had the highest desorption rate with hexane.

The desorption rates were lower than the sorption rates for hexane as well as toluene. However, the diffusivities of desorption for acetone were the same as those of sorption.

For toluene, sorption diffusivities in humic acid and humin were not significantly

different (Table 4-4). However, the desorption diffusivity of toluene in humic acid was slightly lower than those in humin, which could be a result of higher aromaticity and higher affinity in humic acid.

Figure 4-4 and Figure 4-6 show that the sorbed mass of hexane and acetone could not be removed completely at the end of the desorption experiments, 92 hours and 780 hours, respectively. The residual percentage of the sorbed mass was approximately 35% for acetone and 20% for hexane. However, there was no obvious persistence of toluene in humin, as shown in this study.

Lichtfouse et al. (1998) also reported the entrapment of n-alkanes in soil humin based on ^{13}C-NMR data. The low total aromaticity (15.1%) but high total aliphaticity (84.7%) of humin used in this study could cause strong attraction to hexane, a linear aliphatic compound, and subsequently irreversible association. On the other hand, polar-polar interaction between the polar moieties of humin and the polar acetone molecules may be strong enough to retain the acetone molecules in the humin matrix.

For aromatic compounds, the ^{13}C-NMR spectra of Guthrie et al. (1999) suggested noncovalent interaction between pyrene and humin. After studying the interaction between monoaromatic compounds and dissolved humic acids with NMR, Nanny and Maza (2001) indicated that the interactions of benzene and humic acids increased with the percentage of aromaticity of humic acid. Moreover, one of their interactions, the π - π interactions between the aromatic ring of selected monoaromatic chemicals and aromatic components of humic acid, was favored by increasing humic acid aromaticity. Due to the low aromaticity of humin used in this study, our hypothesis is that there is no strong interaction between aromatic compounds, e.g. toluene, and humin due to the low aromaticity of humin; nevertheless, aliphatic compounds could be trapped in the humin matrix due to strong hydrophobic interaction.

The NMR spectra of humin as well as the sorption/desorption experimental results by using three VOCs probes have revealed some evidence of polar-polar and strong aliphatic interactions between the VOC sorbates and humin. The cross-linking property of humin as well as the strong inter-molecular interaction are able to significantly retard the migration of VOCs in humin. Further studies of the entrapment and retarding mechanisms of aliphatic compounds as well as aromatic compounds and quantification of their effect on the transport of VOCs in soils are needed.

4.4 Conclusion

The differences in distribution coefficients for a given solute reflect the higher hydrophilicity in humin than in humic acid. The lowest diffusivity of acetone may result from the high affinity of acetone with humin. The retention of acetone and hexane in humin after thorough purging with VOC-free nitrogen gas was observed. There seems to be strong interaction between the acetone or hexane molecules and the humin matrix. Based on the above results and results presented in other literature (Chang et al., 1997; Piatt and Brusseau, 1998), it may be concluded that the sorption kinetics for VOCs on natural humic substances with a time scale between a few minutes to days is controlled primarily by mass transfer in polymeric humic structures.

Table 4-1. Properties of humin disks

	A1	A2	B1	B2	B3‡	C1	C2	C3
Weight (mg)	100.5	52.0	40.9	40.8	51.8	61.5	72.8	51.8
Thickness (mm)	0.61	0.27	0.21	0.21	0.29	0.34	0.44	0.29
Density (g/cm^3)	1.35	1.58	1.60	1.60	1.47	1.49	1.36	1.47

†All disks are of the same diameters, 12.45 mm.

‡Disk B3 and Disk C3 are the same disk.

Table 4-2. Conditions and results of the sorption and desorption experiments by the gravimetric method.

	Experimental runs							
	A1	A2	B1	B2	B3†	C1	C2	C3
VOC	Acetone	Acetone	Hexane	Hexane	Hexane	Toluene	Toluene	Toluene
VOC concentration (mg/L)	25.8	39.9	28.8	37.4	35.3	5.59	4.29	7.53
VOC pressure (P/P_o)	0.033	0.051	0.040	0.052	0.049	0.039	0.030	0.052
Maximum sorbed mass (μg)	1253	923	110	107	208	96	91	140
K_d ((mg/g)/(mg/L))	0.48	0.44	0.093	0.070	0.11	0.28	0.29	0.36
$D_s x10^9$ (cm^2/sec) ‡	1.1	0.3	6.0	6.0	18	7.0	7.1	7.0
$D_d x10^9$ (cm^2/sec) §	1.1	0.3	2.0	1.5	8.0	4.0	5.5	4.0
Residual mass (μg)	439	323	22	27	35	--	--	--

† Running after experimental run No. C3.

‡diffusivity during sorption

§diffusivity during desorption.

Table 4-3. Distribution coefficients of three VOCs at low concentrations in humic substances.

	Acetone	Hexane	Toluene
Log K_{ow} (mol L^{-1}octanol) (mol L^{-1} water)$^{-1}$†	- 0.24	4.11	2.69
Log K_H (L atm mol^{-1}) †	- 1.68	3.14	0.83
Estimated humin K_d (Karickhoff's eq.)	0.15	0.049	0.38
Estimated humin K_d (Chiou's eq.)	0.071	0.0092	0.098
Estimated humic acid K_d (Karickhoff's eq.)	0.16	0.055	0.43
Estimated humic acid K_d (Chiou's eq.)	0.079	0.010	0.11
Observed K_d for humin (duplicated)	0.48	0.093	0.28
	0.44	0.070	0.29
Observed K_d for Aldrich humic acid‡ (duplicated)	0.082	0.86	4.63
	0.091	--	3.63

†CRC Handbook of Chemical and Physical (1985-1986).
‡Chang et al. (1997).

Table 4-4. Diffusivities of three VOCs at low concentrations in humic substances.

	Acetone	Hexane	Toluene
$D_a \times 10^2$ (in air)†	11	8.6	8.2
$D_w \times 10^5$ (in water)†	1.5	1.1	1.1
$D_s \times 10^9$ (in humin) (duplicated)	1.1	6.0	7.0
	0.3	6.0	7.1
$D_d \times 10^9$ (in humin) (duplicated)	1.1	2.0	4.0
	0.3	1.5	5.5
$D_s \times 10^9$ (in Aldrich humic acid) ‡ (duplicated)	4.4	13.8	7.8
	6.5	--	6.3
$D_d \times 10^9$ (in Aldrich humic acid) ‡ (duplicated)	4.7	3.7	1.3
	--	--	1.1

†Estimated from molecular weight, Schwarzenbach et al. (1993).
‡Chang et al. (1997).

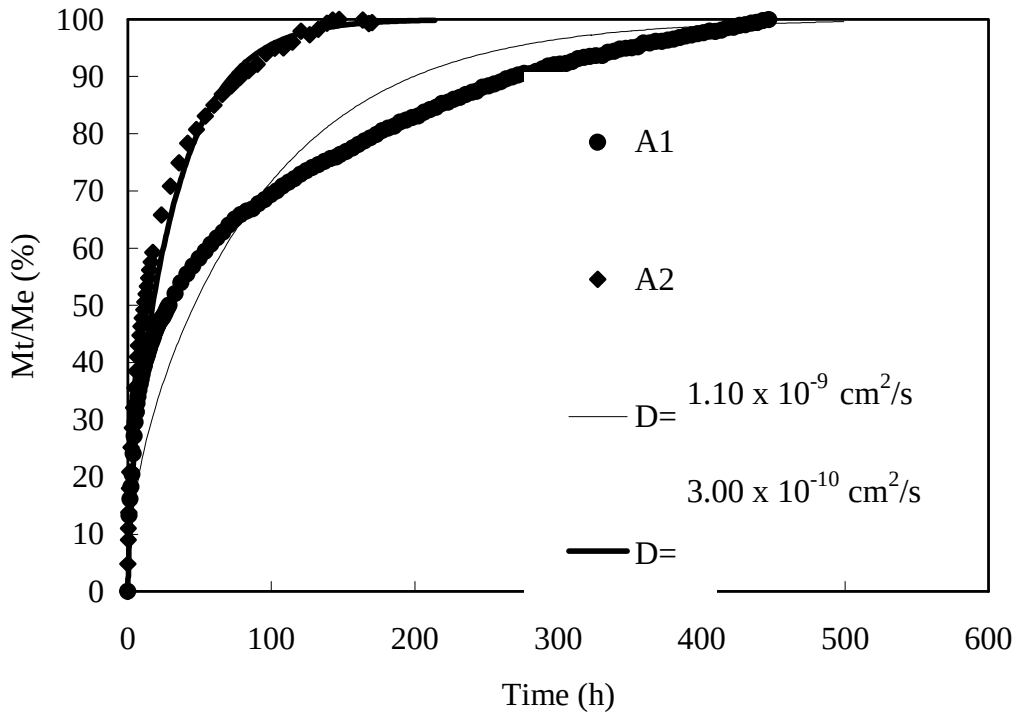

Figure 4-1. The experimental and simulation results of acetone sorption in humin disks.

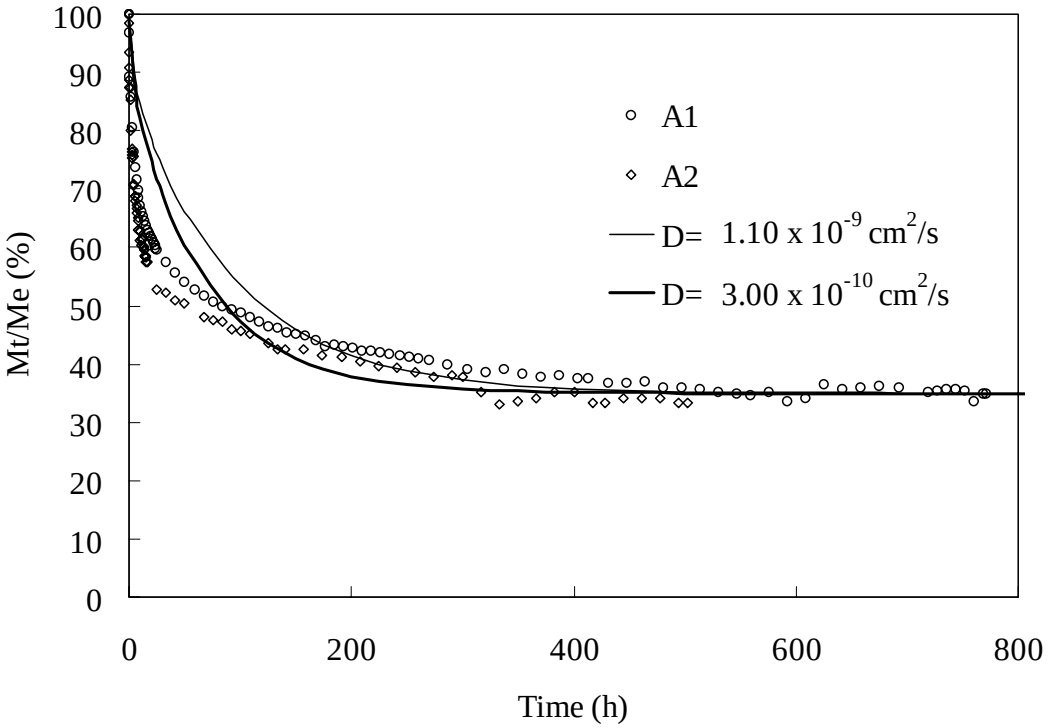

Figure 4-2. The experimental and simulation results of acetone desorption in humin disks.

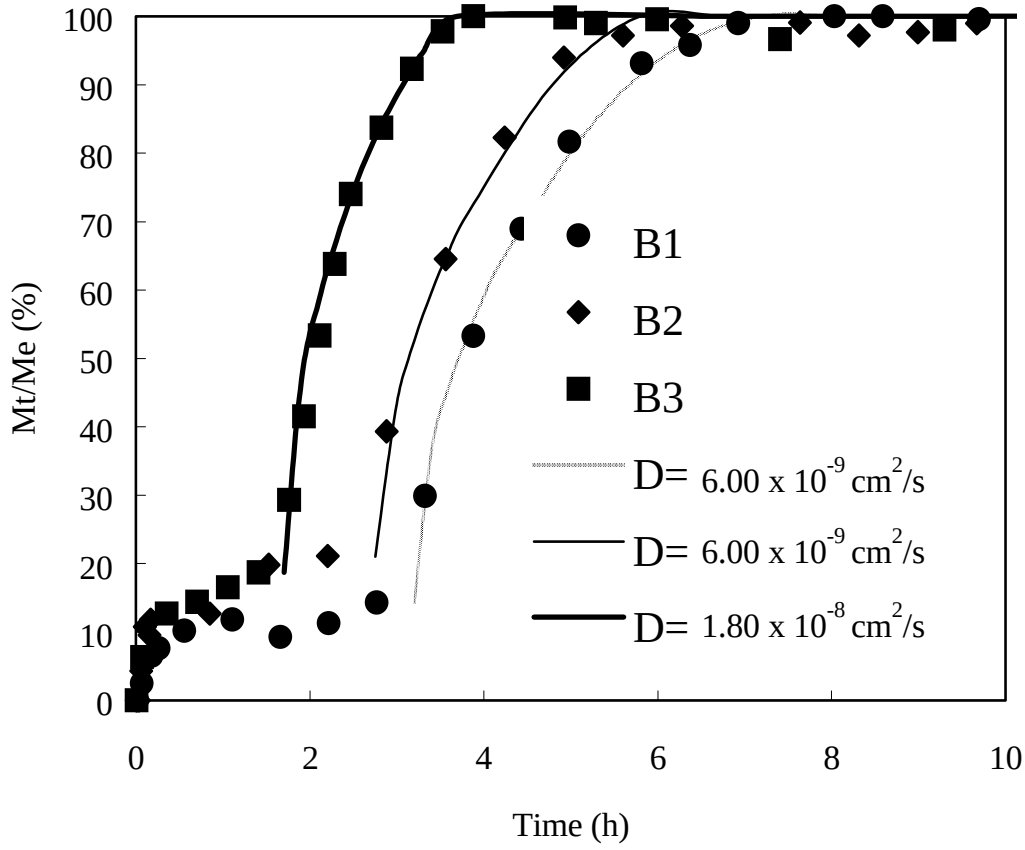

Figure 4-3. The experimental and simulation results of hexane sorption in humin disks.

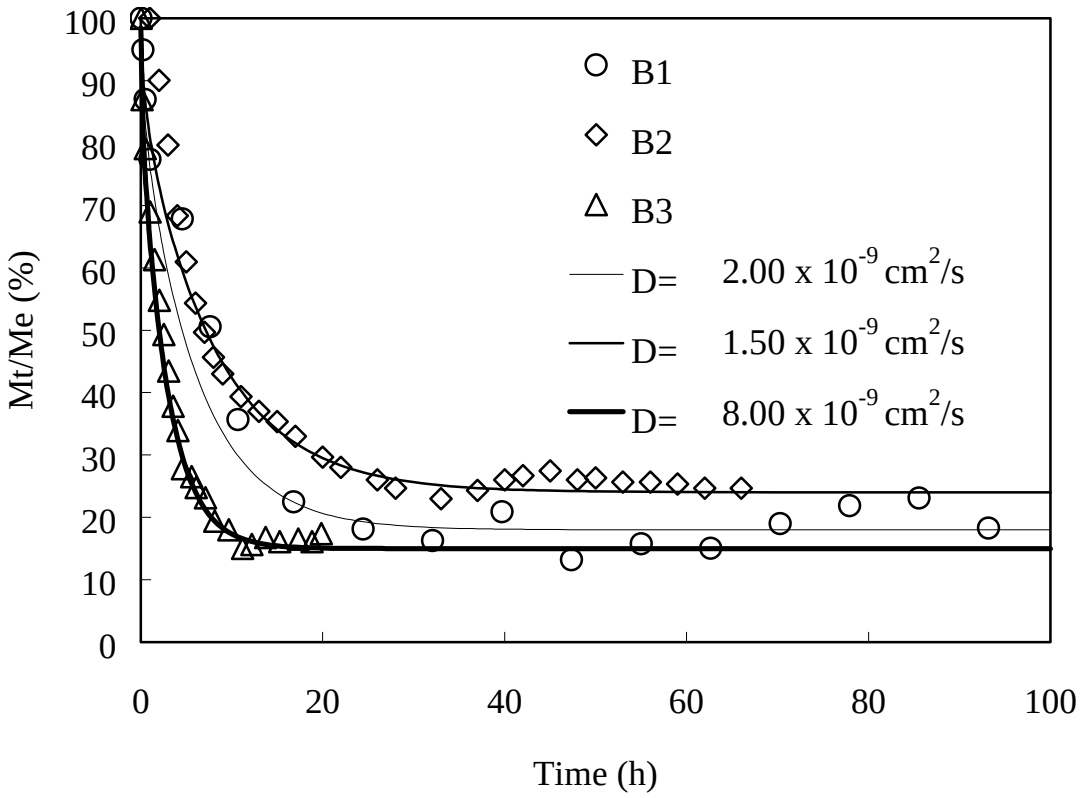

Figure 4-4. The experimental and simulation results of hexane desorption in humin disks.

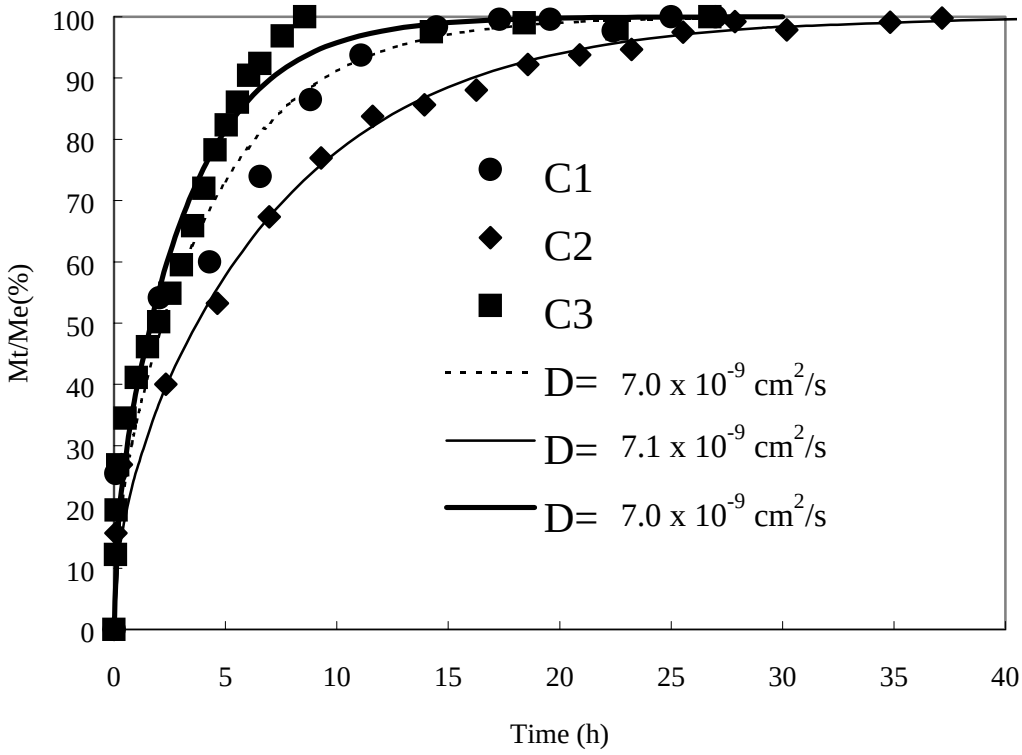

Figure 4-5. The experimental and simulation results of toluene sorption in humin disks.

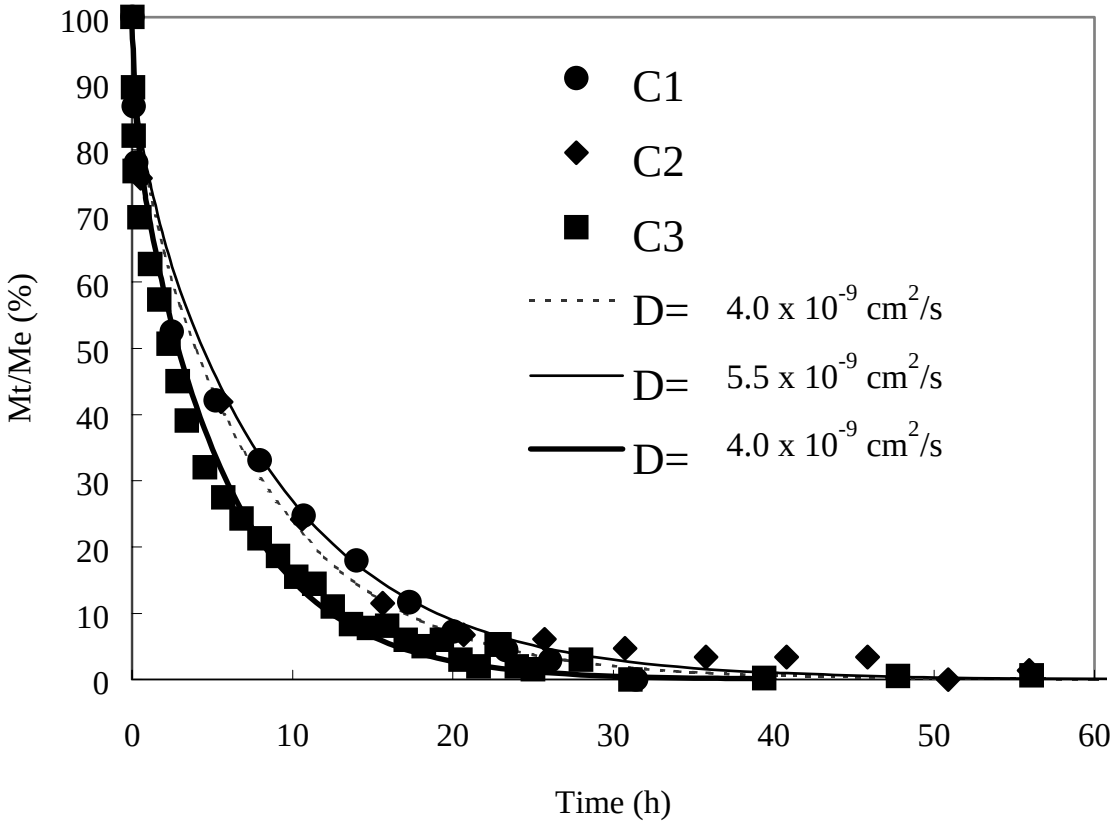

Figure 4-6. The experimental and simulation results of toluene desorption in humin disks.

Chapter 5 Kinetics Study of Toluene Sorption and Desorption in Ca- and Cu- Montmorillonites by FTIR Spectroscopy

5.1 Introduction

Sorption of organic contaminants in soils plays an important role in their transport, fate, and bioavailability in the environment. However, the phenomenon of irreversible sorption or slow desorption of organic pollutants in the laboratory or in the field has been reported. A portion of sorbed organic pollutants was released from soil particles slowly. Some fraction was even retained in the particles irreversibly (Aochi and Farmer, 1995; Pingatello and Xing, 1996). Such retention of the pollutants in soils affects their fate in the environment and the effectiveness of the remediation of contaminated soils and groundwater aquifers.

However, soil is chemically a heterogeneous material with various inorganic and organic constituents. Delineation of the sorption rate and the reversibility of each component is necessary to tell precisely which component contributes to the slow sorption the most and to what extent, and to predict the tendency of migration and attenuation of the pollutants in soils.

Numerous researchers have observed that the sorption of volatile organic compounds (VOCs) on soil particles appears to be a bi-phasic process, in which there is an initial stage of rapid sorption followed by a slow sorption stage. Karickhoff (1980) referred to these two stages as “labile” and “non-labile” stages of sorption. Several researchers interpreted the slow or long-term sorption of VOCs as a result of intra-organic matter diffusion (Leenheer and Ahlrichs, 1971; Ball and Roberts, 1991). Some researchers (Pignatello ;1990 and Schlebaum et al., 1998)suggested that the persistence of organic pollutants in soils resulted from the entrapment of contaminants in soil organic matter. Wu and Gschwend (1986) explained the phenomenon of slow sorption by a radial diffusion model in which the sorbate migrates into and out of the aggregates of organic matter and mineral particles by diffusion.

Mineral surfaces as well as soil organic matter could act as contributing sorbents for slow sorption since their soil samples with very low organic matter showed a

bi-phasic desorption pattern for VOCs (Pavlostathis and Jaglal,1991 and Pavlostathis and Mathavan,1992). Clay minerals offer a gigantic surface area for adsorption as well as surface-catalyzed reactions that we should not overlook. Furthermore, Achoi and Farmer (1995) have demonstrated the formation of a resistant fraction of 1,2-dicholoroethane on clays mixed with potassium bromine under a dry condition. It seems that the relative importance of the roles of soil organic matter and soil minerals on the sorption vary with the type of pollutants and the composition of the soils. This study was conducted only on the sorption of clay minerals and intended to delineate the role of clays on the slow desorption of contaminants from soils.

The gravimetric method with a microbalance has been used to trace the time courses of sorption of VOCs on soil organic matters (Chang et al., 1997; Morrissey, and Grismer, 1999; Shih and Wu, 2001) and on oven-dried clay (Arocha et al.,1996 and Morrissey and Grismer, 1999) all under dry conditions. However, the major constraint associated with the gravimetric methods for the investigation of sorption dynamics is the inability to observe the behavior at the molecular level and under a wet condition.

Molecular-level environmental observation, such as spectrometric methods, can be applied to provide information about the relative quantity, the energetic status and the possible chemical transformation of the compounds.

Therefore, via the thin film/FTIR method under two different levels of humidity, this paper seeks to illustrate the sorption and desorption kinetics of VOCs on clay films, to clarify whether a strong interaction exists between toluene and clays, and to identify the molecular-level mechanism which may contribute to the irreversibility of toluene sorption under dry and humid conditions.

5.2 Material and Methods

5.2.1 Preparation of Clay Films

The clay was treated with 35% hydrogen peroxide and the fraction with particle sizes smaller than 2 μm was collected by the sedimentation method. The Ca(II) and Cu(II) exchanged forms were prepared by treating the clay (< 2 μm) with 1.0 N solutions of $CaCl_2$ or $CuCl_2$, respectively, then centrifuging, and removing the supernatant liquid. The procedure was repeated three times to maximize the exchange of the original cations (mainly sodium). Excess $CaCl_2$ and $CuCl_2$,

respectively, were removed by washing with deionized water until the test for chloride by $AgNO_3$ was negative (Pinnavaia and Mortland, 1971). A drop of the clay suspension was placed on the inner surface of a ZnSe window of a gas cell.

5.2.2 Sorption/Desorption Experiments of Clay films Traced by FTIR

In Figure 3-3, the gas cell had a 5 mm thickness and a 30 mm diameter with two ZnSe windows. All tubings are made of Teflon. The clay film on the inner side of the window of the gas cell was dried and purged with 50 mL/min N_2 gas (HC-free) at least one day to remove sorbed impurities before each experiment. For humid conditions, clay films were incubated with humid nitrogen gas after the drying period. A steady flow of gas was passed through the liquid toluene in a bottle and then mixed with a flow of pure N_2 gas to obtain a desired constant concentration of toluene vapor and the same flow rate as that of the purging gas. The sample cell was purged under either low humidity (RH below 1%) or high humidity (RH above 95%). Desorption experiments were carried out by purging the gas cell with pure N_2 gas at a rate of 50 mL/min for dry experiments or with the moisturized N_2 gas. The experiment was terminated after the change of the intensity of absorbance could not be distinguished.

The concentration of the toluene was determined with Hewlett-Packard 5890II GC, equipped with a flame ionization detector (FID) and a 30 m x 0.53 mm i.d. SPB-5 fused silica capillary column (Supelco Co.). The relative vapor concentrations of toluene (P/Po) were around 0.40 and 0.44 under dry and humid conditions, respectively, and were kept constant during one run of experiment.

The absorbance spectra of IR beam passing through the gas cell windows were obtained on an BIO-Rad FTS 40 spectrometer at 2 cm^{-1} resolutions by averaging 16 scans for a short-term kinetics study and followed by 200 scans for long-term monitoring. The Bio-Rad spectrometer incorporates a Michelson interferometer with a KBr beam splitter and a liquid-nitrogen cooled mercury-cadmium-telluride (MCT) detector. All spectra were ratioed against the optical batch background spectrum before each measurement. No subtraction used in our spectra in case artificials incurred.

5.3 Results and Discussion

5.3.1 Sorption Capacities of Clays

Comparing the steady absorbance of toluene at wavenumber 694 cm^{-1} after sorption equilibrium of Ca-montmorillonite under dry conditions to that under humid conditions, we found more amount of adsorbed toluene on dry clay than that on humid one (Table 5-1). For Cu-montmorillonite, larger difference was observed. However, the average value of intensity of toluene sorbed on Ca- and Cu-montmorillonites under humid conditions are similar.

Chiou (1998) and Petersen et al. (1995) concluded that inorganic matters, e.g. clays, had strong sorbing capacity under dry conditions, however, they were weak absorbents in water. Our observation from the FTIR spectroscopy is consistent with their conclusion. Moreover, Goss et al. (1996) had illustrated that the adsorbed water film was apparently thick enough to diminish the influence of the characteristics of the mineral surface on adsorption at close to 100 % relative humidity. It agrees with our result that there is similar adsorption amount of different cations exchanged clays under high humidity.

Comparing the adsorption intensity of these two montmorillonites under dry conditions, the higher adsorption of Cu-montmorillonite indicates that the mineralogical composition of clay, a chemical parameter of soil, gives a great influence on the sorbing capacity. And the adsorption mechanism of aromatic compounds on Cu-form could be different from that on Ca-form.

5.3.2 Kinetics of Toluene Sorption on Clays

The gas-phase spectra of toluene can be identified by referring to the band assignments of toluene made by Lau and Snyder (1971). Three normal infrared frequency assignments are observed in the region 600 cm^{-1}-1800 cm^{-1}: the ring C-H out-of-plain bending and ring torsion at 694 cm^{-1} and 729 $cm^{-1}$and the ring C-C stretching vibration at 1493 cm^{-1}.

The experimental results indicate that sorption equilibrium can be achieved in a few minutes with a thin clay film (Figures 5-1~5-5). Kubicki et al. (1997) have studied the sorption behavior of salicylate and illite clay using by the attenuated total reflectance Fourier-transform infrared (ATR-FTIR) spectroscopy. They concluded

that the equilibrium time required for hydrophobic organic contaminants in clay minerals was in hours rather than weeks. Furthermore, Johnston et al. (1992) have studied the vapor-phase sorption of *p*-xylene on a self-supporting montmorillonites film. They also observed that a few minutes were needed to reach the equilibrium. Our result was consistent with their observation.

Based on the first-order kinetics assumption, we can get that the sorption rate constants are larger than the desorption rate constants (Table 5-2). It suggests that the sorption process of toluene on clays is faster than the desorption process. In addition, the slow desorption lasts for a long period of time and there is some persistent fraction on both type of clays under a dry condition. Toluene molecules could be trapped in clay matrix during the sorption/desorption process.

5.3.2.1 Sorption Kinetics of Toluene on Ca- montmorillonite

The thin film/FTIR method allows us to monitor the kinetic behavior of the gas/solid reaction. Shown in Figure 5-11, three assignments, 694 cm^{-1}, 729 cm^{-1}, and 1493 cm^{-1}, for the adsorbed toluene on Ca-montmorillonite under dry condition, increase with time. The peak area of the assignment of 694 cm^{-1} obtained by integrating the intensity was used to represent the relative sorbed amount. Figure 5-2 and 5-3 show the amount of sorbate on Ca-montmorillonite varying with time during the experiments under dry and humid conditions, respectively.

It took about 80 seconds to reach equilibrium for toluene on Ca-montmorillonite under dry conditions. During the desorption process, a residual fraction, approximately 10 %, resistant against desorption was observed after sixty days of desorption. Results of duplicated experiments are well in agreement with each other except the slightly scattering of the long-term data due to the low intensity of the infrared frequency. Under humid conditions (Figure 5-3), it took about 100 seconds to reach equilibrium. However, the rate of desorption in humid gas is faster than that in dry conditions. There seems no residual of toluene found in the duplicated experiments in humid conditions.

In the FTIR/thin film method, the spatial dimension of the cell inner space is approximately 5 mm. The time scale of diffusion through the boundary layer estimated by the relationship $t = (\Delta x)^2/D_a$, where Δx is the thickness of the boundary layer (exaggeratedly assuming the same as the cell thickness) and D_a the gaseous diffusivity of toluene (Gilliand, 1934), is 2.75 seconds. This system is clearly not a

boundary-layer-controlled case and the sorption kinetics is controlled by the intrinsic sorption of the clay particles.

The two stages of organic contaminant adsorption on soil aggregates are widely discussed. Arocha et al. (1996) studied the adsorption kinetics of toluene on two soil agglomerates, Yolo silt loam and Na-montmorillonite, and indicated that soil is a biporous sorbent. By proposing that the slow stage was controlled by slower diffusion and adsorption in intragrain micropores, they estimated the macropore and micropore diffusivities on clay. Morrissey and Grismer (1999) also estimated these diffusivities on montmorillonite from the experimental results by using the gravimetric method. According these two papers, the macropore and micropore diffusivities of toluene on montmorillonite range from 5.8×10^{-6} to 9.7×10^{-8} cm^2/sec and 3.7×10^{-12} to 3.5×10^{-15} cm^2/sec, respectively.

The intraparticle diffusion time can be predicted from the equation, $t \quad 0.03 r^2/D$, r the radium, of the time needed to reach 50% sorption (Wu and Gschwend, 1986; Equations 11-166 in Chapter 11, Schwarzenbach et al., 1993). If the micropore diffusion is controlling, the calculated micropore diffusivity of this study is about 6×10^{-12} cm^2/sec for the particle size of 1μm, which is in good agreement with the results of Arocha et al. (1996) and Morrissey and Grismer (1999). Since the particle size which we used was far less than 2μm there was no mass transfer limitation in the clay film system. So the sorption of toluene in clays should be intrinsic reaction rate controlled or micropore diffusion controlled.

5.3.2.2 Sorption Kinetics of Toluene on Cu- montmorillonite

Figure 5-4 shows that it took about 150 seconds for sorption to reach equilibrium under dry conditions. The little difference between the two duplicated experiments might be resulted from the slightly different clay thickness. The desorption rate was lower than that of Ca-montmorillonite under the same condition. The sorbed toluene could not be desorbed completely. The residual fraction was approximately 10 % of the maximum sorbed amount after sixty days of desorption. Under humid conditions, the rate of sorption and desorption became faster than those under dry conditions (Figure 5-5). However, unlike that in dry conditions, the absorbance of peak 694 cm^{-1} showed no residual after long-term desorption.

The estimated first-order rate constants according to the growing and decaying of the intensity at wavenumber 694 cm^{-1} were listed in Table 5-2. The rate constant

ranges from 1.8 to 4.5 min^{-1} for sorption and 0.09 to 2.4 min^{-1} for desorption. For Ca-montmorillonite, the desorption rates are lower than sorption ones approximately one magnitude; moreover, the rate constants in dehydrated conditions are slightly higher than those in humid ones. It indicated that sorption kinetics process of Ca-montmorillonite is not significantly influenced by the humidity. Cu-montmorillonite under dry condition has the lowest sorption/desorption rate constants and the highest sorbing capacity occurs. Seemingly, there is a strong interaction between the sorbate and Cu-montmorillonite.

5.3.3 FTIR Spectra of Sorbed Toluene

Under dry conditions, the FTIR spectra of the two cations exchanged montmorillonites having been exposed to toluene vapor are shown in Figure 5-6 and Figure 5-7. For comparison, a reference spectrum of vapor-phase toluene, and the spectra of Ca- and Cu- montmorillonite without toluene, are also included. Refering to the sorbed-phase toluene (Pinnavaia and Mortland, 1971), four normal modes are selected to be the characteristics for the physically adsorbed toluene molecules on montmorillonite: the C-H out-of-plane skeletal vibration at 694 cm^{-1}, the C-H out-of-plane deformation vibration at 729 cm^{-1}, the C-C stretching vibrations at 1457 and 1493 cm^{-1}, respectively. These observed vibrational frequencies for physical sorption are essentially not shifted (< 2 cm^{-1}) relative to those for the toluene vapor.

For Cu-montmorillonite, all four normal modes were observed except the C-H out-of-plane deformation vibration at 729 cm^{-1} which was shifted to a higher frequency at 735 cm^{-1}. This molecular moiety is known to be quite sensitive to the surrounding (Pinnavaia and Mortland, 1971). The similar shifts were observed, for instance, for toluene in the solid state (Fuson et al., 1960). Moreover, new vibrational bands at 758, 1363, 1487, and 1591 cm^{-1} appeared in 600~1700 cm^{-1} region after one day. Unlike the physical bound form, the CH_3 deformation was shifted to a frequency lowered by 17 cm^{-1} (1380 to 1363 cm^{-1}) and two C-C stretching modes of the complexed toluene are shifted in the same direction by 9 to 18 cm^{-1} (1496 to 1487 cm^{-1} and 1609 to 1591 cm^{-1}). Furthermore, the shift toward high frequency for the vibration (758 cm^{-1} from) 729 cm^{-1} is 4.8 times larger than that for the physically adsorbed form. This result indicates that toluene was chemically bound on Cu-montmorillonite. Pinnavaia and Mortland (1971) also reported the similar peaks for physically and chemically adsorbed toluene on clays under dry conditions.

Under dry conditions after the Cu-montmorillonite being in contact with the toluene vapor, the color of clay changed from light blue to light green. There was no color change neither the peaks assigned to chemisorption observed in the humid sorption experiments. It seems that the water molecules could occupy the strong binding sites and protect the mineral surface. This is in good agreement with the foregoing observation and discussion about the kinetics by Goss et al (1996).

For Ca-montmorillonite, in addition to the physically sorption modes, two new peaks (739 and 1688 cm^{-1}) increase with time consistently in some experimental sets. The peak 739 cm^{-1}on the shoulder of the peak 729 cm^{-1}, a peak representing a quite sensitive molecular moiety to the environment, could be resulted from the same mechanism as 735 cm^{-1} in Cu-form. However, the broad band at 1688 cm^{-1} in the spectrum has no obvious counterpart in the spectra of gaseous toluene or liquid toluene. It could not be an experimental artifact because this band was not found during the sorption of toluene on kaolinite clay mineral in the same experimental system (Cheng, 1999). With the appearance of a single band it is difficult to make any specific conclusion yet. Therefore, further study by other methods is needed.

Ringwald and Pemberton (2000) have studied the adsorption interactions of aromatics and heteroaromatics with hydrated and dehydrated silica surfaces by Raman (a counterpart spectroscopy to FTIR) and FTIR spectroscopies. They indicated that toluene vapor adsorption on silica occurred via weak π-system–hydrogen bonding with silanols on the silica surface. That hydrogen bonding which they mentioned could also happen in our system. Furthermore, Xiong and Maciel (1999) used deuterium NMR to study local motions of benzene adsorbed on Ca-montmorillonite. They concluded that absorbed benzene molecules could enter the interlayer space to form π-complexes with Ca^{2+} first at low temperature and undergo large-angle wobbling of the C6 axis and eventually desorbed from Ca^{2+} when the temperature increased. Consequently, the toluene molecules have opportunities to enter in and out of the clay interlayer. Combining the kinetics result, we proposed that some of the toluene molecules might be strongly trapped in the micropores or the interlayers of Ca-montmorillonite.

5.3.4 Desorption of Toluene on Clays

Comparison of the desorption FTIR spectra of toluene/Cu-montmorillonite to those of toluene/Ca-montmorillonite under anhydrous conditions is shown in Figure 5-7. According to these FTIR spectra of toluene/Cu-montmorillonite, there were

some original toluene peaks as well as some new peaks persistent on Cu-montmorillonite after a desorption time of sixty days.

After dry desorption period, the dry blue clay was purging with moisturized gas to check the humility effect of this organo-clay complex. The color of the dry toluene/Cu-montmorillonite film changed to green color form the original blue after moisturized by the purging gas. Doner and Mortland (1969) and Pinnavaia et al. (1974) indicated that partial dehydration of the Cu-montmorillonite prior to exposure to benzene vapor resulted in the formation of a green surface complex designated as the Type I complex. And the red Type II complex is produced when benzene sorption onto strongly dehydrated Cu-montmorillonite. Moreover, Johnston et al. (1992) observed that the color of the dry p-xylene/Cu-montmorillonite complex turned from dark orange-brown to light orange. The different colors indicate different clay-organic complexes.

There were not many similar unknown peaks observed in the spectra of toluene sorbed on Cu- and Ca-montmorillonites. Furthermore, the color of Ca-montmorillonite during all experiments was not changed. For Cu-montmorillonite, the chemisorption of toluene could be a result of a single electron transfer (SET) reaction which is similar to that of the chemical sorption of benzene/Cu-montmorillonite pair (Doner and Mortland, 1969 and Pinnavaia et al, 1974). And Johnston et al. (1992) have suggested the existence of the SET reaction between *p*-xylene and Cu-montmorillonite with the radical organic cations production from the spectra.

5.3.5 The Slow Desorption

For Ca-clay a desorption time approximately 1000 seconds (Figures 5-2 and 5-3) was needed for either dry or humid conditions. On the basis of this coincidence, we believe that the observed time is for the transfer process into or out of the micropores of these two montmorillonites under our experimental setting in which the mass-transfer limitation has been greatly reduced. However, it took approximately 20 days after the initial desorption of Cu-form under dry conditions to reach the stable absorbance intensity (Figure 5-4). The extended time is needed due to the chemisorption under anhydrous conditions. It is in agreement with the chemisorption in anhydrous conditions discussed above.

The irreversible sorption of toluene on montmorillonite has also been observed

by using the gravimetric method (Morrissey and Grismer, 1999). The authors of that paper indicated that the sorption processes were not instantaneously completed because the sorbate has to reach the sorbent by diffusion through a long distance. Hundal et al. (2001) have studied the sorption of phenanthrene by reference smectites and indicated that sorption of this aromatic compound by smectites was a physical phenomenon. They also concluded that the capillary condensation into a network of nano- or micropores created by quasicrystals was likely to be a dominant mechanism of this aromatic retention by smectites. Several researches (Luthy et al., 1997; Aochi and Farmer, 1995; Aochi et al., 1992; Sawhney and Gent, 1990) have shown that the existence of the network of narrow pores in clay minerals limited the rates of both sorption and desorption for organic species.

The adsorption and desorption FTIR spectra show the sorption mechanisms and the persistent fraction under dry conditions. Morrissey and Grismer (1999) observed larger residual amount, 30%, than ours only after several hours instead of sixty days under air-dried conditions. However, there was not any residual peak on the FTIR spectra observed in this study under humid conditions after the short-term equilibrium. A long-term sorption/desorption experiment for organic contaminants on clays is needed to illustrate the possible effect of aging.

Table 5-1. The equilibrium absorbance intensity of toluene sorbed on clays

	Ca-montmorillonite	Cu-montmorillonite
Dry conditions	0.39	1.27
	0.34	1.33
Humid conditions	0.28	0.24
	0.29	0.34

Table 5-2. The pseudo first-order rate constants (min^{-1})

	Sorption	Desorption
Ca-montmorillonite in dry conditions	2.94	0.534
	4.50	0.612
Ca-montmorillonite in humid conditions	2.50	0.204
	2.81	0.216
Cu-montmorillonite in dry conditions	1.85	0.096
	1.78	0.090
Cu-montmorillonite in humid conditions	2.90	1.90
	2.12	2.42

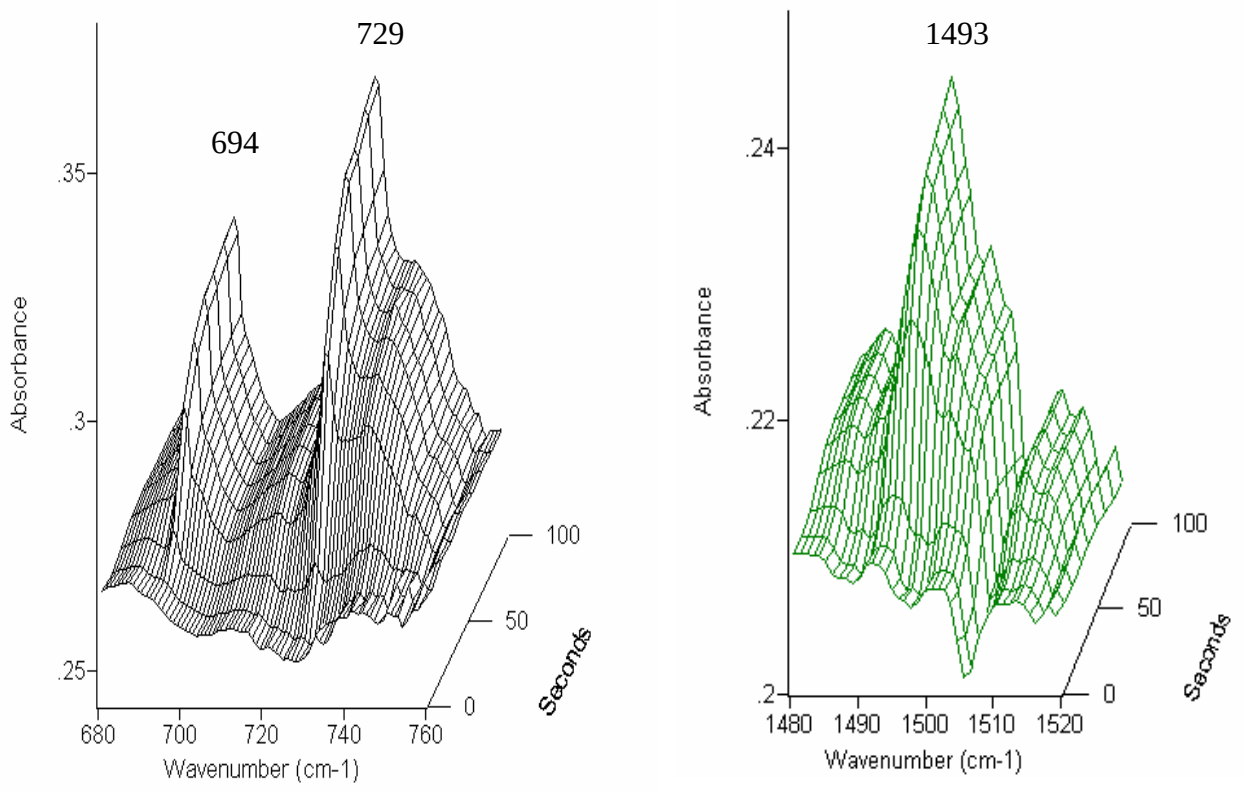

Figure 5-1. The change of FTIR intensity of Ca-montmorillonite exposed to toluene vapor.

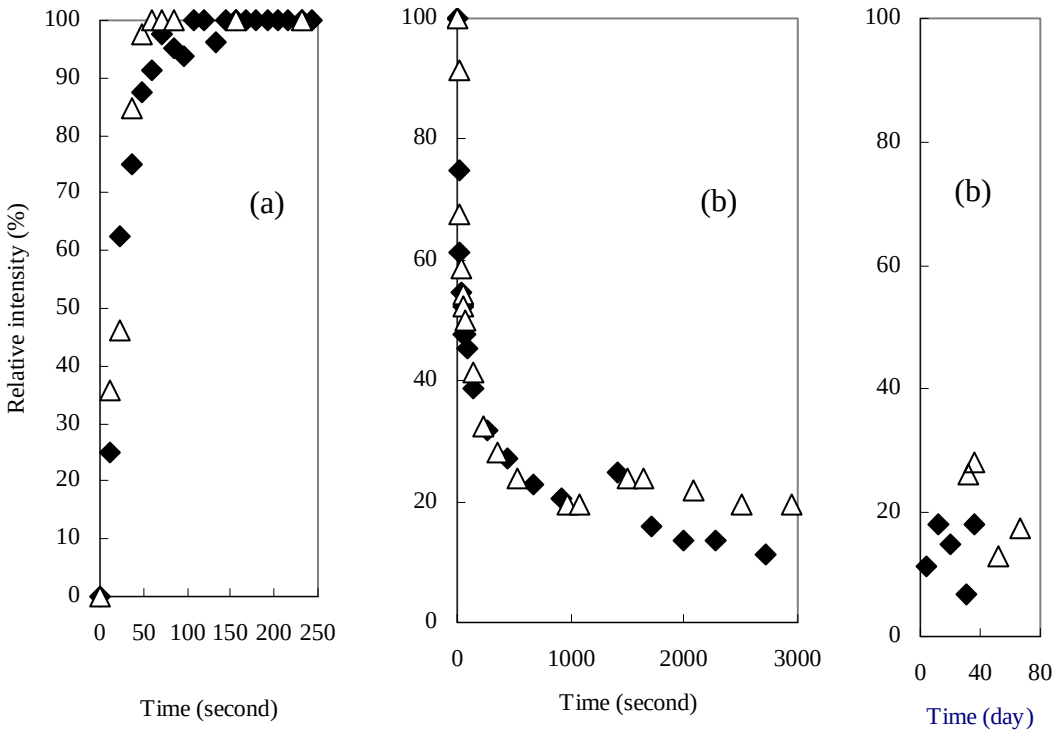

Figure 5-2. The experimental relative absorbance intensity of sorption (a) and desorption (b) of toluene on Ca-montmorillonite at 694cm^{-1} under dry conditions by FT-IR spectrophotometry.

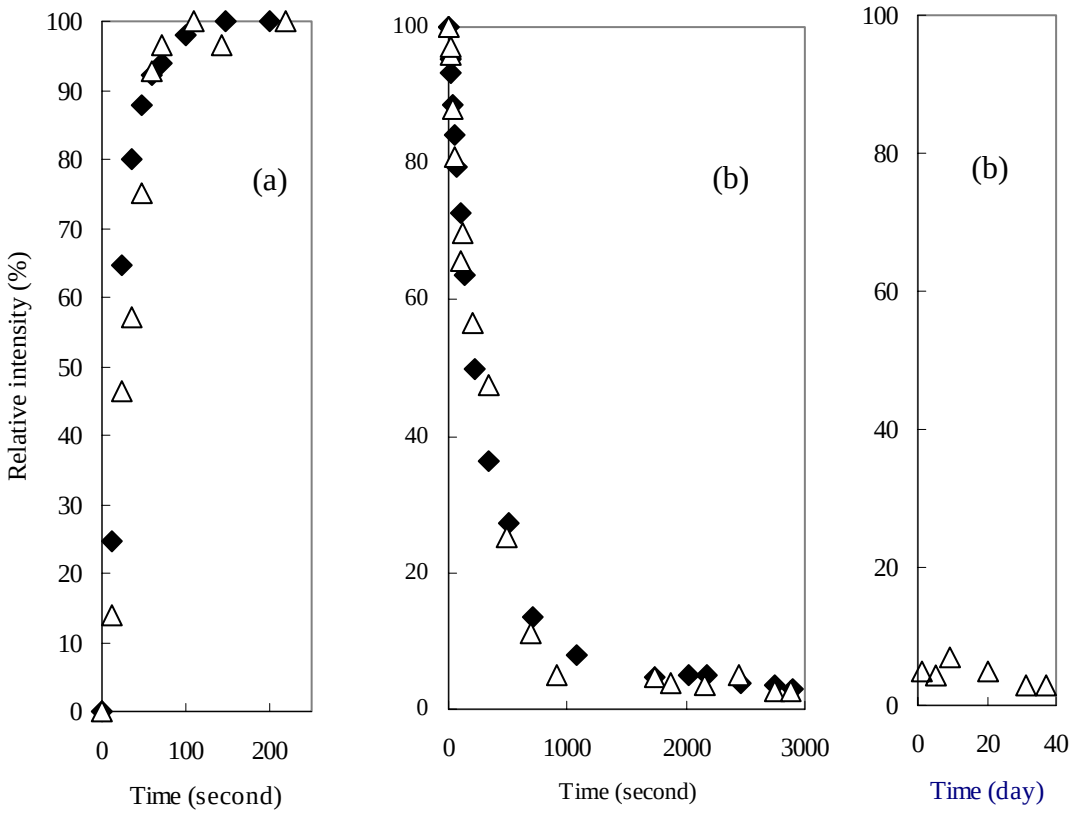

Figure 5-3. The experimental relative absorbance intensity of sorption (a) and desorption (b) of toluene on Ca-montmorillonite at 694cm^{-1} under humid conditions by FT-IR spectrophotometry.

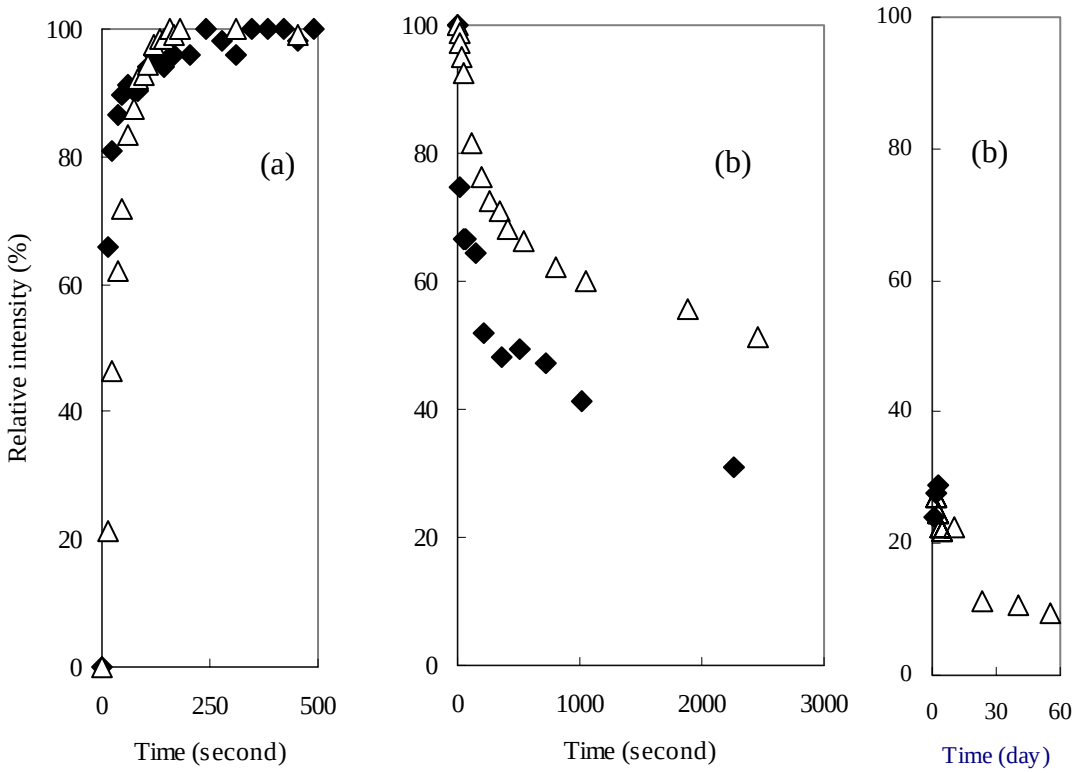

Figure 5-4. The experimental relative absorbance intensity of sorption (a) and desorption (b) of toluene on Cu-montmorillonite at 694cm^{-1} under dry conditions by FT-IR spectrophotometry.

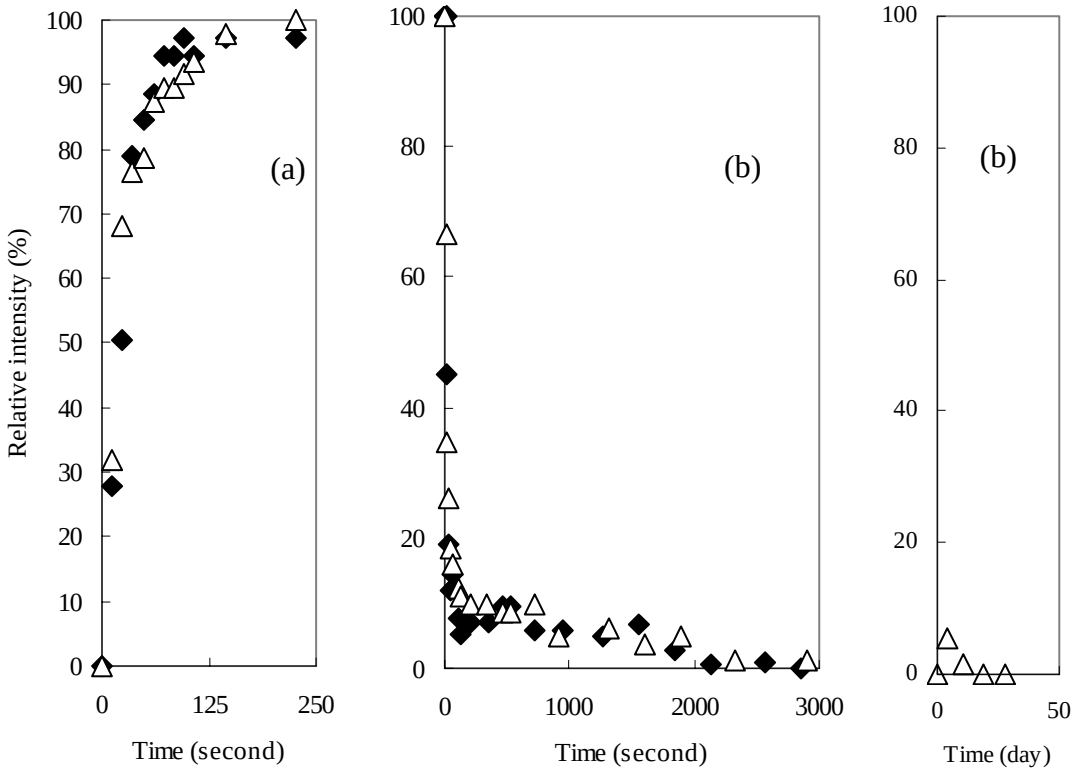

Figure 5-5. The experimental relative absorbance intensity of sorption (a) and desorption (b) of toluene on Cu-montmorillonite at 694cm^{-1} under humid conditions by FT-IR spectrophotometry.

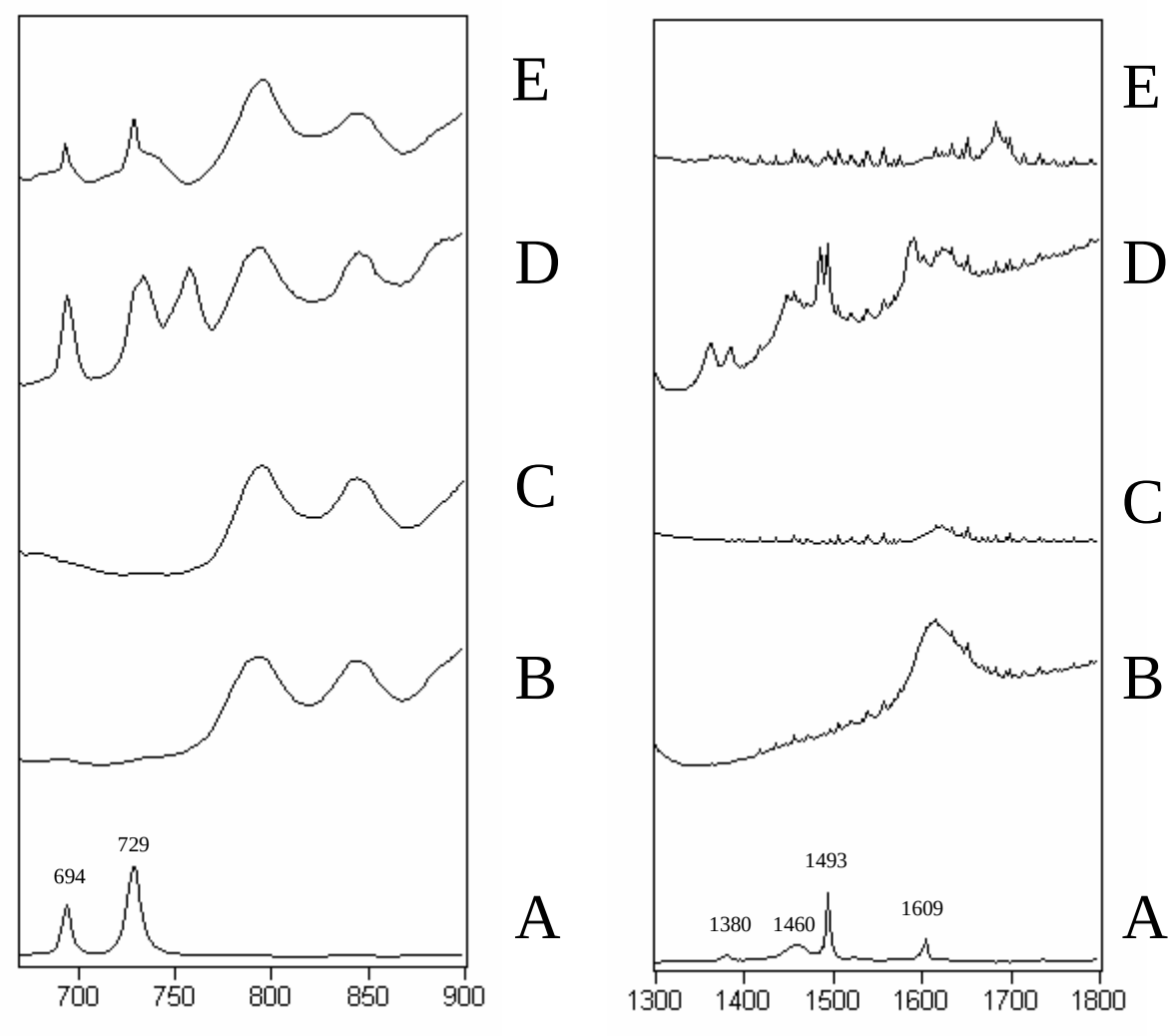

Figure 5-6. The sorption FTIR spectra of toluene on Ca-montmorillonite (E) and on Cu-montmorillonite (D) after reaching sorption equilibrium. (C) denotes pure Ca-montmorillonite, (B) denotes pure Cu-montmorillonite, and (A) denotes pure gaseous toluene.

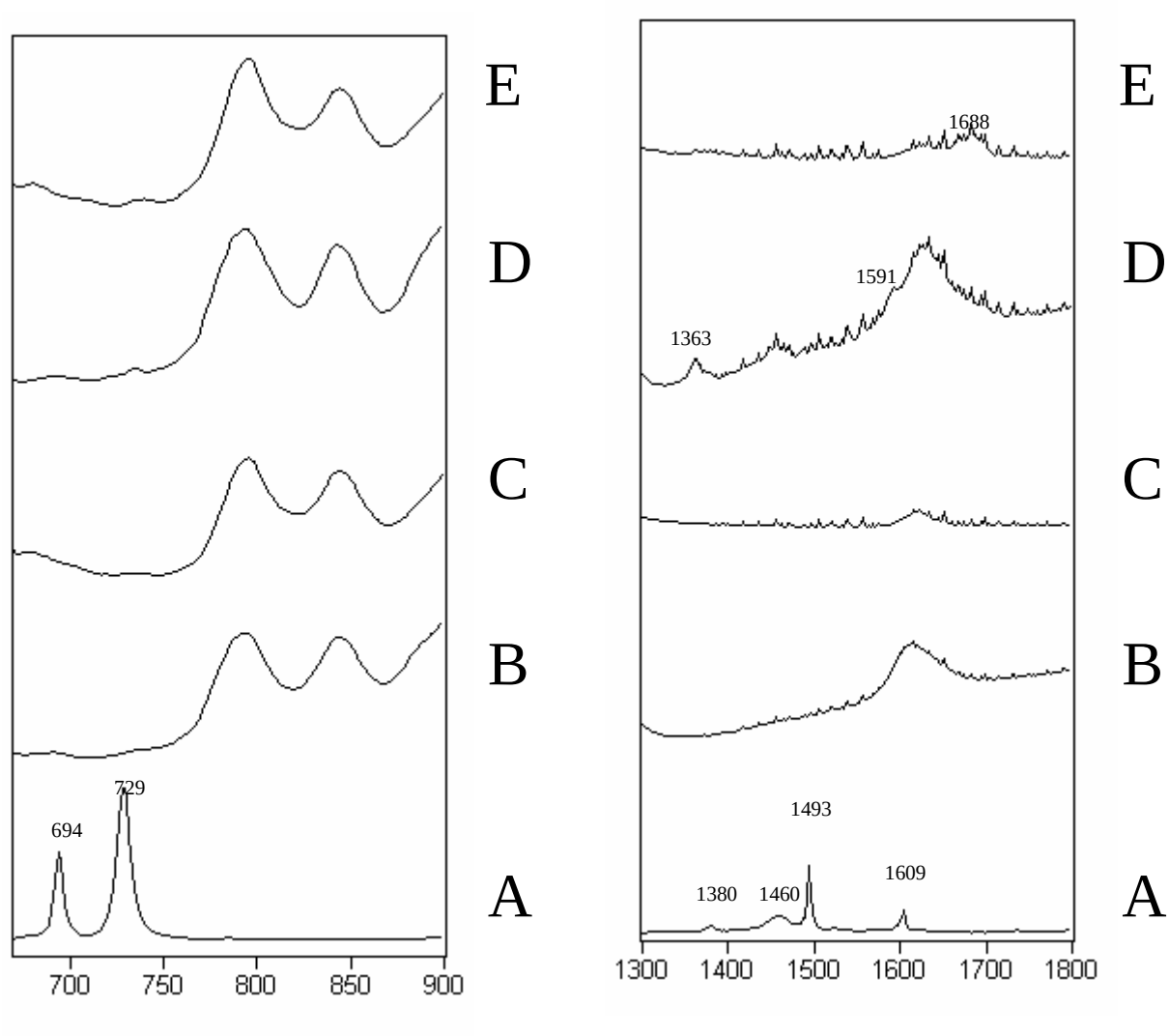

Figure 5-7. The desorption FTIR spectra of toluene on Ca-montmorillonite (E) and on Cu-montmorillonite (D) after sixty days. (C) denotes pure Ca-montmorillonite, (B) denotes pure Cu-montmorillonite, and (A) denotes pure gaseous toluene.

Chapter 6 Sorption of Trichloroethylene in Soil Compartments

6.1 Introduction

The fate of organic contaminants in soils is directly affected by sorption interactions with soil compartments. The sorption rate limitations can influence contaminant transport in the vadose zone and may potentially hinder remediation efforts. The mechanisms responsible for slow sorption processes have been investigated by the complexities and heterogeneities of natural systems. Studies have implicated restricted diffusion through soil organic matter (SOM) and micropores as responsible for the slow release of sorbed contaminants (Luthy et al., 1997). For better understanding and prediction of organic chemical fate and transport, sorption and desorption rates of both soil compartments are required.

Humin represents a highly stable, recalcitrant, and high-molecular-weight fraction of SOM, it may behave differently than the humic acid in the kinetics of sorption. Due to its cross-linked structure, humin may be capable of retaining volatile organic compounds (VOCs) for a significantly longer time and thus contribute to the slow or apparent irreversible sorption.

It has been suggested that halogenated VOCs may be strongly associated with clay minerals by condensation in micropores (Farrell and Reinhard, 1994) or being trapped in inter-layer space (Keyes and Silcox, 1994) and result in irreversible sorption in soils. Furthermore, clay minerals offer a gigantic surface area for adsorption as well as surface-catalyzed reactions that we should not overlook. Achoi and Farmer (1995) and Chang et al. (2003) have observed the resistant fraction of 1,2-dicholoroethane and toluene, respectively, on clays. It seems that the relative importance of the roles of soil organic matter and soil minerals on the sorption vary with the type of pollutants and the composition of the soils. This study was conducted on the sorption of trichloroethylene (TCE) on both humic substances, including humic acid and humin, and clay minerals, Ca- and Cu- exchanged montmorillonites.

Shortcomings of batch and column systems to measure sorption kinetics were

inadequate resolution for early time sorption or desorption and difficulty of measuring very low rates of uptake or release, respectively. Both of these two experimental methods, the gravimetric and spectroscopic methods, used in this study allowed continuous measurement with high sensitivity. The gravimetric method with a microbalance has been used to trace the time courses of sorption of VOCs in soil organic matters (Chang et al., 1997; Shih and Wu, 2002ab). Molecular-level environmental observation is needed to provide information about the possible chemical transformation of the compounds. The thin film/FTIR method was developed (Chang et al, 2003, Shih and Wu, 2004) to investigate the sorption kinetics of VOCs on soil compartments.

In this study, TCE, a nonpolar, halogenated hydrocarbon, was used as the sorbate to delineate the sorption behavior of VOCs with SOM. SOM disks were prepared and used to study the rate of transport of TCE in SOM matrix with artificially exaggerated mass transfer distance via a microbalance. Thin SOM films were also used to mimic natural SOM in a near-natural soil environment. On the other hand, thin film/FTIR method was used to illustrate the sorption and desorption kinetics of TCE on clay films, to clarify whether a strong interaction exists between TCE and clays, and to identify the molecular-level mechanism which may contribute to the irreversibility of TCE sorption under dry and humid conditions.

6.2 Materials and Methods

Gravimetric method

Humin is obtained by digestion of Shamaoshan-like soil in Taiwan with a mixture of concentrated HF and HCl to remove inorganic minerals in our previous study (Shih and Wu, 2002a). Humic acid powder was purchased from Aldrich Chemical Co. These two SOM powder were pressed into thin disk in 12.45mm diameter under a pressure of 12.7N/m^2 for 1 min. The disks were oven-dried (105^oC) overnight and stored in a dessicator before use.

The gravimetric experimental apparatus and procedure for SOM disks used for sorption have been described in detail elsewhere (Shih and Wu, 2002a). Briefly, the disk was hung on the platinum stirrup on the weighing arm of an electric microbalance (Cahn 200). After a constant weight of the disk was reached via purging with

hydrogen-free nitrogen gas, a steady flow of gas (50mL/min) containing TCE vapor was introduced into the glass chamber. The disk was exposed to the TCE gas flowing through. The concentration of TCE was determined by a gas chromatography equipped with a flame ionization detector (Hewlett-Packard 5890II).

The diffusion model and its incorporation into the gravimetric method have been described in our previous studies (Shih and Wu, 2002a). By using the diffusion model, diffusivity can be determined from the uptake or loss of the film during sorption or desorption.

Thin film/fourier transform infrared method

Montmorillonite was obtained from the Source Clay Mineral Repository of the Clay Mineral Society. The clay was treated with 35% hydrogen peroxide and the fraction with particle sizes smaller than 2 μm was collected by the sedimentation method. The Ca(II) and Cu(II) exchanged forms were prepared by treating the clay (< 2 μm) with 1.0 N solutions of $CaCl_2$ or $CuCl_2$, respectively, then centrifuging, and removing the supernatant liquid. The procedure was repeated three times to maximize the exchange of the original cations (mainly sodium). Excess $CaCl_2$ and $CuCl_2$, respectively, were removed by washing with deionized water until the test for chloride by $AgNO_3$ was negative (Pinnavaia and Mortland, 1971). A drop of the clay suspension was placed on the inner surface of a ZnSe window of a gas cell.

The experimental apparatus was shown and presented in details by Chang et al (2003) and Shih and Wu (2004). In short, the gas cell had a 5 mm thickness and a 30 mm diameter with two ZnSe windows. The sample cell was purged with nitrogen gas (50 mL/min) carrying TCE vapor and humidity (RH below 1% for dry conditions and above 95% for humid conditions) during sorption experiments and without TCE during desorption experiments. The absorbance spectra of IR beam passing through the gas cell windows were obtained on an BIO-Rad FTS 40 spectrometer at 2 cm^{-1} resolutions by averaging 16 scans for a short-term kinetics study.

6.3 Results and Discussion

Sorption of TCE in Humic Acid

The sorption and desorption experiments of TCE with humic acid were performed in a microbalance and the results were shown in Fig 6-1. The weight of the humic acid disk is 62.5 mg and its thickness is 0.51mm. The partial pressure of TCE is 0.028± 0.00068. There was a two-stage sorption process observed (Fig. 6-1). A first sorption stage with a relatively small sorption capacity during the first 2.5 h is followed by a second sorption stage with a much higher capacity lasting for several hours. Similar two-stage results have been reported for the sorption of VOCs in humic acid via Chang et al. (1997) and for the sorption of organic compounds in polymers (Kishimoto and Matsumoto, 1964).

The calculated apparent diffusivities of TCE in a humic acid disk are 2.0×10^{-8} cm^2/sec for sorption and 4.0×10^{-9} cm^2/sec for desorption, respectively. The values are on the same order of the diffusivity of TCE in humic and fulvic acid layers on soils (Piatt and Brusseau 1998) but lower than the diffusivity of the compound in water by a factor of 1000.

The organic coating thickness on soils was around 20 μm (Piatt and Brusseau, 1998). According to this length scale and the diffusivity, the time scale which toluene molecules need to penetrate humic acid matrix will be only a few minutes.

Sorption of TCE in Humin

The weight of the humin disk is 51.8 mg and thickness is 0.29mm. The partial pressure of TCE is 0.032± 0.0017. Due to lack of repeating experimental result, we can not conclude that the sorption of TCE in humin is a two-stage sorption (Fig. 6-2). Two-stage of pattern was not observed in other VOCs sorption experiments either (Shih and Wu, 2002b). The apparent diffusivities of TCE in this humin disk are around 8.0×10^{-9} cm^2/sec for sorption and 5.0×10^{-9} cm^2/sec for desorption, respectively, for the final sorption stages.

We did not find any persistent factions of TCE by microbalance. The sorption of aromatic compound in humic acid and humin extracted from this soil are reversible (Chang et al., 1997; and Shih and Wu, 2002ab). The sorption of TCE to humic acid and

humin, similar to the sorption on toluene which we observed, is found to be reversible and diffusion-controlled.

The sorption of TCE in humic acid and humin shows no irreversible fraction. The interaction between TCE and humic acid or humin will not be a cause of the sequestration of TCE in soils when a remediation technology based on vapor extraction is applied.

Kinetics Study of Short-term TCE Sorption and Desorption in Ca- and Cu-Montmorillonites by FTIR Spectroscopy

The FTIR spectra of Ca- and Cu- montmorillonites exposed to TCE vapor for 15 minutes under dry conditions and wet conditions are shown in Figures 6-3 and 6-4, respectively. The vibrational bands of C-Cl stretching of TCE at 782, 850, 934, 944cm^{-1} appeared in 600~1000 cm^{-1} region under wet and dry conditions. For Ca- or Cu-montmorillonites being exposed to TCE for a short time, there is no obviously new peak persistent on these two clay minerals after desorption.

In this thin film/FTIR experimental system, the width of the cell's inner space is approximately 5 mm. The time scale of diffusion through the boundary layer is around 3 seconds. This system is clearly not boundary-layer-limited, and the sorption kinetics is controlled by the intrinsic sorption rate of the clay particles. According to the growing and decaying area of the intensity at wavenumber 850 cm^{-1}, the sorption and desorption kinetics of TCE on Ca- and Cu- montmorillonites are shown in Fig. 6-5.

It took about 100 seconds for Ca-montmorillonite to reach equilibrium under the dry condition (Fig. 6-5a). The difference between the two duplicated experiments might result from the slight difference of clay thickness. The desorption rate seems similar to the sorption rate. The sorption and desorption kinetics of humidified TCE vapor on Ca-montmorillonite show similar patterns (Fig. 6-5b). Furthermore, there is no significant difference observed in sorption and desorption kinetics no matter dry or wet systems. Most of the sorbed TCE could be desorbed completely from Ca-montmorillonite.

Figures 6-5c and 6-5d show the amount of the sorbate on Cu-montmorillonite varying over time during the experiments under dry and humid conditions, respectively. It took about 100 seconds for TCE on Cu-montmorillonite to reach equilibrium under the dry condition. (During the desorption process, a residual fraction, approximately 10%

of total, which was resistant against desorption, was observed within only 15 minutes of desorption. Under humid condition, it also took about 100 seconds to reach equilibrium (Fig. 6-5d). The rate of desorption in the humid condition is similar to that of the sorption. There seems to be no residual of TCE found in both duplicated experiments in the humid condition.

Scinece there are observations of persistency of halogenated chemicals on clays (Aochi ad Farmer, 1995) and chemical transformation of aromatic chemicals on clays (Chang et al, 2003; Pinnanovia and Mortland, 1971; Doner and Mortland, 1969), a long-term sorption experiment of halogenated VOCs on clays is needed to illustrate the possible effect of aging in the future.

6.4 Conclusion

Two experimental approaches, the microbalance method and the thin film/FTIR method, are used to investigate the sorption kinetics under two different levels of humidity. Sorption/desorption kinetics of TCE and soil components, humic acid, humin and montmorillonite, were performed. The apparent diffusivities of VOCs in a humic acid and humin disk are around 10^{-8} cm^2/sec. The time scale of TCE diffusion into soil humic substances could be only a few minutes. The intrinsic sorption and desorption of TCE on two types of cation exchanged montmorillonites just took a few minutes in either low or high levels of humidity. Most of the sorbed TCE seems removed from soil components in these gas purge systems, the microbalance and thin/film FTIR, in short-term sorption experiments. The sorption of TCE in these two humic substances and montmorillonite shows no irreversible fraction. The interactions between TCE and these two soil components could not be a possible cause of the sequestration of TCE in soils. The mass transfer of contaminants into soil plays the important role on the slow sorption/desorption in soils.

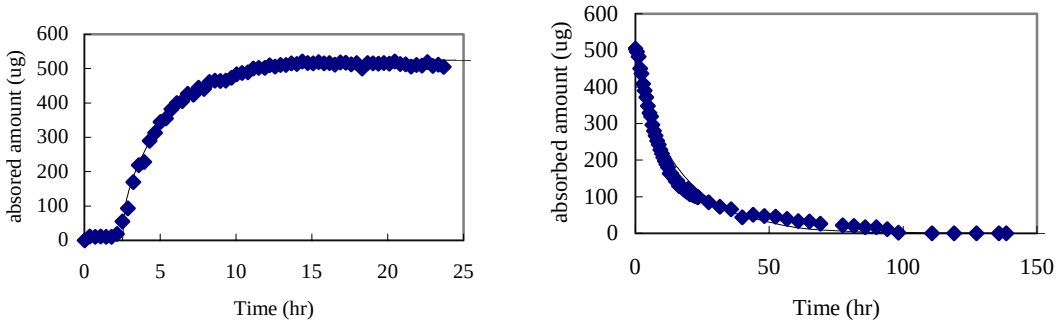

Figure 6-1. The experimental and simulation results of TCE sorption (left) and desorption (right) in a humic acid disk.

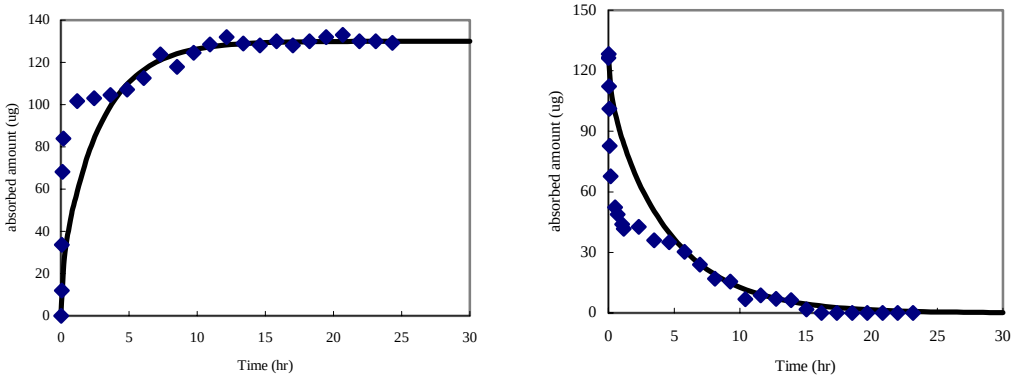

Figure 6-2. The experimental and simulation results of TCE sorption (left) and desorption (right) in a humin disk.

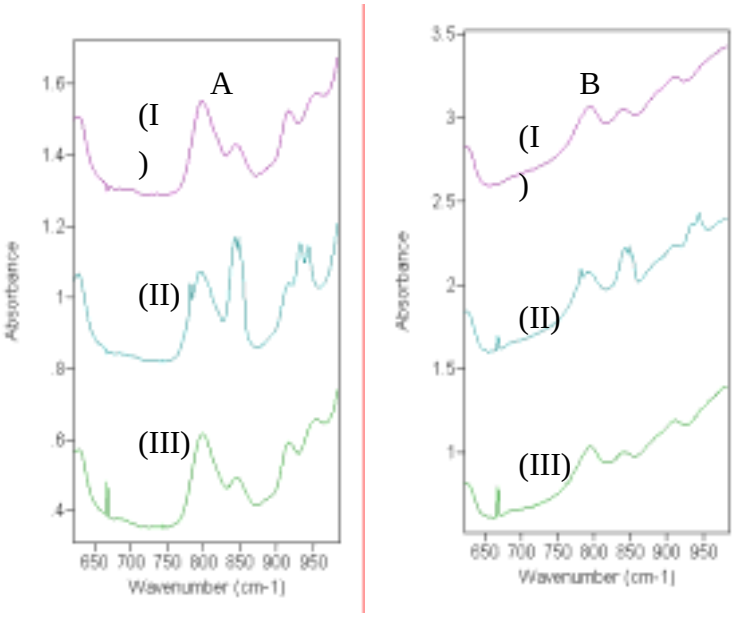

Figure 6-3. The FTIR spectra of tricholoethene on Ca-montmorillonite (A) and Cu-montmorillonite (B) under a dry condition. (I) denotes desorption after sorption of tricholoethene from a montmorillonite for 15minutes, (II) denotes sorption of tricholoethene on montmorillonite for 15 minutes, (III) denotes a pure montmorillonite.

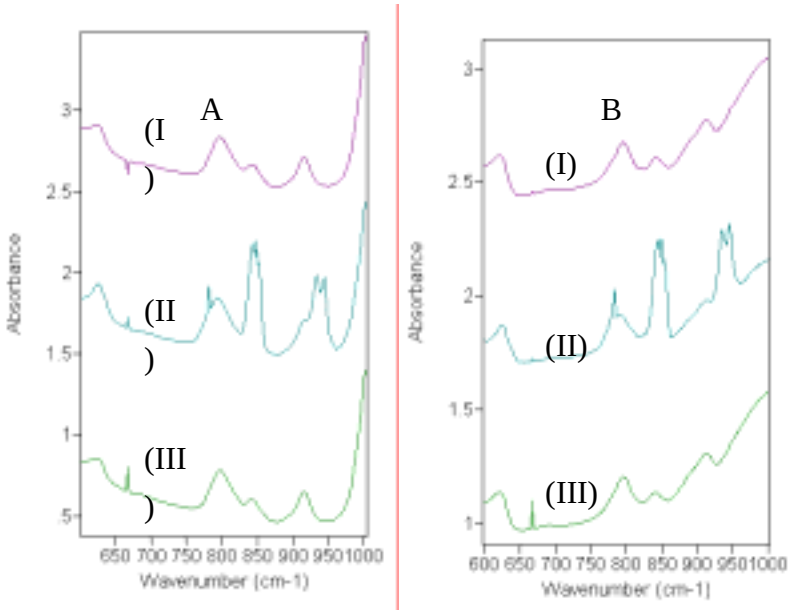

Figure 6-4. The sorption FTIR spectra of tricholoethene on Ca-montmorillonite (A), Cu-montmorillonite (B) under a wet condition. (I) denotes desorption after sorption of tricholoethene from montmorillonite for 15 minutes, (II) denotes sorption of

tricholoethene on a montmorillonite for 15 minutes, (III) denotes a pure montmorillonite.

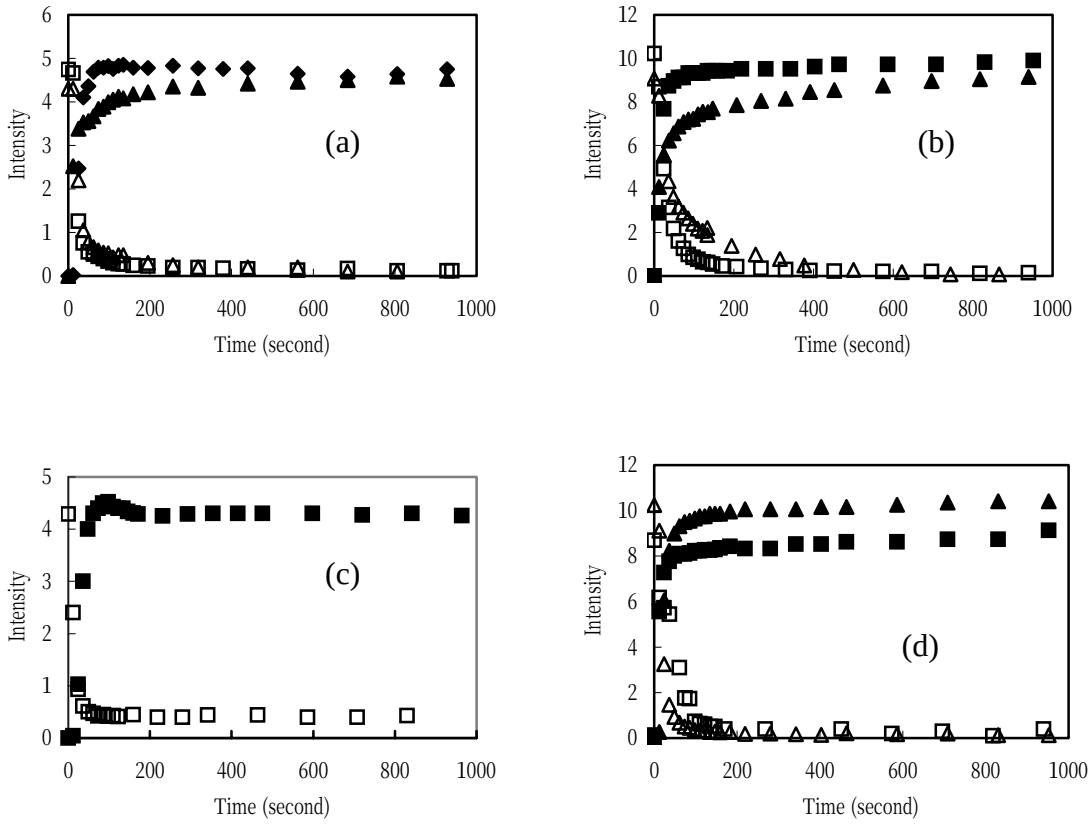

Figure 6-5. The relative absorbance intensity of sorbed TCE on Ca-montmorillonite under a dry condition (a) and a wet condition (b), and on Cu-montmorillonite under a dry condition (c) and a wet condition (d).

Chapter 7 The Influence of the Speciation of Soil Carbonaceous materials on the Sorption of Hydrophobic Organic Compounds (I)-Quantifying and Characterizing Black Carbon in Soil Samples

Shian-chee Wu, Phil Gschwend, John MacFarlene, AmyMarie Accardi-Dey and Yang-hsin Shih

Note: The document is prepared as a record of the research while Prof. Shian-chee Wu was visiting Massachusetts Institute of Technology in 2002. The material in this document has not been reviewed and is not to be sited or referred.

7.1. Introduction

Black carbons (BC), such as soot from the condensation of gaseous carbon and chars from pyrolyses of organic matters, have been found in the natural sediments in significant amount (Gustafsson, 1997; Middelburg, 1999). These carbon species have distinct properties such as rigid molecular structure, high surface area, high sorbing capacity, high chemical, thermal and biological resistance. Their roles on affecting the fate and bioavailability have been discussed recently (Gustafsson, *et al.*, 1997).

Since BC may exist in soil as well, the sources, distribution and the characteristics of BC in soils are of interest. Common soil organic materials include labile (highly biodegradable) organic compounds and biologically stable humic substances. During the isolation of humic substances BC may be left in the resistant fraction of the organic materials and defined as part of the humin. Overlooking the existing of BC in soils may cause underestimation of the quantity of carbon or the sorption capacity for pollutants in soils

The speciation of these resistant organic materials and their sorbing behavior should be identified and tested in order to refine the overall sorption model for soils. On the other hand, the existence of biologically resistant elemental carbon in the soils may become a significant reservoir in the global cycle of carbon.

Therefore, the purposes of this study are

A. to develop an analytical method to identify and to characterizing the carbon species in soils,

B. to investigate the speciation of pyrogenic black carbon in some soil samples qualitatively and quantitatively,

C. to study the sorbing behavior of these carbon species toward hydrophobic organic compounds in water in equilibrium or dynamically.

7.2. Background

Environmental carbonaceous matters (ECMs) can be envisioned as mixtures of many organic and carbonaceous molecules with different molecular weights and chemical structures. Each constituent of ECMs may have its own biological, chemical and heat resisting characteristics, and sorbing behavior toward hydrophobic organic compounds (see Figure 7.1 as a hypothetical example).

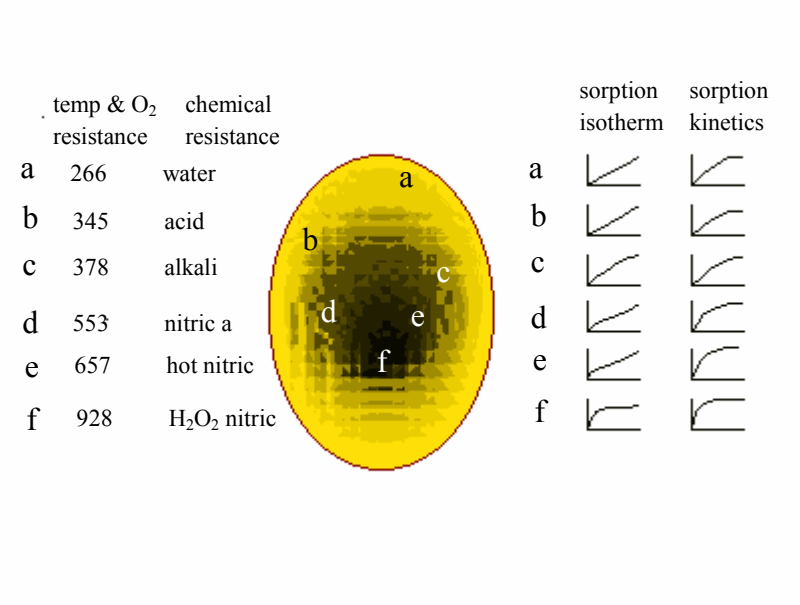

Figure 7.1. A hypothetical example showing the heterogeneity of environmental carbonecious matters in terms of the resistance to heat, the resistance to chemical extractants, sorption isotherm and sorption kinetics. a, b, c, d and e are locations where one carbonecious molecule is sampled and tested.

In the past, ECMs were categorized by operational definitions that were the result of the development of specific separation methods. For example, humic acid is defined as natural organic matter that is soluble in alkali but not in acid during

chemical extraction procedures (Nelson and Sommers, 1982). Using a thermo-oxidation approach, organic carbon (or labile organic matter) is defined as any carbon species (other than the inorganic carbonates) that can be oxidized by heat and oxygen below the temperature of 375 C. Carbon species resistant to oxidation below the temperature of 375 C is defined as black carbon (Figure 7.2).

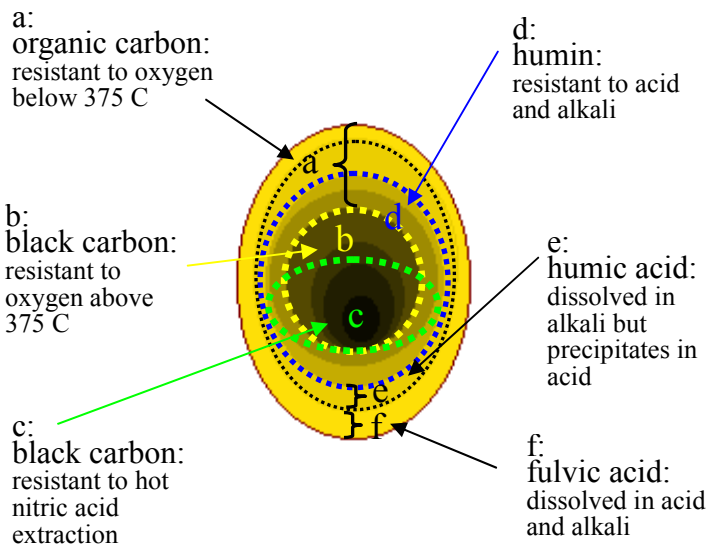

Figure 7.2. Operational definitions of the constituents of ECMs.

These kinds of operational definitions help us to characterize and weigh the ECMs in terms of their contribution to the sorption of hydrophobic organic compounds (HOCs). For a single HOC we may integrate the contribution to sorption of all constituents and obtain the overall sorption behavior. The overall sorption isotherm is

$$q(C) = \Sigma\, f_i \times q_i(C)$$

where $q(C)$ is the overall sorbed concentration of the HOC on sorbent, a function of solute concentration, C; $q_i(C)$ is the concentration of HOC in ith constituent; also functions of concentration, f_i is the weight fraction of ith constituent. Gustafsson et al. (1997) had develop a dual sorption model to describe the sorption isotherm of an environmental sample containing both organic carbon and black carbon. Also, before complete equilibration has been reached, the change of sorbed concentration

with time is

$$d\,q(C)/dt = \Sigma\, f_i \times d\,q_i(C)/dt$$

in which *t* denotes the time.

The thermo-oxidation method has been shown to be a consistent method for removing organic carbon and for quantifying BCs in some specific refractory regions if caution has been taken to avoid the interference from charring of organic carbon (Kuhlbusch, 1995; Currie *et al.*, in press). In addition, BCs from different sources exhibited variations in their rates of disappearance (as shown in thermograms) during temperature-programmed oxidation. This method combined with the detection of the carbon dioxide emission can be used to further differentiate and quantify the composition of BC and may reveal the origin of the BC by comparison to the thermograms of known BC reference materials.

With sufficient information of the thermo-oxidation patterns of BCs, for instance, those of diesel soots, charcoal, graphite and coal, we may establish definitions of BC species based on the operational procedures of thermo-oxidation treatment (Figure 7.3). The more detailed categorizing of BCs will better help us to trace back the sources of the BCs in the soil samples and to predict the overall sorption isotherm and the sorption kinetic behavior of the soil samples.

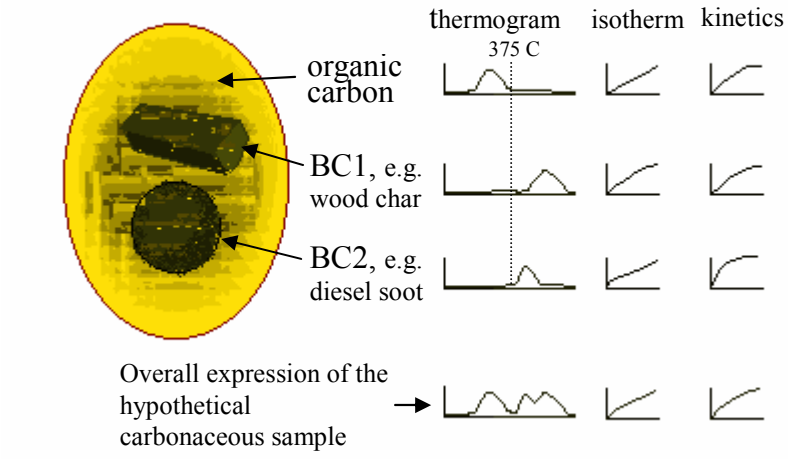

Figure 7.3. A hypothetical model showing the operational definitions match the sources of the ECMs.

7.3. Method development

7. 3.1. Pretreatment of samples

There are a number of methods in the literature used for determining elemental carbon species, which can be classified in three categories: optical, thermal and chemical oxidation methods (Table 7.1). The efficiency of pretreatment procedures in removing organic carbon other than BC defines the BC species. The most commonly used thermal method involves preheating the sample at a medium temperature, 340 C to 375 C varying by methods, and measuring the residual carbon by total elemental analysis. Higher temperatures were used in some methods in conjunction with an oxygen-free pretreatment environment. Stepwise increasing temperature programs were also used which was able to characterize the speciation of element carbon.

Table 7.1 Methods for defining/isolating/quantifying black carbon (BC)

Author(s)	Reference	Methods	Sample source	classification	BC/TOC
Reddy, et al.	ES&T in press	Thermal oxidation: 375 C for 24 h and acidification for removal labile carbon and measuring CO_2 after 850 C 5 h for residue.	1. organics in marine sediment (srm1941A) 2. New York/New Jersey Waterway sediment (srm1944) 3. Urban dust (SRM1649a) (14.0 mg/g) (8% of TOC) 4. Complex mixture of PAHs from coal tar (srm1597)	thermal	1. 0.29 2. 0.18 3. 0.08
Hansin,et al., 1984, in Currie L. A. et al.	*NIST SRM 1649a, J. Res. Natl. Stand. Technol.* in press	**AETH** Optical, by using the EC attenuation	Urban dust (SRM1649a)	optical	0.069
Gustafsson et al., 1997, 2001, in Currie L. A. et al.	*J. Res. Natl. Stand. Technol.* in press	**T375** 24 h at 375 C in the presence of excess oxygen.	Urban dust (SRM1649a)	Thermal oxidation	0.077, 0.079, 0.187
Gustafsson et al., 1997,	ES&T, 1997, 31, 203-209	**T375** 24 h at 375 C in the presence of excess oxygen.	samples from many sources including Mystic Lake sediment and Boston Harbor.	Thermal oxidation	from <0.0001 to 0.95

Table 7.1 Methods for defining/isolating/quantifying black carbon (BC) (continue)

Author(s)	Reference	Methods	Sample source	classification	BC/TOC
Cachier at al., 1989, in Currie L. A. et al.	*J. Res. Natl. Stand. Technol.* In press	**T340** 2 h at 340 C	Urban dust (SRM1649a)	Thermal oxidation	0.346, 0.347
Gundel et al., 1984, in Currie L. A. et al.	*J. Res. Natl. Stand. Technol.* In press	**T500** 50 to 800 C, EC defined by highest temperature peak centered at ca. 500 C. Monitor w/ He-Ne laser for any pyrolytic carbon.	Urban dust (SRM1649a)	thermal-optical, evolved gas analysis	0.500
Birch and Cary, 1996, in Currie L. A. et al.	*J. Res. Natl. Stand. Technol.* In press	**TOT** 60 to 900 w/o oxygen, then cooled to 525 C and w/ 5% O2/He and stepwise to 900 C. Monitor w/ He-Ne laser for any pyrolytic carbon. **Significant potential for charring.**	Urban dust (SRM1649a)	thermal-optical transmission	0.200
Chow et al., 1993, in Currie L. A. et al.	*J. Res. Natl. Stand. Technol.* In press	**TOR** step temp (120, 250, 450,and 550 C) in He, the oxidation of EC in O2 (2% in He) with temp at 550, 700, 800 C. Monitor w/ He-Ne laser for any pyrolytic carbon	Urban dust (SRM1649a)	thermal-optical reflectance	0.432
Puxbaum, 1993, in Currie L. A. et al.	*J. Res. Natl. Stand. Technol.* In press	**TLT** Linear temp ramp of 20 C per minute up to 800 C in O2 (2% in He) with temp at 550, 700, 800 C. Monitor w/ He-Ne laser for any pyrolytic carbon.	Urban dust (SRM1649a)	Thermal optical w/ linear temperature program	0.438
Currie and Kessler, 1999, in Currie L. A. et al.	*J. Res. Natl. Stand. Technol.* In press	**TOK** 560 C isothermally w/ 5% O2/He. Monitor w/ He-Ne laser for loss of any pyrolytic carbon or loss of more labile EC.	Urban dust (SRM1649a)	Thermal kinetic □xidation/intercept	0.109
Currie et al., 2000a in Currie L. A. et al.	*J. Res. Natl. Stand. Technol.* In press	**Ch(N1)T** 1M NaOH twice, 70% HNO3 once, 1M NaOH thrice, 1% HCl once, water twice, and dry. Then 340 C for 2 h and 950 C w/ high purity O2.	Urban dust (SRM1649a)	HNO3-thermal oxidatin	0.224
Marolf, 1998; Slater, 1999, in Currie L. A. et al.	*J. Res. Natl. Stand. Technol.* In press	**Ch(N2)T** The same as i. Except the pretreatment steps with NaOH were omitted.	Urban dust (SRM1649a)	HNO3-thermal-chemical	0.280, 0.283
Klouda, 2001; Schultz, 1962, in Currie L. A. et al.	*J. Res. Natl. Stand. Technol.* In press	**Ch(N3)** Boiling 70% HNO3 for 20min. Then 6N HNO3 overnight. Final residue by combustion	Urban dust (SRM1649a)	Chemical oxidation, hot NO3	0.292

Table 7.1 Methods for defining/isolating/quantifying black carbon (BC) (continue)

Author(s)	Reference	Methods	Sample source	classification	BC/TOC
Masiello et al., 2001; Wolbach and Anders, 1989, in Currie L. A. et al.	*J. Res. Natl. Stand. Technol.* In press	**Ch(Cr)K** 1M Cr2O72- in 2M H2SO4 at 50C up to 406 h. Kinetic analysis of the oxidation process) shows two components (half lives: 0.85h and 1003 h)	Urban dust (SRM1649a)	Chemical oxidation, dichromate	0.458
Verardo, 1997, in Currie L. A. et al.	*J. Res. Natl. Stand. Technol.* In press	**Ch(N4)** Hot, concentrated HNO3, oven drying overnight at 60 C.	Urban dust (SRM1649a)	HNO3,	0.520
Middelburg, J. J. et al., 1999	Marine Cemistry, 65, 245-252, 1999	Thermally oxidation at 375C for 14 h (Gustafsson et al., 1997), or 10 times 30ul of concentratied nitric acid at 50 C (Verardo, 1997).	Marine sediments	Thermal oxidation or HNO3	SC(average of two methods)/OC ranges from 0.13 to 0.61
Birch, M.E.	analyst, May 1998, 123, 851-857	甲、 1. In He 250C 1 min, 500C 1 min, 650C 1 min, 850C 1.5 min, reduce to 650C switch to oxygen mode. 乙、 2. In He 120C 4.5 min, 250C 3.5 min, 450C 4-5 min, 550C 8-10 min, switch to oxygen mode. 丙、 3. In N2: 800C 10 min 丁、 4. In N2: 200C 2 min, 400C 4 min, 560C 6 min (or until stable) 戊、 5. In N2: 200C 2 min, 400C 2 min, 550C 4 min	Urban aerosol and others	Thermal-optical	1. coulometric method, 7.92, fraction, 0.619 2. thermal methods: 1.80-3.00, fraction, 0.14 (method 1), 0.18 (method 3), 0.234 (method 2)
Kuhlbusch, T. A	Environ. Sci. Technol., 29, 2695-2702, 1995.	1. solvent extraction: NaOH (1M), 70% HNO3, 1M NaOH,1 % HCl, twice-distilled water 2. Thermotreatment: 340C ±3C in pure O2 (500ml/min) for 2 h 己、 3. 950C for total C	Residues of vegetation fires	Thermo with pretreatment	0.01-0.36

Table 7.1 Methods for defining/isolating/quantifying black carbon (BC) (continue)

Author(s)	Reference	Methods	Sample source	classification	BC/TOC
Muhlbaier, J. L. and Williams, R. L.	in Particulate Carbon: Atmospheric Life Cycles, Ed: G. T. Wolff and R. L. Klimisch, Plenum Press, NY, 185-198, 1982.	3. Thermotreatment: 350C in air 3. 650C for total C	Particulate carbon from fireplaces, furnaces and vehicles as emission sources	thermo	0.07-0.79

Charring of organic carbon has been shown to occur when determining the BC in the residues of burnt vegetations (Kuhlbusch, 1995). Accardi-Dey (2002, unpublished data) had shown that samples containing protein produced char.

In a preliminary test of the thermo-oxidation method used during this study, some problems occurred while using sodium citrate as an organic carbon reference material in the presence of sufficient oxygen. First, the sample was partially pyrolyzed during heating, which was evidenced by the smell at the vent. This will result in an error by reducing the detected CO_2 concentration and also will likely contaminate the detector system. A post-combustion furnace with a temperature set at about 650 C may be necessary to convert incompletely combusted organic vapor into CO_2 (refer to Kuhlbusch, 1995)

Second, significant amount of black carbon (averagely 31.8% of the original carbon in the samples for two repeated experiments) was formed after the samples had been heated up to 650 C. Another test resulted in sodium citrate crystals with a size of 0.5mm being converted into water, carbon dioxide and grains of char by heating under 375 C for 24 hours with oxygen present.

A similar treatment, but with temperature from 25 C to 925 C, showed sodium citrate crystals were only partially degraded under temperature below 520 C and converted to some highly thermo-resistant carbon which became CO_2 at temperature over 750 C. However, no char was found after grinding the sodium crystals into a powder and mixed with carbon-free sediment before heating (Accardi-Dey, 2002, unpublished data).

Pretreatment with chemical extraction, for example, concentrated HNO_3

extraction combined with thermal methods, could remove most of the labile carbon and significantly avoid charring of organic carbon (Kuhlbusch, 1995). However, losing BC during the treatment is possible and is of concern.

In the following experiments the pretreatment procedure will include reducing the grain size of the sample and oxidizing under 375C for 24 hours. When a temperature program is used for characterization of the BCs (see the next section) the pretreatment will be part of the heating program.

7.3.2. Characterizing of BC

To characterize the BC speciation Kuhlbush (1995) has been using an IR-oven with temperature programs from 100 C to 1000 C at 100C/min. A similar experimental setup is adopted in this study to characterize the BC in soil samples, which include a tube furnace with a temperature control, a NDIR detector for CO2 concentration measurement (Figure 7.4).

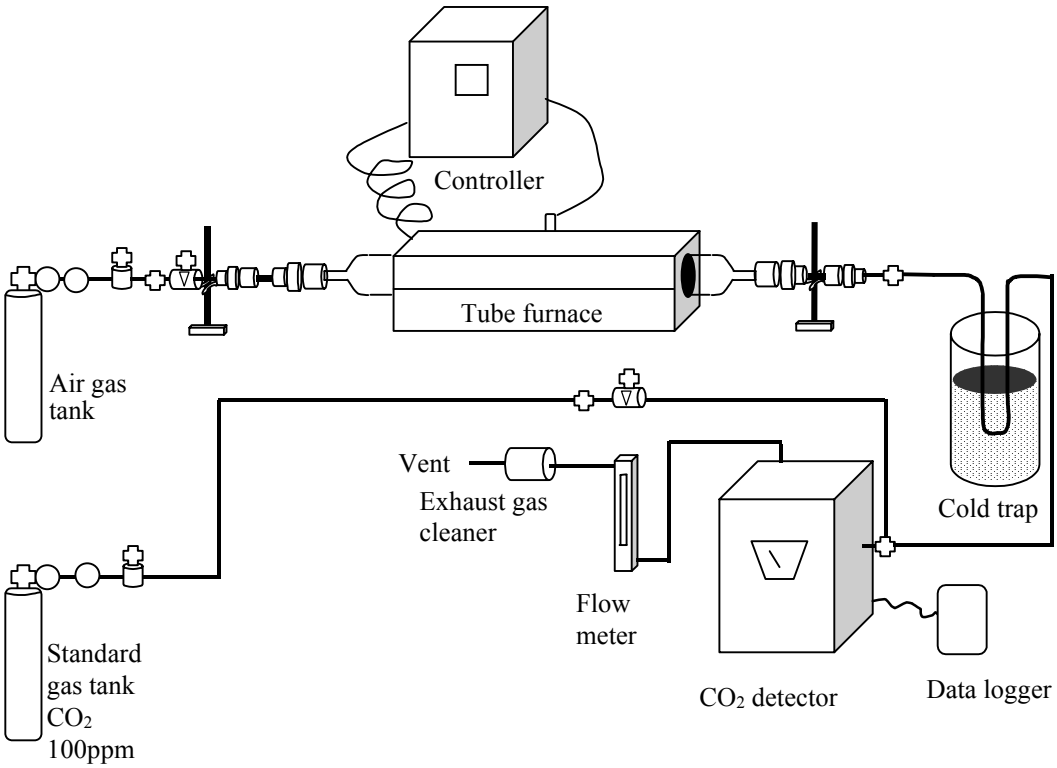

Figure 7.4. Schematic diagram of the experimental setup

7.3.3. Samples

7.3.3.1. Organic carbon references

In addition to sodium citrate, other samples may be used to evaluate the pretreatment efficiency including cellulose, wood and albumin.

7.3.3.2. BC reference

Diesel Particulate Matter or Urban Particulate Matter from NIST may be used (Table 7.2)

7.3.3.3. Soil samples

One of the NIST soils, sediments, and sludge SRM may be used. (Table 7.3) Other soil samples from different places with different types of land uses will be used for comparison.

7.3.3.4. Inorganic carbon removal and size reduction

The sample will be treated with diluted HCl, centrifuged, repeatedly washed with Q-water and centrifuged, then finally dried at 105 C to remove moisture. The sample will be ground into a powder before analysis. The effects of the size of the powders will be tested.

Table 7.2 NIST particulate carbon SRM

SRM	Descriptor	Unit Size	Unit Price	Status
2975	Diesel Particulate Matter	1 g	$216.00	Available
1650	Diesel Particulate Matter	0.5 g	$500.00	Superseded
1650A	Diesel Particulate Matter	100 mg		Out of Stock
1648	Urban Particulate Matter	2 g	$217.00	Available
2783	Air Particulate on Filter Media	2 +2 Blnk	$518.00	Available
1975	Diesel Particulate Extract	4x1.2 mL	$216.00	Available

Table 7.3 NIST soils, sediments, and sludges SRM

SRM	Descriptor	Unit Size	Unit Price	Status
1646A	Estuarine Sediment	70 g	$350.00	Available
1944	New York/New Jersey Waterway Sediment	50 g	$401.00	Available
2586	Trace Elements in Soil (contains lead from paint)	55 g	$255.00	Available
2587	Trace Elements in Soil (contains lead from paint)	55 g	$255.00	Available
2709	San Joaquin Soil	50 g	$259.00	Available (w/carbon data)
2710	Montana I Soil	50 g	$259.00	Available (w/carbon data)
2711	Montana II Soil	50 g	$252.00	Available (w/carbon data)
2781	Domestic Sludge	40 g	$291.00	Available
2782	Industrial Sludge	70 g	$336.00	Available
8407	Tennessee River Sediment	25 g	N/A	Superseded
8704	Buffalo River Sediment	50 g	$187.00	Available

7.3.4. Method validation

In addition to the interference on the measurement of BCs by the pretreatment procedure, the precision and accuracy of the method will be evaluated by performing the following tests:

1. CO_2 concentration linearity (calibration curve),

2. consistency of detected response on the CO_2 emitting event duration time,

3. total recovery (mass balance) of carbon, and

4. the temperature ramping rate on the recovery and peak temperature of an event

7.4. Materials and Methods

7.4.1. Thermo-oxidation procedure

The experimental setup for the temperature-programmed oxidation of the sample is shown in Figure 7.4.

7.4.1.1. Tube furnace and temperature programming

The Lindberg/Blue Hinged Tube Furnaces (Model: HTF55322C) was used for the thermo-oxidation experiments. The oxidation tube was made of quartz allowing operational temperature up to 1100 C. The furnace was powered and controlled by the Control Consoles (Lindberg/Blue, Models: CC58114PC-1) with a temperature controller (Program Controller, Model: UT150).

7.4.1.2. Gases

The carrier and oxidizing gas is Grade Zero 2.0 compressed air with the total hydrocarbons not exceeding 2 ppm (The BOC Group Inc.). No information on the concentration of carbon dioxide in the air is available. Standard carbon dioxide gas (205 ppm in nitrogen, The BOC Group Inc.) was used for calibrating the concentration in the carrier gas.

7.4.1.3. CO_2 emission detection

Carbon dioxide concentration was monitored by an NDIR detector (Horiba, Model: PIR-2000) with the output signal measured in volts.

7.4.1.4. Date recording

Data output was recorded by a signal processor/data logger (MicroDAQ.com, Ltd . Model: HO8-006-04).

7.4.2. Samples and sample pretreatment

Sodium citrate (Analytical Reagent, 99.8%, Mallinckrodt Inc.) was used as reference material of heat-labile organic carbon. This was used either in its original crystal form with size of 0.5 mm or ground to a powder before being burned. The particle size of the powder is not yet available.

Two BC materials have been used in the thermo-oxidation experiments. Activated carbon was obtained from Aldrich Chemical Co., Inc. (Activated Carbon, Darco, 20-40 mesh) and used as received. Diesel particulate matter was obtained from the U.S. Department of Commerce, National Institute of Standards and Technology (Standard Reference Material 1650) which had been treated with heat under 375 C with sufficient aeration for 24 hours and stored in freezer under -10 C for more than 6 months.

One sediment sample from Boston Harbor was used. The sample was thoroughly mixed by grinding and contained 1.3 % total carbon by weight and 0.12% black carbon (Accardi-Dey, 2002, unpublished data).

7.5. Results and discussions

Some experimental results are summarized in table 7.4.

7.5.1. Method evaluation

7.5.1.1. Precision and accuracy

Repeated injections of 5 milliliters of air containing about 3% of CO_2 (introduced between the tube furnace and the detector and under a flow rate of 1.5 standard cubic feet per hour (SCFH)) showed that the relative standard deviation of the detector response was 16.8%, 22.0%, 31% and 44.2% during four different experiments (see Appendix 1). However, the response of the detector to the 119 ppm CO_2 gas standard (dilution of the standard CO_2 gas with the carrier gas) showed very consistent response with signal heights measured at 6.2, 6.0 and 6.2 (arbitrary unit), respectively. The result indicates that the precision of the measurement of CO_2 concentration can be within a relative standard deviation of 2% for a slow changing concentration.

The recoveries of total carbon from the measurement of the CO_2 emission from a heating program of 20 C/min from 25 C to 925 C were 83.9% for the sodium citrate experiment (see Appendix 2) and 60.0% for the activated carbon experiment (see Appendix 3) assuming the carbon ratio in the activated carbon sample is 100%. The low recovery may have resulted from losses due to the partially oxidized

Table 7.4. Summary of experimental results

Experimental number	Sample materials	Treatment/ temperature program	Recovery as CO_2 (%)			% Charring
			< 375 C or first stage	> 375 C or second stage	Total	
1	sodium citrate crystals	Thermo-oxidized from 25 C to 665 C at 25C/min, and hold at 665 for one hour.				27.0
2	sodium citrate crystals	Thermo-oxidized from 25 C to 665 C at 25C/min, and hold at 665 for one hour.				36.6
3	sodium citrate crystals	Thermo-oxidized from 25C to 925C at 20C/min.	37.8 (<540 C, no holding)	46.1	83.9	46.1
4	sodium citrate crystals	Thermo-oxidized from 25C to 375C at 2C/min and hold for 24 hours then 25C to 925C at 20C/min	>55.6 (> 375, no detection for 375 C, 24 hrs)	48.9	>104.5	30.7
5	sodium citrate powder	Grain size reduced by grinding and thermo-oxidized from 25C to 925C at 20C/min	>33.0 (< 375 C; no detection for 375 C, 24 hrs)	33.9	>66.9	33.9
6	sodium citrate	Dissolved in water and mixed with CO_2-free sediments then heat at 375C for one day*	100 (375 C in muffle furnace)		100	0
7	diesel particulate matters	Thermo-oxidized from 25C to 925C at 20C/min.	(7.2 % of total recovered)	(92.8 % of total recovered)	original amount is unknown	
8	diesel particulate matters mixed with glass beads	Thermo-oxidized from 25C to 925C at 20C/min.	(7.2 % of total recovered)	(92.8 % of total recovered)	original amount is unknown	
9	activated carbon	Thermo-oxidized from 25C to 925C at 20C/min.	0.5	59.5	60.0	
10	Boston Harbor sediment	Thermo-oxidized from 25C to 925C at 20C/min.	72 (below 670C)	3.4	75	
11	Boston Harbor sediment	Thermo-oxidized from 25C to 375C at 2C/min, hold for 2 hour and then up to 935C at 20C/min.	76 (below 375 C)	28	104	18 (original BC content is 9% of total carbon)

*Experiment performed by AmyMarie

carbonaceous compounds or pyrolyzed small compounds that may have escaped from the tube furnace without being oxidized to CO_2. However, the recovery of CO2 from natural sediment samples is better, which is 75%. When the heating was at a slower rate, 2 C/min, and with longer holding time at 375 C, 2 hours, the recovery is practically 100% for both sodium citrate and the sediment (104% due to noise of the detected signal).

7.5.2. Thermo-oxidation of organic carbon reference material

The thermogram of the thermo-oxidation of sodium citrate is shown in Figure 7.5. The thermogram shows two regions of CO_2 emission. One region of emission between the temperatures of 250 C and 500 C indicates the oxidation of sodium citrate. The second region of emission between 620 C and 900 C indicates the existence of temperature-resistant BC, which was produced from the charring of sodium citrate.

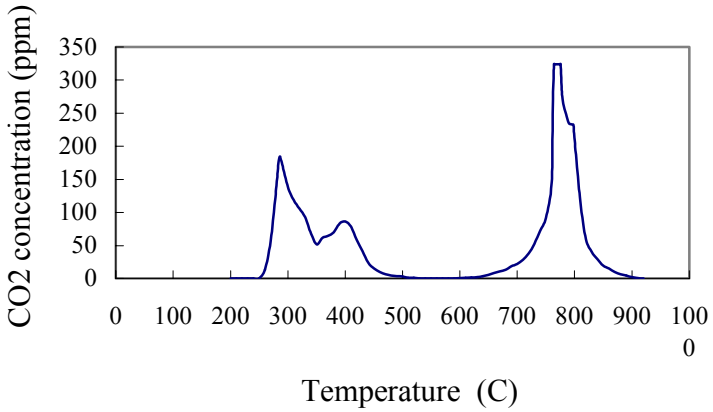

Fig. 7.5 Thermogram of sodium citrate crystals at a heating rate of 20 C/ min

A slower thermo-oxidizing program from 25C to 375C at 2C/min and hold for 24 hours then restarting form 25C to 925C with the ramping rate at 20C/min shows that 55.6% carbon was recovered in the first cycle of heating and 48.9% carbon was in the second cycle with a better recovery of 104.5 (Fig. 7.6). Some amount (18.3% of total carbon) of heat labile carbon was still found in the second cycle emitted as CO_2 below 375 C.

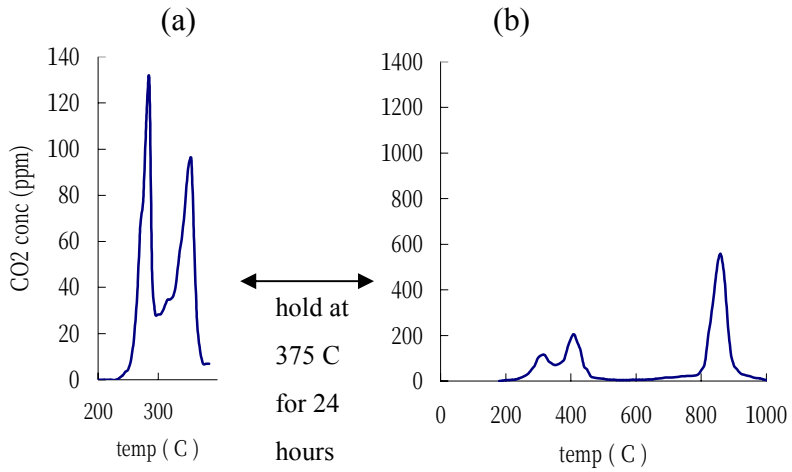

Figure 7.6 The thermogram of sodium citrate crystals (a) first with a slow heating rate at 2 C/min up to 375 C and before (b) restarting at 25 C up to 925 C at 20 C/min. The 10 times difference of the CO2 concentration scale on x-axis is applied to reflect that 10 times higher gas flow per unit increment of temperature during the period (a) than the period (b).

Reducing the grain size of sodium citrate did not help on the total recovery or the removal of heat-labile carbon. (Fig.7.7)

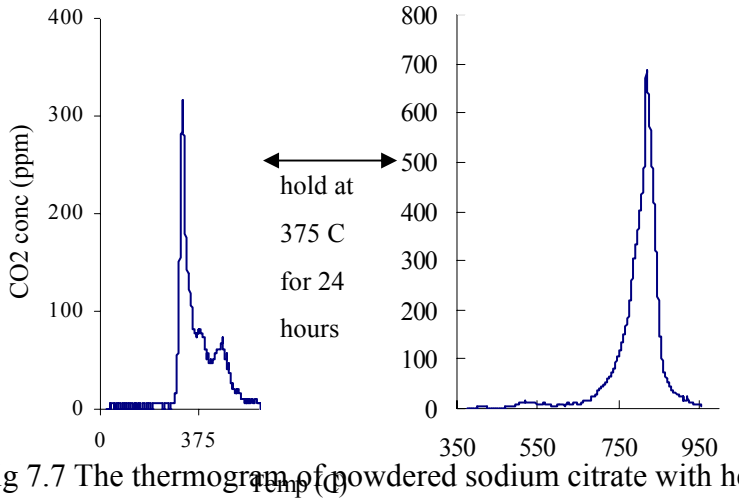

Fig 7.7 The thermogram of powdered sodium citrate with heating rate at 10 C/min and hold at 375 C for 24 hours before continued up to 925 C

7.5.3. Thermo-oxidation of BC reference materials

The thermograms of the combustion of diesel particulate matters, activated carbon and the sediment from Boston Harbor are shown in Fig.7.8, Fig.7.9, Fig.7.10, Fig.7.11 and Fig.7.12, respectively.

Fig. 7.8 shows that the oxidation of diesel soot began at 250 C. The thermo-labile fraction in the thermally pretreated (at 375 C for 24 hours) sample might have come from contamination during storage and handling. Otherwise, the relatively bell-like shape indicates the existence of distributions of the particulate properties. The likely one is the particle size (or molecular size) of the particulate matters. The soot attached on glass beads behaved the same as the soot along (Fig. 7.9). The fluctuation of the CO2 concentration after 700 C is the noise of the detector signal.

The thermogram of activated carbon shows more irregular peaks and higher peak emission temperature (Fig. 7.10). Irregular peaks may due to non-uniform grain sizes and various chemical (molecular structural) forms as well.

The thermograms of the sediment from Boston Harbor is shown in Figure 7.11. Most carbon (72% of theoretical total) was converted to CO2 below 650 C. Small amount (3.4% of the theoretical total) heat-resistant carbon became CO2 between 650 C and 830 C. Slower temperature ramping rate helped on increasing the overall recovery but created more char (Fig.7.12).

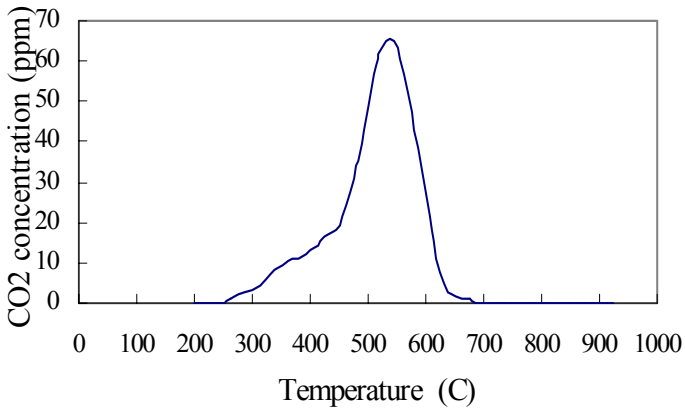

Figure 7.8 Thermogram of diesel particulate matters at a temperature ramping rate at 20 C/min

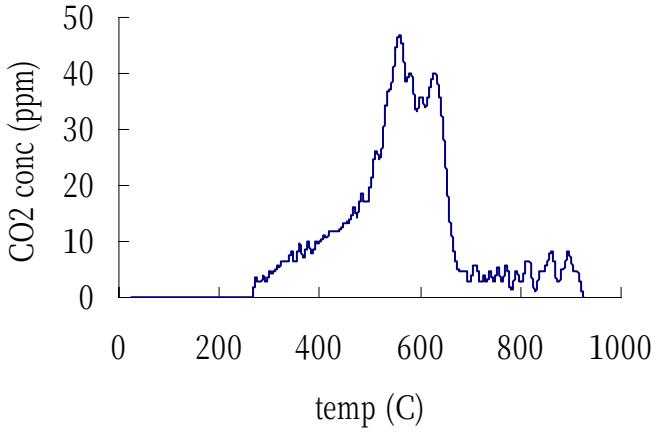

Figure7.9 Thermogram of diesel particulate matters attached on glass beads at a temperature ramping rate at 20 C/min

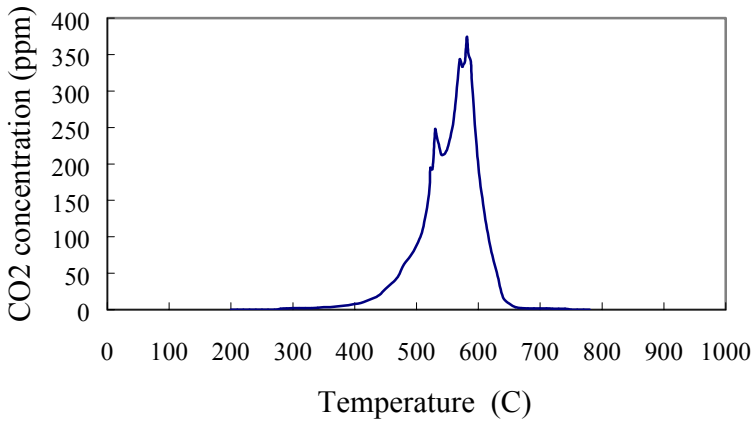

Fig. 7.10 Thermogram of Aldrich activated carbon at a temperature ramping rate at 20 C/min

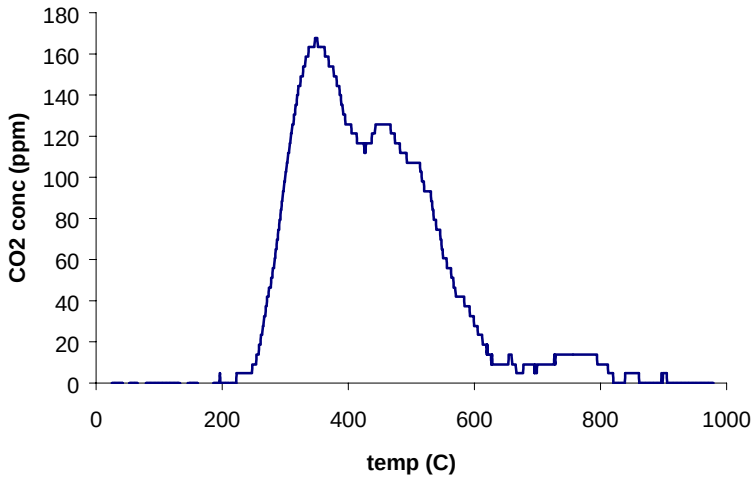

Figure 7.11 The thermogram of the sediment from Boston Harbor with a ramping rate at 20 C/min.

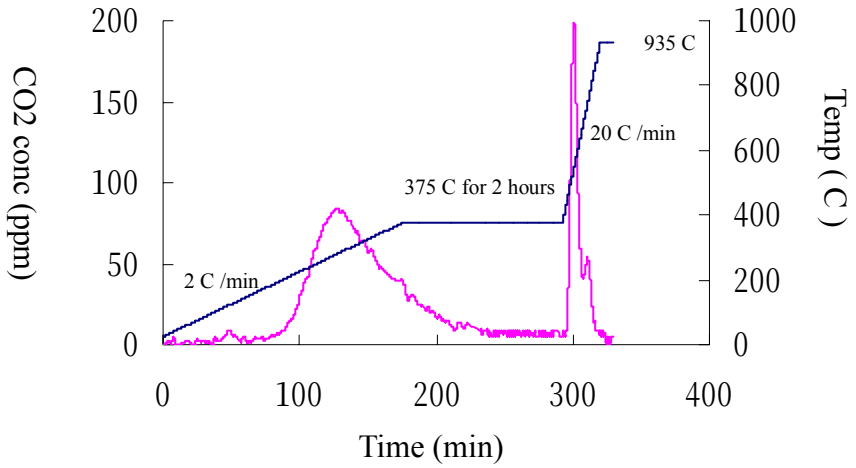

Figure 7.12 The variation of the emitted CO2 concentration and the temperature with time for the sediment from Boston Harbor with a temperature ramping rate at 2 C/min before 375 C, and at 20 C/min up to 935 C after holding at 375 C for 2 hours.

7.6. Summary

The experimental method can efficiently monitor the temperature under which the carbonaceous compounds are converted to carbon dioxide. The precision of the quantification of the carbon mass is acceptable. However, the recovery of the carbon mass is not consistent. A post-furnace catalytic combustion oven may improve the recovery.

Charring is a problem in removing the organic carbon. Reducing the grain size of the sodium citrate or lowering the temperature ramping rate did not lower the possibility of charring. More tests are needed for different sizes, different materials and different temperature ramping rate.

Fingerprints of BCs (thermograms) can be established by using this method, which may help to identify the origins of different BC samples and also help to predict the sorption behavior of them.

7.7. Further evaluation of the methods

Some tests should be done to improve the method.

A. Tests of the pretreatment efficiency and charring on different materials and powder sizes,

B. Repeated experiments on the BC sample with the same temperature program to investigate the method repeatability,

C. Experiments on the BC sample with different temperature ramping rates to look for the completely-oxidizing ramping rate,

D. Experiments using composite samples containing two or more reference BC materials to investigate the ability of the method to differentiate different carbon species,

7.8. Future research

Future research may include

A. Investigating the BC speciation in field samples from different land-use types and establishing the regional and global BC inventory.

B. Categorizing BC species according to their thermo-oxidation characteristics and examining the sorption behavior of each BC group toward HOCs including the sorption equilibrium isotherms and the sorption/desorption rates.

C. Verifying of the multi-component sorption model by comparing the model simulation and the experimental results.

References

Currie L. A. et al., A Critical Evaluatin of Interlaboratory Data on Total, Elemental , and Isotopic Carbon in the Carbonaceous Particle Reference Material, *NIST SRM 1649a, J. Res. Natl. Stand. Technol.* in press.

Gustafsson, O., Haghseta, R., Chen, C., MacFarlane, J. and Gschwend, P. M. Quantification of the Dilute Sedimentary Soot Phase: Implications for PAH Speciation and Bioavailability, *Environ, Sci. Technol.* 1997, 31, 203-209.

Kuhlbusch, T. A. J. Methods for Determining Black Carbon in Residues of Vegetation Fires, *Environ, Sci. Technol.* 1995, 29, 2695-2702.

Middelburg, J. J., Nieuwenhuize, J., van Breugel, P., Black carbon in marine sediments, *Marine Cemistry,* 1999, 65, 245-252.

Nelson and Sommers, Total Carbon, Organic Carbon, and Organic Matter, in *Methods of Soil Analysis* Part 2 Chemical and Microbiological Properties, Page A. L. Eds, 1982

Others (see Table 1)

Chapter 8 Molecular Dynamics Simulations of the Sorption of VOCs in Humic Acid

8.1 Introduction

The sorption behavior of volatile organic compounds (VOCs) in humic substances plays important roles in pollutant fate modeling and remediation of contaminated sites. There were many studies of mechanisms of sorption process. Previous works (Chang et al., 1997; Piatt and Brusseau, 1997; Shih and Wu, 2002a and 2002b) have focused on examining sorption kinetics of VOCs with different types of environmental sorbents. These prior studies focused on measuring rates of sorption and diffusion in complex organo-mineral aggregates or humic substances at larger length scales. Various rate models have been used to simulate contaminant uptake and release in a macroscopic scale. As to the mechanism controlling sorption dynamics, it still remains unclear due to the difficulty in observing its dynamic behavior at the microscopic level (Brusseau and Rao, 1989).

Recently, molecular modeling techniques based on the development of fundamental physical theories and their applications to numerical simulation techniques are applied to environmental issues. For example, some researchers applied the molecular modeling techniques to explain the environmental phenomena such as the persistency of toxaphene in mammals (Vetter and Scherer, 1999) the prediction of polychlorinated hydrocarbons from municipal waste incinerators (Iino et al., 2001), the sorption mechanisms of organic chemicals adsorbed onto clays and minerals (Kubicki et al., 1997; Teppen et al., 1998; Luo and Farrell, 2003) and the interactions of natural organic matter and contaminants (Kubicki and Apitz, 1999). But to our knowledge there is very little molecular modeling work involved in sorption kinetics and thermodynamics study of a contaminant in humic substances.

Therefore, in this work we will first use the molecular dynamics simulation technique to verify our method by comparing the kinetic results of simulation with the real experimental data under dry conditions. Then we will identify the possible mechanism governing the interaction between toluene and humic acid. Finally we will evaluate the thermodynamic property of toluene in humic acid.

8.2 Computational Methods and Structural Model

Structural Model and Molecular Dynamics Simulation. The building block structure of humic acid was described previously (Davis et al., 1997; Kolla et al., 1998). The amide-linked humic acid helical structure is stable and the amide linkage is in agreement with spectroscopic evidence. In this work the basic building block structure of humic acid was produced using the C^2 Builder modules (MSI Inc.). The humic acid model consisting of seven monomers was built by adding one monomer after another gradually and at the same time the energy minimization calculations was carried out to assure its stable confirmation. Finally, the target compound, i.e. toluene molecule, was inserted into the open space formed among chains within humic acid to establish our structural model as shown in Figure 8-1.

Diffusion Coefficient. The calculation for the diffusion coefficient is based on the statistical mechanical principles. In short, the diffusion coefficient is extracted from the proportionality constant according to the Einstein form of diffusion,

$$D = \frac{1}{6}\lim_{t\to\infty}\frac{d}{dt}\left\langle \left(r_i(0) - r_i(t)\right)^2 \right\rangle \qquad (8\text{-}1)$$

with D the diffusion coefficient and $r_i(t)$ the center of mass of the specie i at time t.

Considering a binary system consisting of a natural polymer, humic acid, and a penetrant, toluene molecule, mean square displacement from the dynamics trajectory is equal to the average of the displacement in equation (8-1) for the calculation of diffusion coefficient.

Activation Energy. The effect of temperature on the diffusion coefficient can be described by the Arrhenius equation (Chang et al., 1997; Shih and Wu, 2002; Crank and Park, 1968)

$$D = D_0 \exp(-\frac{E}{RT}) \qquad (8\text{-}2)$$

where D_0 is the diffusion coefficient of the reference state and E is the activation energy of diffusion process. The activation energy for sorption was found by plotting ln D versus 1/T.

8.3 Results and Discussion

8.3.1 Diffusivity of Toluene inside Humic Acid

The proposed humic acid model (Figure 8-1) is based on the combination of the average structural unit of humic acid obtained from chemical analysis. Our structural model of humic acid has very similar feature by gradually adding some monomers to

fill the lattice.

Since the positions of the toluene molecule in humic acid matrix may affect the mobility of toluene, the toluene was inserted at three different positions to get the lowest energy conformation before collecting the dynamic trajectory. The estimated diffusivity of toluene based on equation (8-1) in humic acid is 8.43×10^{-8} cm^2/sec at 300 K. Compared to the diffusivity of 6.6×10^{-9} cm^2/sec for sorption and 1.2×10^{-9} cm^2/sec for desorption at 298 K estimated by Chang et al. (1997), the value of this study is about an order of magnitude larger than the experimental data.

To appreciate this inconsistent result between our calculated diffusion coefficient and experimental estimated diffusion coefficient we found that the density of this humic acid model is 0.92 g/cm^3 instead of 1.23 g/cm^3 as used in experimental works. We propose that the lower density of the polymer will give higher diffusivity thereby increase the mobility of penetrates. Moreover, the humic acid used in the experimental work was the sodium form. The lacking of sodium ions and other cations in our humic acid model may cause the decrease of the density and increasing the simulated diffusivity.

From both molecular simulation and experimental results (Chang et al., 1997; Piatt and Brusseau, 1998; Shih and Wu, 2002), we propose that the penetration of VOC is controlled by diffusion of VOC molecules in humic substance matrix. Also the values of the diffusivity in humic substances are far less than that in the air or in the water.

8.3.2 Some Thermodynamic Characteristics of Diffusion.

The diffusivities are 8.56×10^{-8} cm^2/sec at 325K and 5.71×10^{-6} cm^2/sec at 350 K shown in Figure 8-2. Toluene sorption diffusivity increases with temperature, which is in consistent with the experimental results of Chang et al. (1997). The fact that temperature will increase the rate of diffusion due to giving more energy to facilitate the displacement of the polymer segments and helping the mobility of VOC molecules can be clearly observed in the process of the molecular dynamics simulation.

From Figure 8-2 and equation (8-2), toluene molecules surmount the activation energy barrier of 17.1 kcal/mole when they are squeezing through the macromolecular matrix. This value is slightly higher but in the same order compared to the activation energy of toluene 10.1 kcal/mole for sorption and 15.7 kcal/mole for desorption into humic acid at 15-45 ^oC (Chang et al., 1997). The slightly overestimated activation energy may be resulted from the density difference discussed previously. But the similar trend between the molecular simulation and the macroscopic experimental

results validates that the molecular dynamics method faithfully mimics molecular motion in actual humic acid systems.

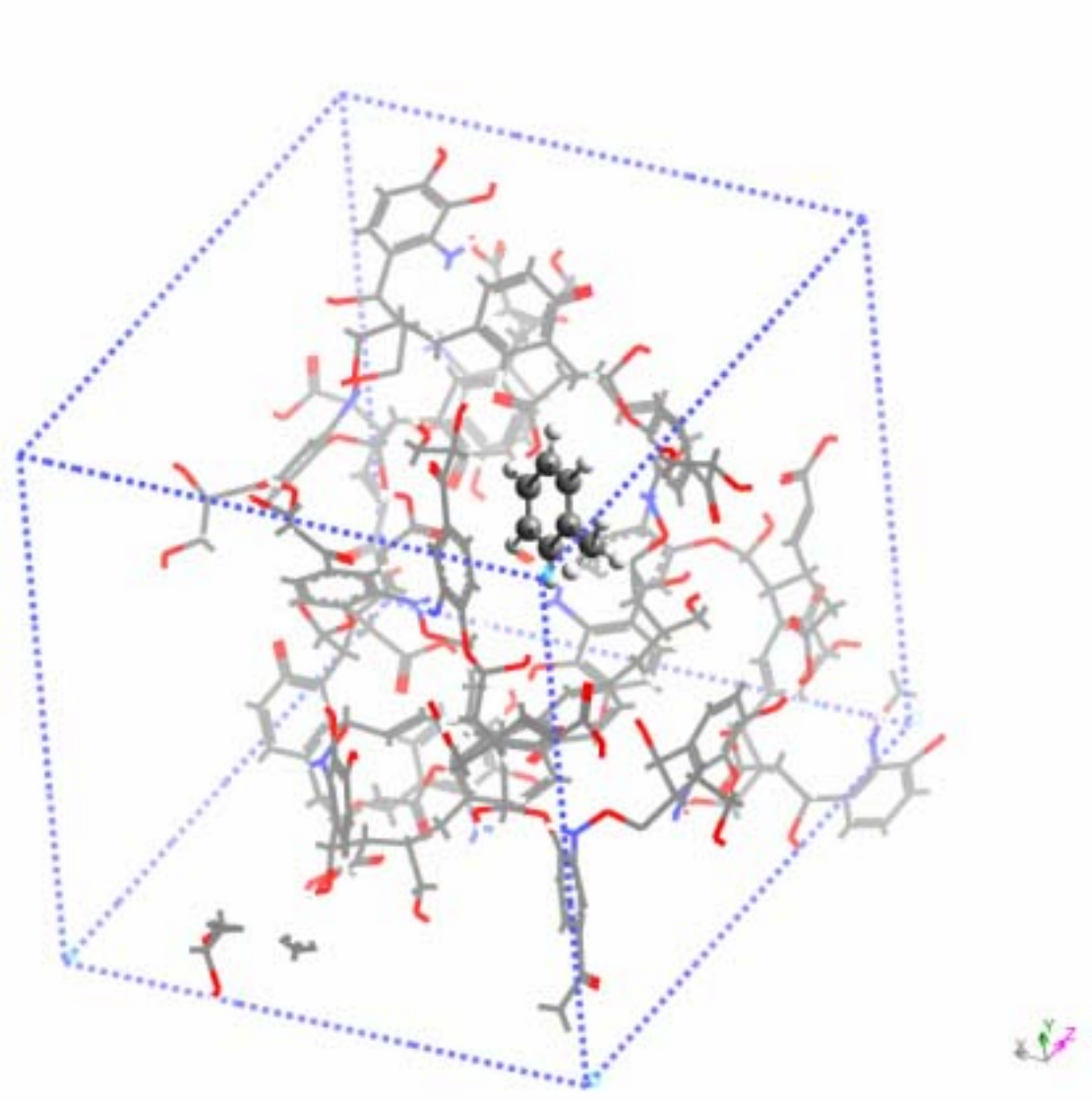

Figure 8-1 The lowest-energy humic acid model containing one toluene molecule (the ball and stick form). Carbon atoms are gray, nitrogen atoms are blue, oxygen atoms are red, and hydrogen atoms are white.

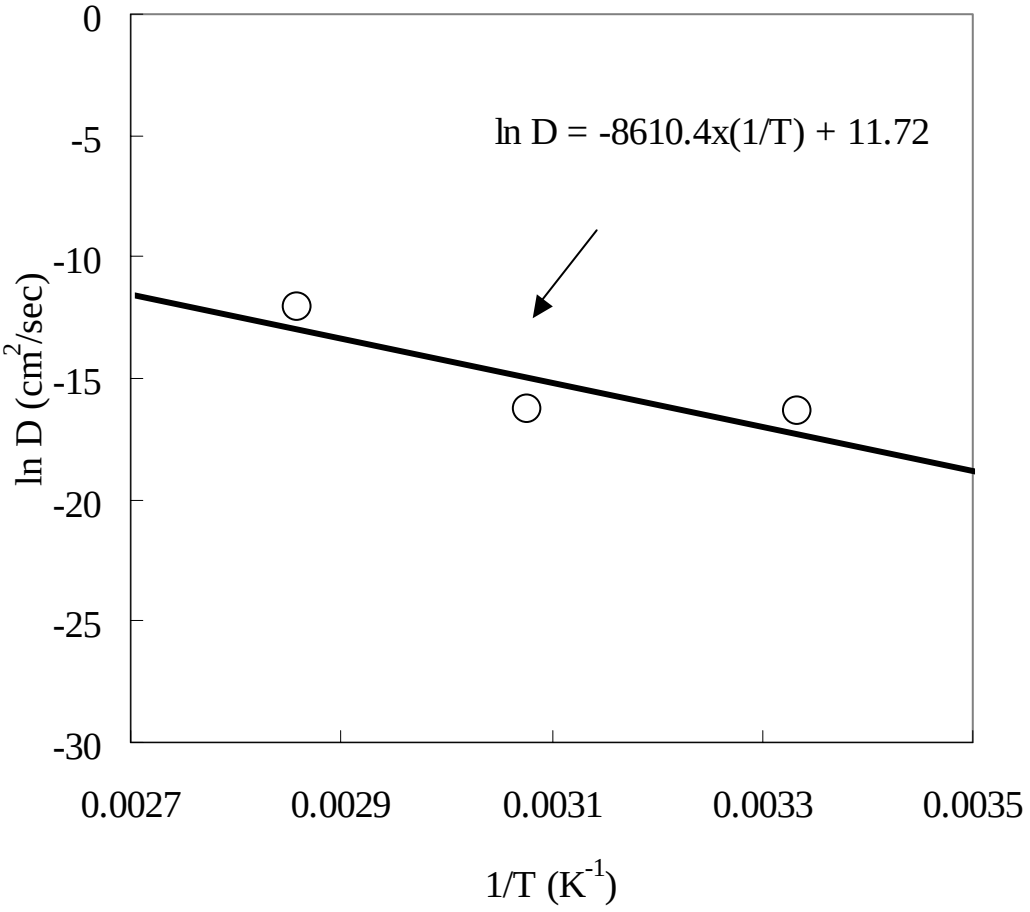

Figure 8-2. ln D versus 1/T (K) for toluene sorption. Temperature ranges from 300 to 350 K.

Chapter 9 The Effect of Soil Chemical Heterogeneity on the Slow Sorption Toluene in Soils

9.1 Introduction

The sorption of organic contaminants in soils is one of the main processes controlling the pollutant fate and the effectiveness of contaminated soil remediation. Irreversible sorption or slow desorption of volatile organic compounds (VOCs) has been reported in the laboratory and the field. A portion of sorbed VOCs is slowly released from soil particles and some fraction will be retained in the particles for a long period of time (Pignatello and Xing, 1996; Aochi and Farmer, 1995; Steinberg et al. 1987). The retaining mechanisms affect the chemical fate in the environment and the remediation effectiveness of contaminated soils and groundwater aquifers.

Soil heterogeneity plays an important role in the sorption/desorption of organic contaminants in soils. Soils are chemically heterogeneous matrix in which there are many inorganic and organic constituents. The chemical heterogeneity complicates the predicting of the fate of a pollutant in soils. Recent review papers summarized the slow sorption/desorption of organic compounds in natural particles (Pignatello and Xing, 1996; Luthy et al., 1997). This phenomenon has been attributed to slow diffusion through micropores of soil particles (Lin et al., 1994; Farrell and Reinhard, 1994), through matrixes formed from condensed organic matter (Weber and Huang, 1996; Huang and Weber,1998), and slow migration in soil organic matter (SOM) (Fu et al., 1994; Brusseau et al., 1991).

Numerous researchers have observed a bi-phasic process for the sorption of VOC on soil particles, in which there is an initial stage of rapid sorption followed by a slow sorption stage. Some researchers (Pignatello, 1990; Schlebaum et al., 1998) suggested that the persistence of organic pollutants in soils was resulted from the entrapment of contaminants in soil organic matter. Wu and Gschwend (1986) explained the phenomenon of slow sorption by a radial diffusion model in which the sorbate migrated into and out of the aggregates of organic matter and mineral particles by diffusion. However, rare literature presents the sorption kinetics of individual soil component. Here, we propose that each component has its unique sorption mechanism and kinetic behavior. Delineation of the sorption rate of each component is necessary.

Therefore, we intended to utilize soils with diversified organic contents to study the contributions of soil organic matter and soil inorganic matter to sorption kinetics. Toluene, a

model compound for mononuclear hydrocarbons, was used as the sorbate to delineate the sorption behavior of VOCs in soils. Humic acid and kaolinite were selected as the two model soil components to represent soil organic matter and soil inorganic matter. The sorption of toluene in humic acid and humin are reversible and diffusion-controlled (Chang et al., 1997; Shih and Wu, 2002a). Sorption of VOCs on soil inorganic matters (SIMs) is believed to be surface adsorption under a low contaminant concentration. Kaolinite, a non-swelling clay mineral and one of the weathered clay minerals, can be one of the model of the SIMs in soils. The sorption kinetics pattern and sorption capacity were examined to show the effect of soil chemical heterogeneity on the sorption behaviors and the controlling mechanisms while the soils were contaminated.

9.2 Materials and Methods

Samples. Kaolinite (KGa-1) was obtained from the Source Clay Mineral Repository of the Clay Minerals Society. Aldrich humic acid powder was purchase from Aldrich Chemical, Milwakee, WI, USA. The particle size of humic acid powder ranged from 100μm to 800μm and the weighted average was around 270μm. There are four soil samples, Taichung (TC), Chungli (CL), Kaikung (KK), and Yangmingshan (YM) soils. These soil samples were collected in Taiwan. Soil samples were air-dried, freed of plant materials, and screened through a 20 mesh (0.84 mm) sieve. Then the soil samples were stored in sealed bottles.

These four soil samples were treated with 30 % H_2O_2 at around 70℃ to remove soil organic matter (SOM) following the procedure described by Kunze and Dixon (1986). These low organic content soils were denoted as TCD from TC soil, LCD from LC soil, KKD from KK soil, and YMD from YM soil, respectively.

Sample Characterization. Surface area and pore size distribution tests were carried out in an ASAP 2000 analyzer (Micrometrics Instrument Corporation). Surface area was calculated from the nitrogen adsorption data using the BET equation. The organic carbon fraction (foc) was determined by a Perkin-Elmer Model 2400 CHN analyzer (Nelson and Sommers, 1982). Inorganic carbon was removed according to Ball et al. (1990).

Sorption/Desorption Experiment. The gravimetric method was described in Chang et al. (1997) and Shih and Wu (2002b). In this study, the experimental apparatus was maintained at 25±0.1 ^{o}C. In short, the sample in the holder rather than a pressed disk was hung on the sample side of a Cahn 200 electric microbalance and enclosed in a glass gas chamber. All of the samples were dried and purged with 50 mL/min N_2 gas (HC-free) to remove sorbed impurity before each experiment. A steady flow of gas was passed through the liquid toluene in a bottle, and then mixed with a flow of pure N_2 gas to obtain a constant

concentration of toluene vapor. Desorption experiments were carried out by purging the gas chamber with 50 mL/min pure N_2 gas. The concentration of the toluene was determined with GC/FID (Hewlett-Packard 5890II).

9.3 Result and Discussion

Characteristics of Soils. The soil properties of these eight soil samples were shown in Table 9-1. The organic content of four origin soils increases in the order of TC, CL, KK, and YM. After removing SOM, the residual organic carbon content follows the same trend. The proportion of residual SOM is averagely 17±6.0% of the original total SOM. Surface area is in reverse order to the SOM content except CL soil, which has the highest value of surface area. According to the soil texture analysis by Chang (1998), surface area was predominately contributed by the clay in CL soil. The surface area is still large after removing most of the SOM in CL soil since the clay in CL dominates the source of surface area. Interestingly, surface area of KKD soil and YMD soil, which are KK soil and YM soil after treatment to remove organic matter, is higher than KK soil and YM soil, respectively. In YMD soil, 25% of the surface is micropore surface, however, none has been found in the original YM soil. The increased surface area may be the mesopore or micropore surfaces previously covered by SOM.

Sorption of Toluene on Two Soil Components. The ratio of the sorbed amount to the ultimate sorbed amount of toluene on kaolinite and in the humic acid are shown in Figure 9-1. The experimental conditions and the results of sorption experiments of kaolinite and humic acid are summarized in Table 9-2. It took about 4 hours for the sorption of toluene on kaolinite to reach steady state. The time for the sorption of toluene in humic acid to reach a steady state is longer than that of the sorption on kaolinite.

Sorption Kinetics on Clays. The sorption kinetics of toluene on kaolinite shows only one step (Fig. 9-1). One step sorption for several organic sorbates on different clay minerals by the same gravimetric method was also observed by Morrissey and Grismer (1999). Although mineral surfaces as well as soil organic matter could contribute to slow sorption reported by Paviostathis and Mathavan (1992) and Pavlostathis and Jaglal (1991), the sorption of toluene on kaolinite took few hours to complete, which is faster than the sorption into humic acid. And the intrinsic sorption time of toluene on different cation-exchanged montmorillonite thin films was just a few minutes shown in Shih and Wu (2003).

Kaolinite, a common clay mineral in soils, provides large surface area for the sorbates to attach on. The surface adsorption on kaolinite reaches equilibrium more easily than the penetration/partition of toluene in humic acid.

Diffusion into Humic Substances. The sorption of toluene into humic acid powder took about 15 hours, and showed a period of lag time at the beginning (Fig. 9-1). The penetration of VOCs is believed to be controlled by diffusion of VOC molecules in humic substances matrix (Chang et al., 1997; Shih and Wu, 200a2a and 2002b; Piatt and Brusseau, 1998). The average diffusivity of toluene into humin is 7.0×10^{-9} cm^2/sec at 25 ^oC (Shih and Wu, 2002a). The value is on the same order for the diffusivity of toluene in humic acid (Chang et al., 1997; Piatt and Brusseau, 1998). Diffusivities for toluene in humic and fulvic acids are in the order of 3.84×10^{-9} cm^2/sec and 8.51×10^{-10} cm^2/sec, respectively (Piatt and Brusseau, 1998). By using the diffusivity of toluene in humic acid and the approximate diameter of humic acid powder, the time needed to diffusion into humic acid powder was around 13hours. This time period is very close to the diffusion time of toluene into humic acid after a lag period shown in Fig. 9-1. This result is coincident with the diffusion mechanism of VOCs into humic acid disks.

Sorption Process of Soil Samples. A two-stage sorption processes was observed in all soil samples (Fig. 9-2 and 9-3). For soils with low contents of SOM, TC and CL soils, the first stage of the sorption process took up to one hour, and followed by a waiting time of 1.7 hours to continue onto the second stage. The second sorption process took longer time than the first stage. The similar sorption pattern was observed in TCD and CLD soils, the hydrogen peroxide treated TC and CL soils, respectively. The fractions of the sorbing capacity of the first stage of these soils are higher than 70%. It shows that the sorption on soil inorganic matter is the dominant mechanism in these two soils with low SOM content under dry conditions.

Comparing to other soils, YM soil showed the least sorption percentage for the first stage. After removing most of the SOM, the sorption percentage of the first stage increased significantly in YMD soil (Fig. 9-2). This enhancement could be the result of opening up the sites for surface adsorption after removing SOM.

The experimental conditions and the results of the sorption experiments were shown in Table 9-3. All experiments were performed under low toluene partial pressure. The relative saturation pressure (P/P_o) of toluene ranges from 0.019 to 0.086 and the concentration ranges from 2.5 mg/L to 11.3 mg/L. In this concentration range, the distribution coefficient K_d (mg/g)/(mg/L-gas) between the solid phase and the gaseous phase is assumed constant and defined as

$$K_d = \frac{q_e}{C_g} \tag{9-1}$$

where q_e is the equilibrium sorbed amount (mg/g) and C_g is the toluene concentration

(mg/L).

Soil organic substances predominate the sorption capacity of soils under humid conditions. The relative abundance of SOM (represented by the organic carbon fraction) follows the order YM > KK > CL >TC. The distribution coefficients of these soils seem to follow the same trend; however, the K_d of CL, 0.67, is slightly higher than that of KK, 0.41. The same pattern was observed in the hydrogen-peroxide-treated soils.

Sorption amount of organic contaminants in dry soils is controlled not only by the partition or sorption into SOM but also by the surface adsorption on the surface. The amount of organic contaminants adsorbed on the surface of soils can be estimated by the surface area of soils and the surface-based distribution constant.

By using two parameters, organic carbon fraction and surface area, distribution coefficient can be quantified via the following equation:

$$K_d = a\, f_{oc} + b\, SA \qquad (9\text{-}2)$$

where f_{oc} (dimensionless) is the organic carbon fraction in soils, SA (m^2/g) is the surface area of soils, and the *a* (L-gas/g-carbon) and *b* (L/ m^2) are constants. These two constants were obtained by the multiple-variables regression of the distribution coefficients to the two soil properties, f_{oc} and SA, of these eight soils. So the *a* constant is 0.104 ± 0.0109 (L-gas/g-carbon) and *b* is 0.0320 ± 0.00221 (L/ m^2). The good correlation was presented by the R-square, 0.96 and F-value, 60.3, respectively.

The comparison between the predicted distribution coefficients from equation (2) and the experimental values is shown in Fig. 9-4. It shows that we can estimate the distribution coefficients of neutral organic contaminants in soils by these two soil properties under a dry condition and a low pollutant concentration range. Two distribution parameters, the adsorption constant, K_{ds}, and the partition coefficient, K_{dc}, can be extracted from K_d by this formula.

Two Sorption Processes. The surface adsorption rate of VOCs on the SIMs is faster than that of the sorption of VOCs into humic substances (Fig. 9-1). Therefore, it is reasonable to suggest that the fast sorption process of soil samples is contributed mainly by the adsorption on mineral surfaces.

The level of the first plateau between the two sorption stages is supposedly indicating as the first sorption fraction for the two soils with higher SOM (Fig. 9-2). And the second sorption fraction is the sorbed amount between the first plateau and the ultimate plateau. The results are shown in Table 9-4. In soils with low SOM contents, the first sorption fraction dominates the total amount. The first sorption fraction is generally proportional to

the surface area while the second fraction increases with the increasing of SOM.

In the sorption equilibrium aspect, the first term in eq. (9-2), the contribution from surface adsorption, is denoted as K_{ds}. The second term, the contribution from the soil organic matter, is deonoted as K_{dc}. These two fractions can be estimated from eq. (9-2) and are shown in Table 9-4. The surface adsorption fraction, K_{ds}, is generally larger than the SOM sorption fraction, K_{dc}, except KK and YM soils due to their higher SOM content than others.

Implication of the Findings. In choosing an appropriate soil remediation technology, we are facing the difficulty of estimating the sorption capacity and kinetics behavior of heterogeneous soils. Now the finding that each component behavior essentially independently and the sorption capacity at any time of sorption can be estimated by superimposing the capacity of each component together helps us to estimate the sorption amount and the overall mechanisms of a composite soil sample. By using only two soil property measurements, organic carbon fraction and surface area, the distribution coefficient of VOCs between the water and the soil as well as the rate of sorption can be estimated.

9.4 Conclusion

Sorption kinetics of volatile organic compounds (VOCs) affects the remediation, prediction, and fate of these pollutants in soils. The soil chemical heterogeneity further complicates the transport process of VOCs in their fates in soils. The sorption kinetics of two common soil components, humic acid and kaolinite, shows two different sorption patterns. Sorption on kaolinite is believed to be the surface adsorption, however, sorption into humic acid could be explained by two sorption mechanisms, solvation and partition into humic substances. In soils, the two-stages sorption process of toluene is obvious. The first stage is supposedly the surface adsorption and the second stage is the sorption into organic substances. The sorption mechanisms of these two stages can be quantified by two parameters, soil organic fraction and surface area. Better understanding of the sorption kinetics and the effects of soil chemical heterogeneity greatly help on the prediction of the fate of chemicals in the environment and improve the efficiency of the contaminated soil remediation actions.

Table 9-1. Soil properties

	TC	CL	KK	YM	TCD[b]	CLD[b]	KKD[b]	YMD[b]
f_{oc}	0.010	0.016	0.031	0.12	0.0023	0.0034	0.0044	0.012
surface area (m^2/g)	8.5[a]	23.3[a]	6.42	3.80	7.70[a]	25.95[a]	7.65	47.05

[a]: measured by Chang (20).

[b]: TCD, CLD, KKD, and YMD are TC, CL, KK, and YM after being treated by H_2O_2 to remove organic matter.

Table 9-2. Sorption of toluene on two soil components

	Kaolinite	Humic acid
weight (mg)	183.4	70.0
P/P_o[a]	0.021	0.019
	(0.0013)	(0.00079)
concentration (mg/L)	2.8	2.5
sorbed weight (μg)	255	205

[a]: The number shown is the average of three measurements. And the number in the parentheses is the standard deviation of the three measurements.

Table 9-3. Experimental conditions and results of toluene sorbed on soils

	TC	CL	KK	YM	TCD	CLD	KKD	YMD
soil weight (mg)	154.8	160.4	151.0	47.0	142.9	175.2	166.3	351.5
P/P_o	0.037 (0.0032) [a]	0.042 (0.00031)	0.036 (0.0016)	0.086 (0.00022)	0.043 (0.00077)	0.047 (0.0018)	0.038 (0.00045)	0.019 (0.0034)
concentration (mg/L)	4.9	5.5	4.7	11.3	5.7	6.2	5.0	2.5
sorbed weight (μg)	260	591	293	738	163	870	305	1532
K_d (mg/g/mg/L)	0.34	0.67	0.41	1.39	0.20	0.80	0.37	1.74

[a]: The number shown is the average of three measurements. And the number in the parentheses is the standard deviation of the three measurements.

Table 9-4. Experimental and predictive two-stages sorption results

	TC	CL	KK	YM	TCD	CLD	KKD	YMD
1st stage sorbed ratio (%)[a]	74.0	86.0	71.5	30.0	71.9	89.4	83.6	76.5
2nd stage sorbed ratio (%)[b]	26.0	14.0	28.5	70.0	28.0	10.6	16.4	23.5
K_{ds} (mg/g/mg/L)[c]	0.29	0.79	0.22	0.13	0.26	0.88	0.26	1.60
K_{dc} (mg/g/mg/L)[d]	0.07	0.11	0.22	0.83	0.02	0.02	0.03	0.08
K_{ds}/K_d (%)	80.3	87.6	50.2	13.5	94.3	97.3	89.3	95.0
K_{dc}/K_d (%)	19.7	12.4	49.8	86.5	5.7	2.7	10.7	5.0

[a]: the first sorbed toluene ratio can be estimated by the level of the first plateau between two stages in Fig.9-2 and 9-3.

[b]: the difference in sorption fraction between the first plateau and the ultimate plateau in Fig.9-2 and 9-3.

[c]:the prediction of the distribution coefficient on soil surface by equation (2).

[d]: the prediction of the distribution coefficient in soil organic carbon by equation (2).

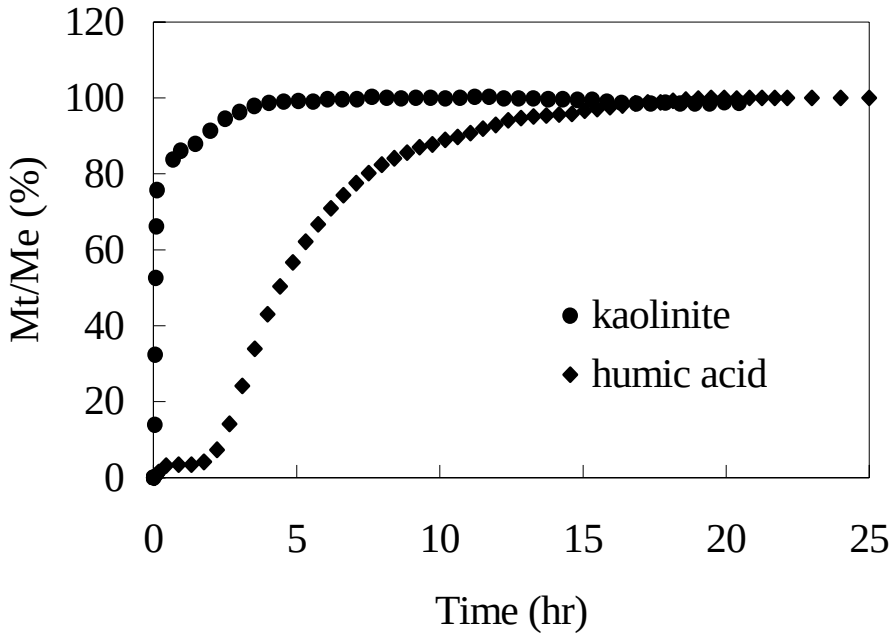

Fig. 9-1 The results of toluene sorption on kaolinite and humic acid.

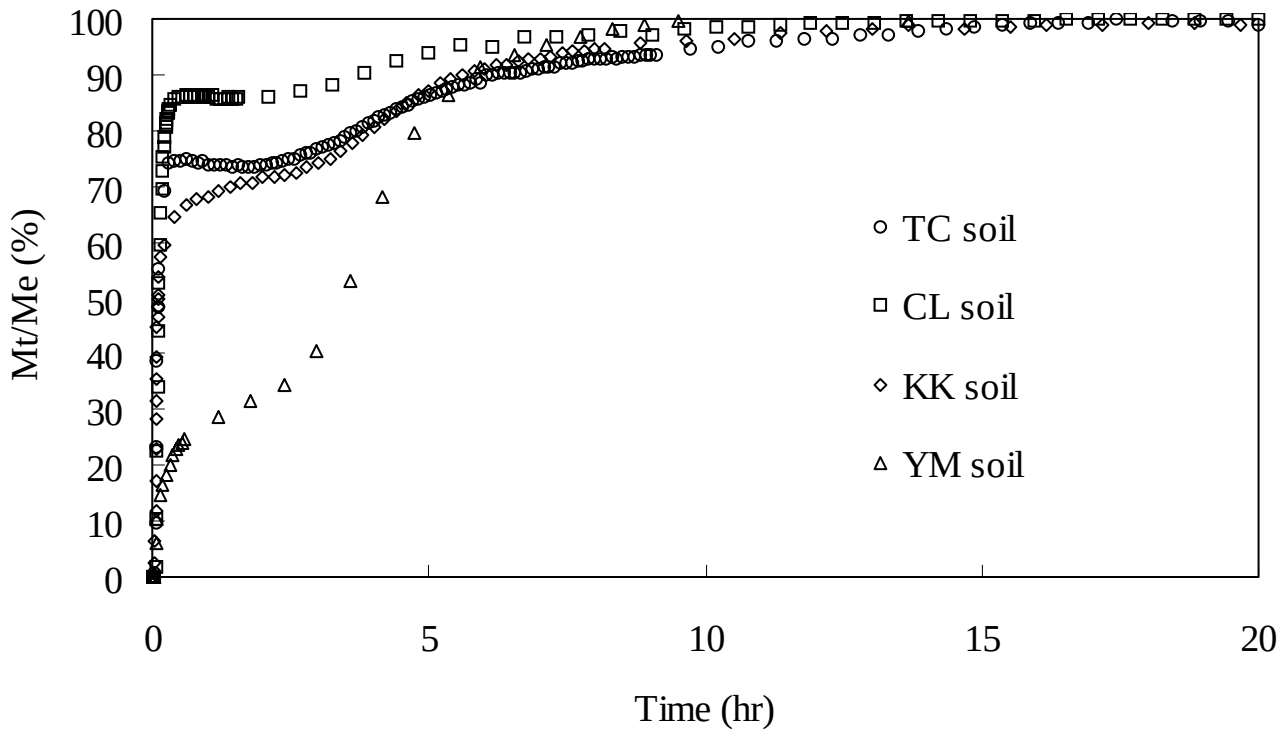

Fig. 9-2 The results of toluene sorption on four soils: Taichung (TC) soil, Chungli (CL) soil, Kaikuang (KK) soil, and Yangmingshan (YM) soil.

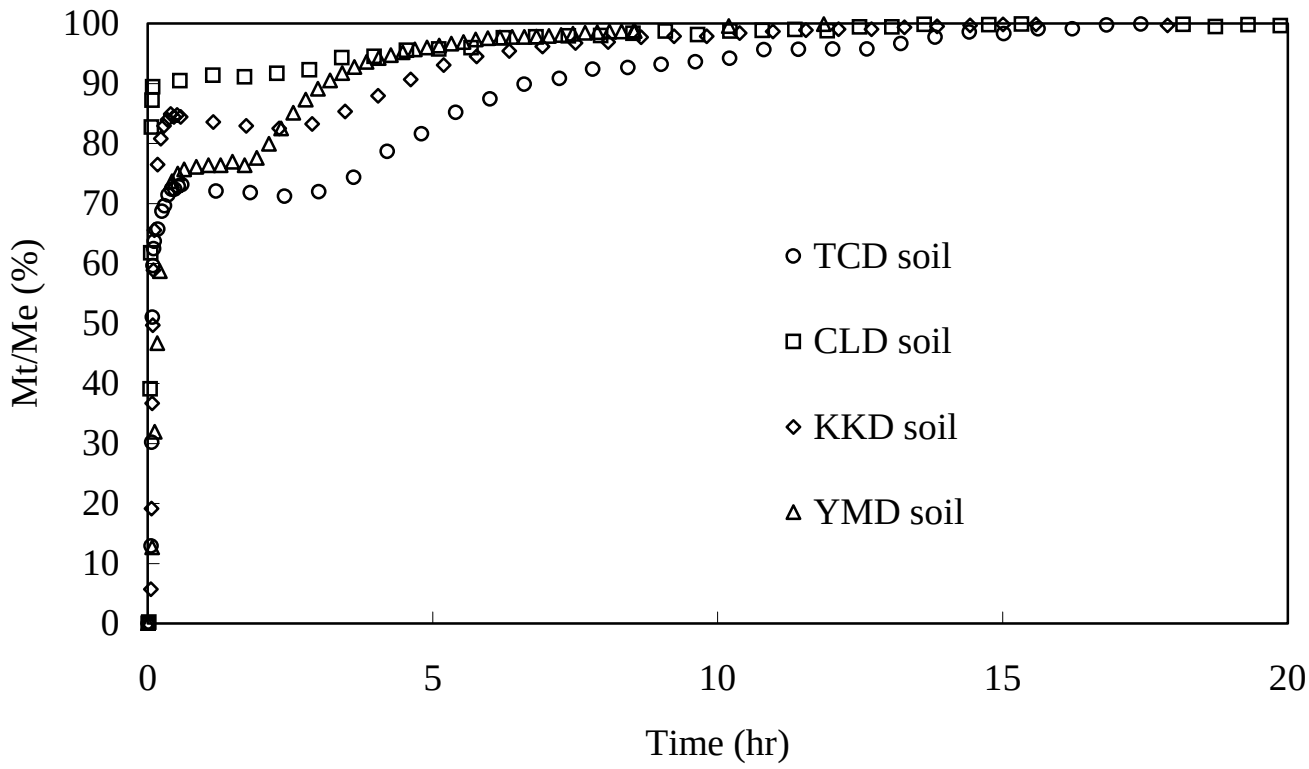

Fig. 9-3 The results of toluene sorption on four soils after removing most SOM. TCD soil, CLD soil, KKD soil, and YMD soil denote: Taichung soil, Chungli (CL) soil, Kaikuang (KK) soil, and Yangmingshan (YM) soil with low SOM content, respectively.

5

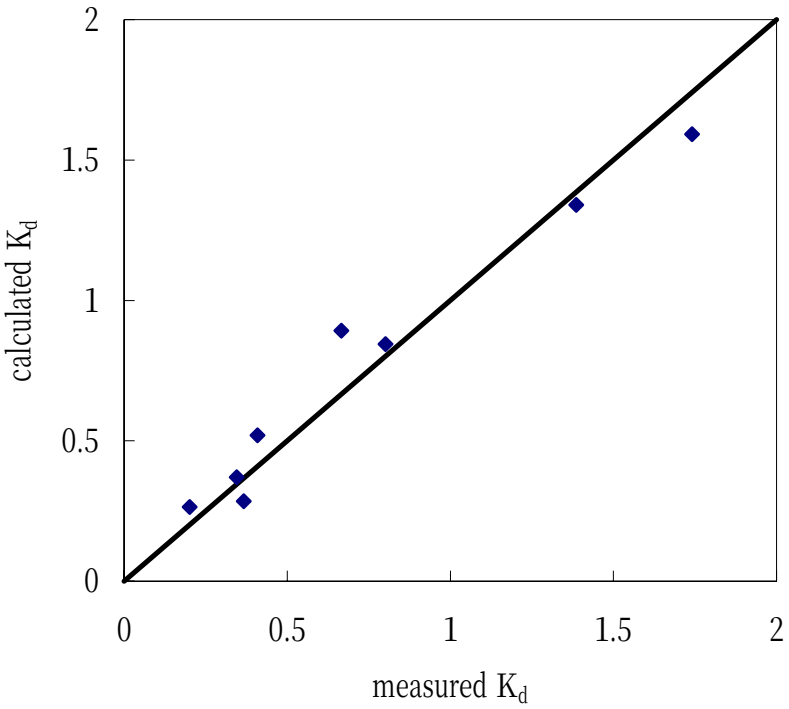

5

Fig. 9-4 The distribution coefficients of toluene between the solid phase and the gaseous phase plotted against values calculated through equation (9-2).

Chapter 10 Summary

10.1 Summary of the results

The effects of soil heterogeneity on the transport of pollutants in the groundwater can be described by a set of distributed mass-transfer coefficients. A numerical model was developed in which the groundwater aquifer was divided into a mobile phase and several immobile, or stagnant, phases. The movement of pollutants is governed by advection and dispersion in the mobile phase, and by mass transfer between mobile and immobile phases.

The distributed mass-transfer coefficient approach is able to model the transport of pollutants where there is heterogeneous soil texture and mass-transfer limited partition kinetics. The experimental and simulation results also indicate that in a length scale larger than that of a laboratory soil column the phenomenon of non-equilibrium transport or tailing is resulted mainly from the mass-transfer limited migration of the sorbate into the stagnant region inside the immobile phases. The problem of modeling each of these immobile phases due to the lack of geological information can be improved by using a distributed mass-transfer coefficient set, which is related to some of the easily obtained soil properties such as the length scale of the system of concerned, the moisture content and the heterogeneity of the soil texture profile. Also the soil video imaging system can be used to identify and locate the layers with high hydraulic conductivity and layers with low hydraulic conductivity, or say the heterogeneity of the soil column with quite low cost and in short time, which will be a promising tool to help on the characterizing, modeling and remediation of a contaminated site.

Each component of the chemically heterogeneous soil exhibits a unique sorption behavior toward organic sorbates; and therefore influences greatly the fate and the remediation efficiency of organic pollutants. Humin, instead of composite soil organic matter or mineral complex, was used to investigate the possibility of irreversible sorption under both dry and humid conditions. The gravimetric and spectroscopic methods were applied to observe the sorption behaviors of organic compounds to humin and clay mineral via compressed either a disk form or a thin film. A FTIR experimental method allowed us to observe the sorption kinetics of VOCs on these soil components in either a system near the natural humidity or a dehydrated system on a short time scale. Furthermore, a new approach to use the molecular simulation method

to predict the sorption kinetics results, i.e. the diffusivities, was validated in this research. Overall, the experimental and theoretical findings of this research indicate that sorption processes of VOCs in humin and clays are diffusion-control and micropore-diffusion-control, respectively.

The sorption kinetics of toluene in pressed humin disks was investigated by tracking the weight change of the disks with a microbalance. For the apparent diffusivity of toluene in the disks, it ranged from 10^{-8} to 10^{-9} cm^2/s and increased with temperature. And desorption diffusivity was about one-half that of sorption. No significant permanent residue of sorbed molecules was observed with the FTIR method on a thin humin film under either low or high-humidity conditions. These results are consistent with the gravimetric method, indicating that the sorption of toluene in humin is a reversible process and mainly diffusion-controlled.

Comparing the sorption kinetics of two hydrocarbons with different polarity, hexane and acetone, in humin, it was found that the apparent diffusivity of acetone and hexane in the disks ranged from 10^{-8} to 10^{-10} cm^2/s. The lowest diffusivity of acetone may result from the high affinity of acetone with humin. From the differences in distribution coefficients for these given solutes, it reflects the higher hydrophilicity in humin. Moreover, higher sorbing capacity for more polar VOCs as well as C^{13}-NMR data indicates that humin was more hydrophilic than Aldrich humic acid. The retention of acetone and hexane in humin after thorough purging with VOC-free nitrogen gas was observed. On the completion of the desorption experiments, there were approximately 35% and 20% sorbate residue for acetone and hexane, respectively. Humin could be a controlling soil component for the sequestration process of organic contaminants except the monoaromatic compounds, i.e. toluene. Based on the above results and results presented in other literature (Chang et al., 1997; Piatt and Brusseau, 1998.), it may be concluded that the sorption kinetics for VOCs on natural humic substances with a time scale between a few minutes to days is controlled primarily by mass transfer in polymeric humic structures.

For soil inorganic matter, one expanding clay mineral, montmorillonite, which exhibits a unique sorption behavior toward organic sorbates was investigated by tracking the intensity change with a FTIR/thin film method to study the sorption kinetics of toluene in dry and humid conditions. Two cation-exchanged forms of montmorillonite were used to identify the sorption mechanism of toluene in

Ca-montmorillonite. For the sorption under humid conditions, similar toluene sorbed intensities were found on Ca -and Cu– montmorillonites; however, higher intensity of toluene was showed on Cu-form under dry conditions than under humid condition. The sorption capacity of Ca-form is lower than those of Cu-form under a dehydrated system. This result indicate that the sorption process of toluene to Ca-montmorillonite could be different from that of toluene/Cu-from system. Among the first-order- rate constants of toluene on these two montmorillonites, the sorption and desorption rates of toluene on Cu-form under dry conditions are the lowest. Furthermore, the peak shift in the spectrum and the color change of Cu-montmorillonite may be resulted from the chemisorption of toluene on clay. There is no similar observation for Ca-montmorillonite. Consequently, there seems to be no chemical interactions between the toluene molecules and Ca-montmorillonite according to the IR spectra. There may be micropore diffusion control in these two montmorillonites; in addition, the single electron transfer chemisorption occurred in Cu-montmorillonite.

The sorption and desorption of trichloroethylene (TCE) in humic acid and humin disks was investigated by microbalance. The apparent diffusivity of TCE in these two humic substances was in the 10^{-8} to 10^{-9} cm^2/s magnitude. There are no residual sorbed TCE observed via a microbalance. The intrinsic sorption/desorption time scale of TCE on two cation exchanged montmorillonites was only few minutes by the thin film/FTIR method. So these two humic substances, humic acid and humin, and montmorillonite do not contribute to the sequestration process of TCE in soils.

Molecular dynamic simulation was used to solve the problem of sorption kinetics of organic pollutants in humic substances. Toluene, a main contaminant in soil/groundwater pollutant sites, and humic acid, a main soil organic matter, are selected to validate this method by comparing to real experimental data. The computer simulated results of the sorption kinetics and thermodynamics of toluene in humic acid are in good agreement with the experimental data. This method helps us to get useful information without the risk of applying the toxic contaminants and producing a lot of contaminants after the experiments. Moreover, our studies have shown that the molecular dynamics simulation of volatile organic compounds in humic substance is able to yield meaningful result.

After studying soil chemical heterogeneity, we found the intrinsic sorption is fast for VOCs into humin, humic acid, and montmorillonite. So they do not contribute to

the sequestration process in soils. The mass transfer of contaminants into soil plays the important role on the slow sorption/desorption in soils.

References

Achtnich, C., E. Fernandes, J. Bollag, H. Knackmuss, and H. Lenke. 1999. Covalent binding of reduced metabolites of [$^{15}N_3$]TNT to soil organic matter during a bioremediation process analyzed by ^{15}N NMR spectroscopy. *Environ Sci Technol* 33:4448-4456.

Almendros, G., M. E. Guadalix, F. J. Gonzalez-vila, and F. Martin. 1996. Preservation of aliphatic macromolecules in soil humins. *Org. Geochem.* 24:651-659.

Aochi, Y. O., and W. J. Farmer. 1995. Spectroscopic evidence for the rate-limited accumulation of a persistent fraction of 1,2-dichloroethane sorbed onto clay minerals. *Environ. Sci. Technol*. 29:1760-1765.

Aochi, Y. O., and W. J. Farmer. 1997. Role of microstructural properties in the time-dependent sorption/desorption behavior of 1,2-dicholoroethane on humic substances. *Environ. Sci. Technol*. 31:2520-2526.

Aochi, Y. O., W. J. Farmer, and B. L. Sawhney. 1992. In situ investigation of 1,2-dibromoethane sorption/desorption processes on clay mineral surfaces by diffuse reflectance infrared spectroscopy. *Environ. Sci. Technol*. 26: 329-335.

Archa, M., A. P. Jackman, and B. J. Mccoy. 1996. Adsorption kinetics of toluene on soil agglomerates: Soil as a biporous sorbent. *Environ. Sci. Technol*. 30, 1500-1507.

Ball, W. P., and P. V. Roberts. 1991. Long-term sorption of halogenated organic-chemicals by aquifer material. 2. intraparticle diffusion. *Environ. Sci. Technol*. 25,1237.

Ball, W. P., C. H. Buehler, T. C. Harmon, D. M. Mackay, and R. V. Roberts. 1990. Characterization of sandy aquifer material at the grain scale. *J. Contam. Hydrol*. 5:253-295.

Bedient, P. B., and H. S. Rifai. 1994. *Groundwater contamination: transport and remediation.* Englewood Cliffs, N. J. :PTR Prentice Hall.

Boyd, S. A., M. M. Mortland, and C. T. Chiou. 1988. Sorption characteristics of organic compounds on hexadecyltrimethylammonium-smetite. *Soil Sci. Soc. Am. J*. 52:652-657.

Brusseau, M. L., and P. S. C. Rao. 1989. The influence of sorbate-organic matter interactions on sorption nonequilibrium. *Chemosphere*. 18, 1691-1706.

Brusseau, M. L., R. E. Jessup, and P. S. C. Rao. 1991. Nonequilibrium sorption of organic chemicals: elucidation of rate-limiting processes. *Environ. Sci. Technol.* 25:134-142.

Chang, G. P. 1982. *The study on solvent diffusion coefficient in the drying of coated film of polymer solution*. Thesis, National Taiwan University, Taipei, Taiwan.

Chang, M. 1998. *Sorption and desorption kinetics of volatile organic vapor in soil*, Dissertation, National Taiwan University, Taipei, Taiwan.

Chang, M., S. Wu, and C. Chen. 1997. Diffusion of volatile organic compounds in pressed humic acid disks. *Environ. Sci. Technol.* 31:2307-2312.

Chefetz, B., A., Deshmukh, P. G. Hatcher, and E. A. Guthrie. 2000. Pyrene sorption by natural organic matter. *Environ. Sci. Technol*. 34:2925-2930.

Cheng, P. 1999. *The mechanisms of slow sorption of volatile organic compounds on clay minerals.* Thesis, National Taiwan University, Taipei, Taiwan.

Cheshire, M. V. 1979. *Nature and origin of carbohydrates in soils*. Academic Press, New York.

Chiou, C. T. 1998. Soil sorption of organic pollutants and pesticides. p. 4517-4554. *In* R. A. Meyers (ed.) *Encyclopedia of environmental analysis and remediation.* John Wiley & Sons. New York.

Chiou, C. T., and D. E. Kile. 1994. Effects of polar and nonpolar groups on the solubility of organic compounds in soil organic matter. *Environ. Sci. Technol.* 28:1139-1144.

Chiou, C. T., and D. E. Kile. 1998. Deviations from sorption linearity on soils of polar and nonpolar organic compounds at low relative concentrations. *Environ. Sci. Technol*. 32: 338-343.

Chiou, C. T., D. E. Kile, and R. L. Malcolm. 1988. Sorption of vapors of some organic liquids on soil humic acid and its relation to partitioning of organic compounds in soil organic matter. *Environ. Sci. Technol*. 22:298-303.

Chiou, C. T., D. E. Kile, D.W. Rutherford, G. Sheng, and S. A. Boyd. 2000. Sorption of selected organic compounds from water to a peat soil and its humic-acid and humin fractions: potential sources of the sorption nonlinearity. *Environ. Sci. Technol*. 34:1254-1258.

Chiou, C. T., J. Lee, and S. A. Boyd. 1990. The surface area of soil organic matter. *Environ. Sci. Technol.* 24:1164-1166.

Chiou, C. T., P. E. Porter, and D. W. Schmedding. 1983. Partition equilibria of nonionic organic compounds between soil organic matter and water. *Environ Sci Technol* 17:227-231.

Chiou, C. T., S. E. Mcgroddy, and D. E. Kile. 1998. Partition characteristics of polycyclic aromatic hydrocarbons on soils and sediments. *Environ Sci Technol* 32:264-269.

Crank J, Park GS. 1968. Diffusion in Polymers. Academic Press, London, UK.

CRC Handbook of Chemical and Physical, 66th Ed, CRC Press, Boca Raton, FL, 1985-1986.

Culver, T. B., Brown, R. A. and Smith, J. A., 2000, Rate-limited sorption and desorption of 1,2-dichlorobenzene to a nature sand soil column, *Environmental Science & Technology*, 34, 2446-2452.

Culver, T. B., Hallisy, S. P., Sahoo, D., Deitsch, J. J. and Smith, J. A., Modeling the desorption of organic contaminants from long-term contaminated soil using

distributed mass transfer rates, *Environ. Sci. Technol*. 31, 1581-1588, 1997.

Currie L. A. et al., A Critical Evaluatin of Interlaboratory Data on Total, Elemental , and Isotopic Carbon in the Carbonaceous Particle Reference Material, *NIST SRM 1649a, J. Res. Natl. Stand. Technol.* in press.

Davis, G., A. Fataftah, A. Cherkassiy, E. A. Ghabbour, A. Radwan, S. A. Jansen, S. Kolla, M. D. Paciolla, L. T. Sein, Jr., W. Buermann, M. Balasubramanian, J. Budnick, and B. Xing. 1997. Tight metal binding by humic acids and its role in biomineralization. *J. Chem. Soc., Dalton Trans*. 4047-4060.

Deitsch , J. J, Smith, J. A., Culver, T. B., Brown, R. A. and Riddle, S. A., 2000, Distributed-rate model analysis of 1,2-dichlorobenzene batch sorption and desorption rates for five natural sorbents, *Environ. Sci. Technol*. 34, 1469-1476.

Del Nobile, M. A., G. Mensitieri, L. Nicolais, and R. A. Weiss. 1995. Gas transport through ethylene-arcylic acid ionomers. *J. Polym. Sci. B.* 33:1269-1280.

Doner HE, Mortland MM. 1969. Benzene complexex with Cu (II) montmorillonite. Science. 166: 1406-1407.

Farrell, J., and M. Reinhard. 1994. Desorption of halogenated organics from model solids, sediments, and soil under unsaturated conditions. 2. Kinetics. *Environ. Sci. Technol.* 28:63-72.

Farrell, J., D. Grassian, and M. Jones. 1999. Investigation of mechanisms contributing to slow desorption of hydrophobic organic compounds from mineral solids. *Environ. Sci. Technol*. 33, 1237-1243.

Fu, G., A. T. Kan, and M. Tomson. 1994. Adsorption and desorption hysteresis of PAHs in surface sediment. *Environ. Toxicol. Chem.* 13:1559-1567.

Fuson N., C. Garrigou-Lagrange, and M. L. Josien. 1960. Spectre infrarouge et attribtion des vibration des toluenes. *Spectrochim. Acta* 16, 106-127.

Gilliland, E. R. 1934. Diffusion coefficients in gaseous systems. *Ind. Eng. Chem.* 26:681-685.

Goss, K. –U., and S. J. Eisenreich. 1996. Adsorption of VOCs from the gas phase to different minerals and a mineral mixture. *Environ. Sci. Technol.* 30, 2135-2142.

Grabor E. R., and M. D. Borisover. 1998. Evaluation of the glassy/rubbery model for soil organic matter. *Environ Sci Technol* 32:3286-3292.

Grasset , L., and A. Ambles. 1998. Structure of humin and humic acid from an acid soil as revealed by phase transfer catalyzed hydrolysis. *Org. Geochem.* 29:893-897.

Griffioen, J., Suitability of the first-order mass transfer concept for describing cyclic diffusive mass transfer in stagnant zones, *J. Cont. Hydrology*, 34, 155-165, 1998.

Guo, C. J., D. De Kee, and B. Harrison. 1995. Free volume model and diffusion of organic solvents in natural rubber. *J. Appl. Polym. Sci.* 56:823-829.

Gustafsson, O., F. Haghseta, C. Chan, and P. M. Gschwend. 1997. Quantification of the dilute sedimentary soot phase: implications for PAH speciation and

bioavailability. *Environ. Sci. Technol.*, 31, 203-209.

Guthrie, E. A., J. M. Bortiatynski, J. D. Van Heemst, J. E. Richman, K. S. Hardy, E. M. Kovach, and P. G. Hatcher. 1999. Determination of [^{13}C]pyrene sequestration in sediment microcosms using flash pyrolysis-GC-MS and ^{13}C NMR. *Environ. Sci. Technol*. 33:119-125.

Haile, J. M. 1997. In *Molecular Dynamics Simulation: Elementary Methods*, Wiley: New York.

Hatcher, P. G., I. A. Breger, G. E. Maciel, and N. M. Szeverenyi. 1985. Geochemistry of humin. p. 275-302. *In* G. R. Aiken et al. (ed.) *Humic substances in soil, sediment, and water*. John Wiley & Sons, New York,

Hatcher, P. G., M. Schnitzer, L. W. Dennis, and G. E. Maciel. 1983. Soild–state ^{13}C-NMR of sedimentary humic substances: new revelations on their chemical composition. p. 37-81. *In* R. F. Christman and E. T. Gjessing (ed.) *Aquatic and terrestrial humic materials.* Ann Arbor Science Publishers, MI.

Hatcher, P. G., M. Schnitzer, L. W. Dennis, and G. E. Maciel.1981. Aromaticity of humic substances in soils. *Soil Sci. Soc. Am. J*. 45:1089-1094.

Hillel, D. 1980. In *Fundamentals of Soil Physics*; Academic Press: London, Chapter 2.

Hu, W, J. Mao, B. Xing, and K. Schmidt-Rohr. 2000. Poly(methylene) crystallites in humic substances detected by nuclear magnetic resonance. *Environ Sci Technol* 34:530-534.

Huang, W.; Weber, W. J., Jr. 1998. *Environ. Sci. Technol*. 32, 3549-3555.

Hundal, L. S., M. L. Thomspon, D. A. Laird, and M. Carmo. 2001. Sorption of phenanthrene by reference smectites. *Environ. Sci. Technol*. 36, 3456-3461.

Iino, F., K. Tsuchiya, T. Imagawa, and B. K. Gullett. 2001. An isomer prediction model for PCNs, PCDD/Fs, and PCBs from municipal waste incinerators. *Environ. Sci. Technol*. 35, 3175-3181.

Ingamells, C. O. 1970. Lithium metaborate flux in silicate analysis. *Anal. Chim. Acta* 52:323-334.

Johnston, C. T., T. Tipton, S. L. Trabue, C. Erickson, and D. A. Stone, Stone.1992. Vapor-phase sorption of *p*-xylene on Co-exchanged and Cu-exchanged SAZ-1 montmorillonite. *Environ. Sci. Technol*. 26, 382-390.

Karickhoff, S. W., D. S. Brown, and T. A. Scott. 1979. Sorption of hydrophobic pollutants on natural sediments. *Water Res*. 13:241-248.

Keyes BR, Silcox GD. 1994. Fundamental study of the thermal desorption of toluene from montmorillonite clay particles. *Environ. Sci. Technol*. 28:840-849.

Kleineidam, S., H. Rügener, B. Ligouis, and P. Grathwohl. 1999. Organic matter facies and equilibrium sorption of phenanthrene. *Environ. Sci. Technol*. 33, 1637-1644.

Kohl, S. D. and J. A. Rice. 1998. The binding of contaminants to humin: A mass balance. *Chemosphere* 36, 251-261.

Kolla, S., L. T. Sein, Jr., M. D. Paciolla, and S. A. Jansen. 1998. *Recent Res. Adv. Phy. Chem.* 2, 22.

Kubicki JD, Apitz SE. 1999. Model of natural organic matter and interactions with organic contaminants. Organic Geochem 30: 911-927.

Kubicki, J. D., M. J. Itoh, L. M. Schroeter, and S. E. Apitz. 1997. Bonding mechanisms of salicylic acid adsorbed onto illite clay: An ATR-FTIR and molecular orbital study. *Environ. Sci. Technol*. 31, 1151-1156.

Kuhlbusch, T. A. J. Methods for Determining Black Carbon in Residues of Vegetation Fires, *Environ, Sci. Technol.* 1995, 29, 2695-2702.

Kunze, G. W.; Dixon, J. B. In *Methods of Soil Analysis, Part 1, Physical and Mineralogical Properties 2nd Ed.,* Kulte, A. Eds; American Society of Agronomy: Madison, 1986, pp 91-99.

Lau, C. L., and R. G. Snyder. 1971. A valence force field for alkyl benzenes- toluene, p-xylene, m-xylene, mestilyene, and some of their deuterated analogues. Spectrochimica Acta. 27A, 2073-2088.

Li, Y., and G. Gupta. 1994. Adsorption/desorption of toluene on clay minerals. *J. Soil Contam.* 3, 127-135.

Lichtfouse, E., C. Chenu, F. Baudin, C. Leblond, M. D. Silva, F. Behar, S. Derenne, C. Largeau, P. Wehrung, and P. Alberecht. 1998a. A novel pathway of soil organic matter formation by selective preservation of resistant straight-chain biopolymers: chemical and isotope evidence. *Org. Geochem*. 28:411-415.

Lichtfouse, E., P. Wehrung, and P. Albrecht. 1998b. Plant wax *n*-alkanes trapped in soil humin by noncovalent bonds. *Naturwissenschaften* 85:449-452.

Lin, T., J. C. Little, and W. W. Nazaroff. 1994. Transport and sorption of volatile organic compounds and water vapor within dry soil grains. *Environ. Sci. Technol.* 28:322-330.

Little, J. C., Daisey, J. M., and Nazaroff, W. W. 1992. Transport of subsurface contaminants into building: An exposure pathway for volatile organics. *Environ. Sci. Technol.*, 26, 2058-2066.

Long, F. A., and L. J. Thompson. 1954. Water induced acceleration of the diffusion of organic vapors in polymers. *J. Polym. Sci*. 14:321-327.

Lorden, S. W., Chen, W., and Lion, L. W., Experiments and modeling of the transport of trichloroethene vapor in unsaturated aquifer material, *Environ. Sci. Technol*., 32, 2009-2017, 1998.

Luo J and J. Farrell. 2003. Examination of hydrophobic contaminant adsorption in mineral micropores with grand canonical Monte Carlo simulations. Environ Sci Technol 37: 1775-1782.

Luthy, R. G., G. R. Aiken, M. L. Brusseau, S. D. Cunningham, P. M. Gschwend, J. J. Pignatello, M. Reinhard, and S. J. Traina, W. J. Weber, Jr., and J. C. Westall. 1997. Sequestration of hydrophobic organic contaminants by geosorbents. *Environ. Sci. Technol.* 31:3341-3347.

Malcolm, R. L., and P. MacCarthy. 1986. Limitations in the use of commercial humic acids in water and soil research. *Environ Sci Technol* 20:904-911.

Michaels, A. S., and H. J. Bixler. 1961. Flow of gases through polyethylene. *J. Polym. Sci.* 50:413-439.

Middelburg, J. J., Nieuwenhuize, J., van Breugel, P., Black carbon in marine sediments, *Marine Chemistry,* 1999, 65, 245-252.

Miller, C. T., Christakos, G., Imhoff, P. T., McBride, J. F., and Pedit, J. A., Multiphase flow and transport modeling in heterogeneous porous media: challenges and approaches, *Advances in Water Resources*, 21, 2, 77-120, 1998.

Molecular Simulation Inc., San Diego, CA.

Morrissey, F. A., and M. E. Grismer. *J.* 1999. *Contam. Hydrol*. 36, 291-312.

Nanny, M. A., and J. P. Maza. 2001. Noncovalent interactions between monaromatic compounds and dissolved humic acids: a deuterium NMR T_1 relaxation study. *Environ Sci Technol* 35:379-384.

Nelson and Sommers, Total Carbon, Organic Carbon, and Organic Matter, in *Methods of Soil Analysis* Part 2 Chemical and Microbiological Properties, Page A. L. Eds, 1982

Nelson, D.W.; Sommers, L. E. In *Methods of Soil Analysis, Part 2, Chemical and Microbiological Properties 2nd Ed.,* Page, A.L. Eds; American Society of Agronomy: Madison, 1982, pp 539-579

Paviostathis, S. G., and G. N. Mathavan.1992. Desorption Kinetics of Selected Volatile Organic Compounds from Field Contaminated Soils. *Environ. Sci. Technol*. 26, 532-538.

Pavlostathis, S. G.; Jaglal, K. 1991. *Environ. Sci. Technol*. 25, 274-279.

Perminova, I. V., N. Y. Grechishcheva, and V. S. Petrosyan. 1999. Relationships between structure and binding affinity of humic substance for polycyclic aromatic hydrocarbons: relevance of molecular descriptors. *Environ. Sci. Technol*. 33:3781-3787.

Petersen, L. W., P. Moldrup, Y. H. El-Farhan, O. H. Jacobsen, T. Yamaguchi, and D. E. Rolston. 1995. *J. Environ. Qual.* 24,752-759.

Piatt, J. J., and M. L. Brusseau. 1998. Rate-Limited Sorption of hydrophobic organic compounds by soils with well-characterized organic matter. *Environ. Sci. Technol*. 32:1604-1608.

Pignatello, J. J. 1989. In *Reactions and Movement of Organic Chemicals in Soils*; Sowhney, B. L., and K. Brown. Eds.; SSSA Special Publication No. 22; Soil Science Society of America: Madison, WI; Chapter 3.

Pignatello, J. J. 1990. Slowly reversible sorption of aliphatic halocarbons in soils. II. Mechanistic aspects. *Environ. Toxiol. Chem*. 9:1117-1126.

Pignatello, J. J., and Xing, B., Mechanisms of slow sorption of organic chemicals to natural particles, *Environ. Sci. Technol*., 30, 1, 1-11, 1996.

Pinnavaia, T. J., and M. M. Mortland. 1971. Interlamellar metal complexes on layer silicates. I. Copper (II)-Arene complexes on montmorillonite. *J Phys Chem* 75, 3957-3962.

Rabideau, A. J. and Miller, C. T., Two-dimensional modeling of aquifer remediation influenced by sorption nonequilibrium and hydraulic conductivity heterogeneity, *Water Res. Research*, 30(5), 1457-1470, 1994。

Rao, P. S. C., Jessup, R.E., Rolston, D. E., Davidson, J. M., and Kilcrease, D. P., Experimental and mathematical Description of nonadsorbed solute transfer by diffusion in spherical aggregates, *Soil Sci. Soc. Am. J.*, 44, 684-688, 1980.

Rice, J. A., and P. MacCarthy. 1990. A model of humin. *Environ. Sci. Technol.* 24:1875-1877.

Rigol, A., M. Vidal, M., G. Rauret., C. A. Shand, and M. V. Cheshire. 1998. Competition of organic and mineral phases in radiocesium partitioning in organic soils of Scotland and the area near Chernobyl. *Environ. Sci. Technol*. 32:663-669.

Ringwald, S. C. and J. E. Pemberton. 2000. Adsorption interactions of aromatics and heteroaromatics with hydrated and dehydrated silica surfaces by Raman and FTIR spectroscopies. *Environ. Sci. Technol*. 34: 259-256.

Rogers, C. E. 1985. Permeation of gases and vapours in polymers. p. 11-73. *In* J. Comyn (ed.). *Polymer permeability.* Elsevier Applied Science, London.

Rügner, H., S. Kleineidam, and P. Grathwohl. 1999. Long term sorption kinetics of phenanthrene in aquifer materials. *Environ. Sci. Technol*. 33, 1645-1651.

Russell, J. D., D. Vaughan, D. Jones, and A. R. Fraser. 1983. An IR spectroscopic study of soil humin and its relationship to other soil humic substances and fungal pigments. *Geoderma* 29:1-12.

Sawhney, B. L., and M. P. N. Gent. 1990. Hydrophobicity of clay surface: sorption of 1,2-dibromoethane and trichloroethene. *Clay Clay Minerals*, 38, 14-20.

Schlebaum, W, Badora, A., Schraa, G., and Van Riemsdijk, W. H. 1998. *Environ. Sci. Technol*., 32, 2273-2277

Schneider, N. S., J. A. Moseman, and N. Sung. 1994. Toluene diffusion in butyl rubber. *J. Polym. Sci.* B 32:491-499.

Schnitzer, M. 1982. Organic matter characterization. In *Methods of soil analysis. Part 2- Chemical and microbiological properties. 2nd edition.* Page, A. L., Miller, R. H., Keeney, D. R. Eds.; American Society of Agronomy, Inc. and Soil Science Society of America, Inc. Publisher, Madison, WI, USA, pp 581-593.

Schulten, H-R. 1997. Mechanisms and effects of resistant sorption processes of organic compounds in natural particles. *Div. Environ. Chem. Prep. Extend. Abs.* 37, 130-131.

Schwartz, R.C. , Juo, A.S.R. and McInnes , K.J., Estimating parameters for a dual-porosity model to describe non-equilibrium, reactive transport in a fine-textured soil, Journal of Hydrology, 229, P.149–167, 2000.

Schwarzenbach, R. P., P. M. Gschwend, and D. M. Imboden. 1993. *Environmental organic chemistry*. John Wiley & Sons, New York.

Sein, L. T., Jr.; Varnum, J. M.; Jansen, S. A. *Environ. Sci. Technol*. **1999**, 33, 546.

Senesi, N, and E. Loffredo. 1998. The chemistry of soil organic matter. In Sparks DL, eds, *Soil Physical Chemistry*; CRC, New York, NY, USA. pp 239-370.

Shih, Y., and S. Wu. 2002a. Kinetics of Toluene Sorption in Humin under Two Different Levels of Relative Humidity. *J. Environ. Qual*..31: 970-978.

Shih, Y., and S. Wu. 2002b. Sorption Kinetics of Selected Volatile Organic Compounds in Humin. *Environ. Toxicol. Chem*..21: 2067-2074.

Shih, Y., and S. Wu. 2003. Kinetics of Toluene Sorption and Desorption in Ca- and Cu- Montmorillonites Investigated with FTIR Spectroscopy under Two Different Levels of Humidity. *Environ. Toxicol. Chem.* (in review)

Steinberg, S. M., J. J. Pignatello, and B. L. Sawney. 1987. Persistence of 1,2-dibromoethane in soils: entrapment in intraparticle micropores. *Environ. Sci. Technol*. 21:1201-1208.

Stevenson, F. J. 1982. *Humus chemistry: genesis, composition, reactions*. John Wiley & Sons, New York.

Tao, T., and G. E. Maciel. 1998. ^{13}C NMR study of Co-contamination of clays with carbon tetrachloride and benzene. *Environ. Sci. Technol*. 32, 350-357.

Tell, J. G., and C. G. Uchrin. 1991. Relative contribution of soil humic acid and humin to the adsorption of toluene onto an aquifer solid. *Environ Contam Toxicol* 47:547-554.

Teppen, B. J., C.-H. Yu, D. M. Miller, and L. Schäfer. 1998. Molecular dynamics simulations of sorption of organic compounds at the clay mineral/aqueous solution interface. *J. Comput. Chem*. 19, 144-153.

Theodorou, D. N. 1996. Molecular Simulations of Sorption and Diffusion in Amorphous Polymers. In *Diffusion in Polymers;* Neogi, P. Eds.; Marcel Dekker: New York, pp 67.

USDA-NRCS. (United State Department of Agriculture, National Resources Conservation Service.) 1993. Soil sampling and database of alpine forest soils in Taiwan. Lincoln, Nebraska, USA.

Vahdat, N. 1991. Estimation of diffusion coefficient for solute-polymer systems. *Appl. Polym. Sci.* 42:3165-3171.

Vetter, V, and G. Scherer. 1999. Persistency of toxaphene components in mammals that can be explained by molecular modeling. *Environ. Sci. Technol*. 33, 3458-3461.

Weber W. J., P. M. Mc Ginley, and L. E. Katz. 1991. Sorption phenomena in subsurface systems: Concepts, models and effects on contaminant fate and transport. *Water Research*, 25, 499-528.

Weber, W. J., Jr., P. M. Mcginley, and L. E. Katz. 1992. A distributed reactivity model for sorption by soils and sediments 1. Conceptual basis and equilibrium assessments. *Environ. Sci. Technol.* 26, 1955-1962.

Weber, W. J., Jr.; Huang, W. 1996. *Environ. Sci. Technol*. 30, 881-888.

White JC, Hunter M, Nam K, Pignatello JJ, Alexander M. 1999. Correlation between biological and physical availabilities of phenanthrene in soils and soil humin in aging experiments. *Environ Toxicol Chem* 18:1720-1727.

Wilson, J. L., and Lin, J., Dueling time constants : competing processes in aquifer contamination and remediation, 1997 International Conference on Groundwater Quality Protection – Remedial Technology and Management Policy for NAPL Contamination, Taipei, Taiwan, ROC, 269-303, 1997。

Wu, S., and P. M. Gschwend. 1986. Sorption kinetics of hydrophobic organic compounds to natural sediments and soils. *Environ. Sci. Technol*. 20:717-725.

Wu, S.C., and Gschwend, P. M., Numerical modeling of sorption kinetics of organic compounds to soil and sediment particles, *Water Resources Res*.,24, 1373-1383, 1988.

Xing, B., and J. J. Pingnatello. 1997. Dual-mode sorption of low-polarity compounds in glassy poly(vinyl chloride) and soil organic matter. *Environ. Sci. Technol.* 31, 792-799.

Xiong, J., and G. E. Maciel. 1999. Deuterium NMR studies of local motions of benzene adsorbed on Ca-montmorillonite. *J. Phys. Chem. B.* 103, 5543-5549.

Young, T. M. and W. J. Weber, Jr. 1995. A distributed reactivity model for sorption by soils and sediments. 3. Effects of diagenetic processes on sorption energetics. *Environ. Sci. Technol.* 29, 92-97.

Zhang, Z. and Brussear, M. L., Nonideal transport of reactive solutes in heterogenous porous media, 5. Simulating regional-scale behavior of a trichloroethene plume during pump-and-treat remediation, *Water Res. Research*, 35(10), 2921-2935, 1999。

Appendix I

The list of the published and submitted papers from this project is as following:

A. Journal papers:

1. Yang-hsin Shih and Shian-chee Wu, "Sorption Kinetics of Toluene in Humin under Two Different Levels of Relative Humidity", *Journal of Environmental Quality*, 31, 970-978, 2002. (SCI) (2001 Impact factor: 1.155)

2. Yang-hsin Shih and Shian-chee Wu, "Sorption Kinetics of Selected Volatile Organic Compounds in Humin", *Environmental Toxicology and Chemistry*, 21, 2067-2074, 2002. (SCI) (2001 Impact factor: 1.964)

3. Chang, Meei-ling; Wu, Shian-chee; Chen, Pei-jen and Cheng, Shu-chun, Infrared Investigation of the Sequestration of Toluene Vapor on Clay Minerals, Environmental Toxicology and Chemistry, 22, No. 9, 2003, pp. 1956-1962. (SCI) (2002 Impact factor: 2.013)

4. Yang-hsin Shih and Shian-chee Wu, "Kinetics of Toluene Sorption and Desorption in Ca- and Cu- Montmorillonites Investigated with FTIR Spectroscopy under Two Different Levels of Humidity", Submitted to *Environmental Toxicology and Chemistry*, 2003. (SCI) (2001 Impact factor: 1.964)

5. Yang-hsin Shih, Jyh-shing Lin, Shian-chee Wu, and Lien-feng Lee, "Molecular Dynamics Simulations of the Sorption of Toluene in Humic Acid", Submitted to *Environmental Science & Technology*, 2003. (SCI) (2001 Impact factor: 2.707)

6. Yang-hsin Shih and Shian-chee Wu, "The Effect of Soil Chemical Heterogeneity on the Slow Sorption of Toluene in Soils", To be Submitted to *Environmental Science & Technology*, 2003. (SCI) (2001 Impact factor: 2.707)

B. Conference papers:

1. Yang-hsin Shih and Shian-chee Wu, Denitrification in Two Taiwan Soils and Its Impacts on Leachate quality, Proceedings of the 7th IAWQ Asia-Pacific Regional Conference, Volume II, 1641-1644, Taipei, Taiwan, October 18-20, 1999.

2. Shian-chee Wu, Yang-hsin Shih, Meei-ling Chang, and Pei-jen Chen, "Sorption of Toluene on Humin and Montmorilonite under Dry and Humid Conditions Traced by Microbalance and FTIR", Preprints of Extended Abstracts of the 220th ACS National Meeting, Volume 40, 187-190, Washington, D.C., August 20-24,2000.

3. Yang-hsin Shih, Meei-ling Chang, and Shian-chee Wu, “Slow Sorption and Desorption Kinetics of Volatile Organic Contaminants in Soil”, Proceedings of the 7th Mainland-Taiwan Environmental Protection Academic Conference, Vol. (1), Wuhan, China, April 20-26, 2001.

4. Yang-hsin Shih, Shian-chee Wu, and Meei-ling Chang, “FTIR Kinetics Study of Vapor-phase Sorption of Toluene on Cu- and Ca- exchanged Montmorillonites”, Preprints of Extended Abstracts of the 222nd ACS National Meeting, Volume 41, Chicago, IL., U.S.A., August 26-30, 2001.

5. 王美雪、吳先琪、陳維基、許心蘭，土壤不均質性對有機污染物在土壤中傳輸之影響及模擬，中華民國環境工程學會第十六屆廢棄物處理技術研討會，國立高雄第一科技大學，高雄，台灣，2001。

6. Yang-hsin Shih and Shian-chee Wu, “Gravimetric Evidence of a Persistent Fraction of Volatile Organic Contaminant Sorbed in Soil Compartments”, Proceedings of Extended Abstracts of the 20th International Meeting of International Humic Substance Society, Boston, MA, U.S.A., July 21-26, 2002.

7. 王美雪、吳先琪、蕭宏杰，SVE系統之示蹤劑試驗及模擬，第一屆海峽兩岸土壤及地下水污染整治研討會，台灣土壤及地下水環境保護協會，台北，台灣，2002年。

8. Doong, Ruey-an; Sun, Yun-chang; Chang, Meei-ling; Wu, Shian-chee, Distribution of Persistent Organic Pollutants and Heavy Metals in Sediments from Erh-jen River, Taiwan, SETAC/ASE AsiaPacific 2003, Christchurch New Zealand, Sep. 28 – Oct. 1, 2003, p. 143.

9. 卓坤慶、吳先琪、王美雪、羅致良、王凱中、陳慎德，應用慢釋氧物質處理受石油碳氫化合物污染之地下水－現地模場試驗，中華民國環境工程學會第一屆土壤與地下水技術研討會，國立中興大學，台中，台灣，2003。

10. Yang-hsin Shih and Shian-chee Wu, “Sorption Kinetics of Trichloroethylene in Humic Acid and Montmorillonite”, Accepted in the 4th International Conference of Remediation of Chlorinated and Recalcitrant Compounds, Monterey, CA, U.S.A., May 24-27, 2004.

C. Master and Ph. D. thesis:

1. Yu-ling Liang, The long-time adsorption mechanisms of toluene on clay minerals, Master Thesis, National Taiwan University, 2002.

2. Yang-hsin Shih, The effect of soil heterogeneity on the sorption and desorption of organic contaminants in soil, Ph.D. Dissertation, National Taiwan University, 2002。

3. Yu-wen Huang, Chemical Transformation and Sorption/Desorption Kinetics of Chlorinated Volatile Organic Compounds on Clay Minerals, Master Thesis, National Taiwan University, 2003.

Appendix II

The reports and presented conference papers for three conferences are in the following pages.

國科會補助專家學者出席國際學術會議報告

89 年 9 月 13 日

報告人姓名	吳先琪	服務機構 ※ 及職稱	國立台灣大學環境工程學研究所 教授
會議期間 地點	89 年 8 月 20 日至 89 年 8 月 25 日 美國華盛頓特區	本會核定 補助文號	
會議 名稱	(中文)第二百二十屆美國化學學會國際會議 (英文)American Chemical Society 220th National Meeting		
發表 論文 題目	(中文)以微量天秤與紅外光光譜法觀測乾濕狀態下甲苯在腐植素與蒙特石之吸附 (英文)Sorption of toluene on humin and montmorillonite under dry and humid conditions traced by microbalance and FT-IR		

報告內容應包括下列各項：

一、參加會議經過
二、與會心得
三、考察參觀活動(無是項活動者省略)
四、建議
五、攜回資料名稱及內容
六、其他

※服務機關若係大專院校，請註明科系名稱。

※報告內容請另以稿紙書寫工整，俾本部輯印成冊送各相關單位參考應用。

行政院所屬各機關人員出國報告書提要

撰寫時間：89 年 9 月 13 日

姓名	吳先琪	※服務機關名稱	國立台灣大學環境工程學研究所	聯絡電話	(0)23629435 (H)27373624
出生年月日	41 年 2 月 9 日		職稱	教授	
出席國際會議名稱	(中文)第二百二十屆美國化學學會國際會議 (英文)American Chemical Society 220th National Meeting				
到達國家及地點	美國華盛頓特區	出國期間	89 年 8 月 20 日至 89 年 8 月 25 日		
內容提要	筆者於八十九年八月十九日受邀出發參加於 2000 年 8 月 20 日至 25 日在美國華盛頓特區舉行之第二百二十屆美國化學學會國際會議（American Chemical Society 220th National Meeting）。今年獲得國科會的補助能參與此國際會議並於大會中受邀發表論文。由於此國際學術會議規模相當地大，並在會場的展覽館中有來自各國的廠商參展最目前有關研究化學領域的設備、分析以及監測儀器。 這次所發表的論文題目為" 以微量天秤與紅外光光譜法觀測乾濕狀態下甲苯在腐植素與蒙特石之吸附 "，由於這是第一次實際利用直接由土壤萃取出「腐植素」並打成片狀來測量擴散係數，再加上率先運用自行設計之 ZnSe 小視窗的紅外線光譜法觀測吸附現象，因此論文發表的過程中引起很大的回響與討論。這次會議的最大的一項收穫就是與參展的研究人員間的互動，另外有一些廠商的儀器設備、書商的最新出版物以及電腦模擬軟體等都可以當作日後在實驗室研究的參考。 所發表之論文如後頁所附。				
出席機關人審所核屬意見					
層審轉核機意關見					
研處考理會意見					
旅行社之服務情形	旅行社名稱	萬商旅行社	□優良 ■良好 □尚可 □差		

※服務機關若係大專院校，請註明科系名稱。

行政院國科員會補助國內專家學者出席國際學術會議報告

90 年 9 月 20 日

附件三

報告人姓名	施養信	服務機構及職稱	台灣大學環工所 博士候選人
會議時間地點	90 年 8 月 26 日 至 90 年 8 月 30 日 美國芝加哥	本會核定補助文號	NSC 90-2211-E-002-054-
會議名稱	(中文) 第二百二十二屆美國化學學會國際會議 (英文) The 222nd American Chemical Society's National Meeting		
發表論文題目	(中文) 傅氏紅外線光譜法研究氣態甲苯與銅和鈣置換蒙特石之吸附動力學 (英文) FTIR Kinetics Study of Vapor-Phase Sorption of Toluene on Cu- and Ca-Exchanged Montmorillonites		

報告內容應包括下列各項：

七、參加會議經過

八、與會心得

九、考察參觀活動(無是項活動者省略)

十、建議

十一、 攜回資料名稱及內容

十二、 其他

請詳見隨後附件。

行政院所屬各機關人員出國報告書提要

撰寫時間： 90 年 9 月 20 日

<table>
<tr><td>姓　　名</td><td>施養信</td><td>服務機關名稱
(請註明科系名稱)</td><td>國立台灣大學環境工程學研究所</td><td>連絡電話、</td><td>(0)23629435</td></tr>
<tr><td>出　生　日　期</td><td colspan="2">61 年 3 月 5 日</td><td>職　　稱</td><td colspan="2">博士班研究生</td></tr>
<tr><td>出席國際會議名稱</td><td colspan="5">第二百二十二屆美國化學學會國際會議</td></tr>
<tr><td>到達國家及地點</td><td colspan="2">美國芝加哥</td><td>出國期間</td><td colspan="2">自 90 年 8 月 25 日
迄 90 年 8 月 30 日</td></tr>
<tr><td>內　容　提　要</td><td colspan="5">筆者於九十年八月二十五日出發參加於 2001 年 8 月 25 日至 30 日在美國芝加哥舉行之第二百二十二屆美國化學學會國際會議（American Chemical Society 222nd National Meeting)。由於此國際學術會議規模相當地大，大會除了有多篇論文發表外，並在會場的展覽館中有來自各國的廠商參展最目前有關研究化學領域與環境化學的設備、分析以及監測儀器。
這次所發表的論文題目為” 傅氏紅外線光譜法研究氣態甲苯與銅和鈣置換蒙特石之吸附動力學”，由於這是第一次實際利用自行設計之 ZnSe 小視窗的紅外線光譜法觀測黏土礦物吸附有機物之動力現象，因此論文發表的過程中引起很大的回響與討論。這次會議的最大的一項收穫就是與參展的研究人員間的互動，各研究群所發表的是最新發展的成果，另外有一些廠商的儀器設備、書商的最新出版物以及電腦模擬軟體等都可以當作日後在實驗室研究的參考。</td></tr>
<tr><td>出席人所屬機關審核意見</td><td colspan="5"></td></tr>
<tr><td>層轉機關審核意見</td><td colspan="5"></td></tr>
<tr><td>研考會處理意見</td><td colspan="5"></td></tr>
<tr><td>旅行社之服務情形</td><td>旅行社名稱</td><td colspan="2">萬商旅行社</td><td colspan="2">□優良 ■良好 □尚可 □差</td></tr>
</table>

※服務機關若係大專院校，請註明科系名稱。

國科會補助專家出席國際會議報告

報告人姓名：施養信　服務機關：台灣大學環境工程學研究所

一、　參加會議經過

台灣大學環境工程學研究所博士班研究生施養信於九十年八月二十五日出發參加於 2001 年 8 月 25 日至 30 日在美國伊利諾州芝加哥舉行之第二百二十二屆美國化學學會國際會議（American Chemical Society 222nd National Meeting）。今年因教育部經費用罄，故未能獲得教育部的補助，在此同時大部分基金會之申請時間已截止，所以未獲其他基金會補助。但幸運地貴會有通過並給於我們計畫中所編列之博士生出席國際會議經費，故能參與此國際會議並於大會中口頭宣讀發表論文，並獲 222nd ACS National Meeting's Merit Award。

由於此國際學術會議規模相當地大，環境化學組這個領域就有四個子題會議同時召開，另外有機化學、無機化學、分析化學、物理化學等組別，各組會議是同時進行的，能在此會場中趕場聆聽各國一流的專家學者的演講，真是一大享受，可以參加此次會議真是獲益良多。並在會場的展覽館中有來自各國的廠商參展最目前有關環境污染防治的設備、分析以及監測儀器。在整個與會其間，除了與筆者專長之有機污染物傳輸與儀器分析研究領域的各國研究學者討論並交換研究心得外，並於會外對目前一些污染整治之新技術進行討論。此外在研討會期間，筆者全程參與，盡可能地與與會人員討論，俾發揮影響力，且了解最新的研究趨勢。

二、　與會心得

筆者這次所發表的論文題目為" 傅氏紅外線光譜法研究氣態甲苯與銅和鈣置換蒙特石之吸附動力學", 由於這是第一次實際利用自行設計之 ZnSe 小視窗的紅外線光譜法觀測吸附現象，此法避免傳統用 KBr 打片因 KBr 所可能造成之干擾，因此論文發表的過程中引起很大的回響與討論。大家的焦點都放在銅蒙特石吸附甲苯之變化特性、乾濕狀態下之不同特徵峰、及 ZnSe 小視窗的紅外線光譜法的自行設計問題上。當然與會的學者專家也提出一些寶貴的意見，值得作為日後研究的參考。

參與這次會議最大的收穫除了在學術交流外，當然不免有些遺憾，畢竟在短短幾天內大會進行相當多篇的論文發表，還是有些議題沒能參與到。不過還是能夠參考大會所發的論文摘要以及所購買的論文光碟片。這

次會議的令一項收穫就是與參展的廠商間的互動，畢竟各廠商所參展的設備都是最新發展的，有一些設備的設計以及分析監測的原理都可以當作日後在實驗室研究的參考。因此我收集了不少各廠商的儀器資料，雖然增加了行李的重量，但卻覺得相當值得，收穫剖豐。

三、 建議

由於這是一年一度的大型國際會議，參與會議人士眾多，從各國來的專家學者、研究生、工程師、業者以及政府的環保部門等。看到眾多人士對環保的重視、為改善環境而努力，筆者心生感動。國內目前的環境保護工作雖然一直在推行，但很多政策成效並不佳。因此建議除了專家學者多多的參與此種國際會議外，政府民間單位亦多鼓勵參與。希望政府、學界及民間單位多繼續參與國際交流，這對國內環保工作一定有正面的效果。

四、 攜回資料

1. 環境化學組長篇論文摘要光碟一份。
2. 儀器展等資料。

五、 其他

所發表之論文如後頁所附。

行政院國科員會補助國內專家學者出席國際學術會議報告

92 年 10 月 2 日

附件三

報告人姓名	吳先琪	服務機構及職稱	台灣大學環工所 教授
會議 時間 會議 地點	92 年 9 月 28 日 至 92 年 10 月 1 日 紐西蘭 基督城	本會核定補助文號	NSC 91-2211-E-002-062
會議名稱	(中文) 第一屆環境毒物與化學亞洲國際會議 (英文) SETAC/ASE Asia Pacific 2003		
發表論文題目	(中文) 二仁溪表面底泥持久性有機物與重金屬之分佈特性研究 (英文) Distribution of persistent organic pollutants and heavy metals in sediments from Erh-jen River, Taiwan		

報告內容應包括下列各項：

十三、 參加會議經過

十四、 與會心得

十五、 考察參觀活動(無是項活動者省略)

十六、 建議

十七、 攜回資料名稱及內容

十八、 其他

請詳見隨後附件。

行政院所屬各機關人員出國報告書提要

撰寫時間： 92 年 10 月 2 日

姓　　名	吳先琪	服務機關名稱	國立台灣大學環境工程學研究所	連絡電話、	(0)23629435
出生日期	41 年 2 月 9 日		職　　稱	教授	
出席國際會議名稱	第一屆環境毒物與化學亞洲國際會議 SETAC/ASE Asia Pacific 2003				
到達國家及地點	紐西蘭 基督城		出國期間	自 92 年 9 月 28 日 迄 92 年 10 月 1 日	
內容提要	本第一屆環境毒物與化學亞洲國際會議，於二 OO 三年九月二十八日至十月一日在紐西蘭基督城 (Christchurch, New Zealand)的國際會議中心舉行。此會議由環境毒物與化學學會(Society of Environmental Toxicology and Chemistry, SETAC)亞洲分會主辦，吸引全球三十個國家、超過三百五十位專家學者與會，交換研究心得，促進合作與友誼，以提供作為處理及控制毒性物質發展的基石。台灣地區則有清華大學與及台灣大學的代表與會。 大會將此次會議的主軸訂為「Solutions to pollution」，希冀藉由此次會議提供能解決環境問題的可行方案。正式的會議則在二十九日正式展開，除邀請三位 plenary 及五位 keynote 演講者外，也收錄一百九十五篇口頭宣讀論文及一百三十九篇壁報論文。而因應大會主軸與近年來毒性化學物質的研究趨勢，特將主題分為內分泌干擾物質(endocrine disrupting chemicals, EDCs)、持久性有機物(persistent organic pollutants, POPs)、風險評估、生物標誌與評估、復育技術、及生態毒性監測與評估等主要研究範疇。 此次會議筆者口頭宣讀的論文被安排在第三天的「持久性有機物」專題中發表，題目為「二仁溪表面底泥持久性有機物與重金屬之分佈特性研究」(distribution of persistent organic pollutants and heavy metals in sediments from Erh-jen River, Taiwan)。 主辦單位對於本次的會議相當用心，除將開會地點安排於紐西蘭的第二大城市外，並於會議期間提供具茶點及午宴。使與會者能有足夠的時間研讀壁報論文並與作者討論。會後在閉幕典禮上，大會也頒發了許多學生獎項，如最佳口頭宣讀論文獎、及最佳壁報論文獎等，不僅提昇了研究生參與會議的意願，也藉此鼓勵研究生進行高品質的研究。				
出席人所屬機關審核意見					

層轉機關 審核意見			
研考會 處理意見			
旅行社之 服務情形	旅行社 名稱		□優良 ■良好 □尚可 □差

※服務機關若係大專院校，請註明科系名稱。

國科會補助專家出席國際會議報告

報告人姓名：吳先琪　服務機關：台灣大學環境工程學研究所

一、　　參加會議經過

本次會議於 2003 年九月二十八日至十月一日在紐西蘭基督城(Christchurch, New Zealand)的國際會議中心舉行。此會議由環境毒物與化學學會(Society of Environmental Toxicology and Chemistry, SETAC)亞洲分會主辦。SETAC 是國際環境毒物化學及生態風險評估相當重要的一個組織，所主辦的專業會議主要著重於毒性與危害性物質的處理與控制技術，今年則是第一次在亞洲地區舉行相關會議，吸引全球三十個國家、超過三百五十位專家學者與會，台灣地區則有清華大學、弘光科技大學與及台灣大學的代表與會。

大會將此次會議的主軸訂為「Solutions to pollution」，希冀藉由此次會議提供能解決環境問題的可行方案。。正式的會議則在二十九日正式展開，除邀請三位 plenary 及五位 keynote 演講者外，也收錄一百九十五篇口頭宣讀論文及一百三十九篇壁報論文。而因為網路時代的來臨，本次大會也創新收錄三十五篇網路論文(virtual paper)，論文作者將欲宣讀的投影片內容公告於網路上，與會者則藉由網路的連線瞭解論文的內容並與作者進行討論，相當引人注意。

大會主軸與近年來毒性化學物質的研究趨勢，特將主題分為內分泌干擾物質(endocrine disrupting chemicals, EDCs)、持久性有機物(persistent organic pollutants, POPs)、風險評估、生物標誌與評估、復育技術、及生態毒性監測與評估等主要研究範疇。

此次會議董瑞安教授與筆者口頭宣讀的論文被安排在第三天的「持久性有機物」專題中發表，題目為「二仁溪表面底泥持久性有機物與重金屬之分佈特性研究」(distribution of persistent organic pollutants and heavy metals in sediments from Erh-jen River, Taiwan)。筆者針對二仁溪底泥中持久性有機物中的有機氯農藥(organochlorine pesticide, OCPs)及多氯聯苯(polychlorinated biphenyls, PCBs)的含量與分佈特性進行研究，並配合重金屬濃度分佈特性來瞭解污染潛能與可能的污染源。

二、 與會心得

本次會議之討論議題，除了地區性的海洋、極地及熱帶等毒性物質分布之外，特別著重於持久性有機物(persistent organic pollutants, POPs)、內分泌干擾物質(endocrine disruptors)及生態毒物學(ecotoxicology)。顯示這幾個議題已經成為眾人所關心的環境問題。

國內對 POPs 的管制雖已開始，但是對於實質的環境流佈及危害情形所投入之研究不多。這次研討會有許多篇亞洲地區有關 POPs 流佈的報告，所研究之區域遍不亞洲地區，對象則包括土壤、底泥、人體(人乳等)及野生動物。國內缺乏完整的資料，無法與他國做比較，在政府評估管制效果上，恐也較困難。

至於內分泌干擾物質的研究則方興未艾。許多以往認為無害的化學物質在這次研討會中，均討論到其對環境生物生殖能力潛在的影響。在 Keynote speaker 的演說中也闡述化學結構對環境荷爾蒙毒性之影響及這些物質對環境生物的衝擊。我國尚未對環境荷爾蒙單獨立法管制，對於新化學物質是否有內分泌干擾特性也未進行評估，實是有些危險。

生態毒理學很早就是評估物質毒性的基礎，後來被實驗毒理學取代，因其不確定性較高。但是由於多年來國外許多研究累積了不少環境生物毒性影響的數據，使生態毒理學的準確性提高、且更切合實際。這次研討會有許多篇報告，討論毒性物質的環境暴露途徑及劑量與影響的關係。這方面的研究對於建立管制標準、保護生態系統的安全是非常需要的。國內對於都毒性物質在生態系統中之暴露途徑，及其對環境生物之危害性的研究相當缺乏，在亞洲各國中是屬落後的。

三、 建議

除了傳統的環境污染物移除與復育方面的研究，對於危害生態系健康的毒性物質，如 POPs，環境荷爾蒙等，應該投注更多的心力去建立他們在環境中流佈及對生態系統影響的理論及預測模式，如此才能適度的對這些物質加以管制，防止其對生物造成危害。

許多以往認為無害的物質，近年來新的實驗發現具有某種危害性。這方面的資料在國內未有有系統的收集與整理，以便及早在立法、分析調查技術、環境流佈現狀及各種可能管制措施對產業與生活之影響方面掌握先機。待發現其危害或國外已加以管制時再匆匆立法管制，常常會因為缺乏足夠的背景資料佐證，訂定標準時就造成大家討價還價的情形，往往定出不合實際的法規。這方面之基礎研究實在應該加強，以因應這些新毒性物質之衝擊。

四、 攜回資料

SETAC/ASE Asia Pacific 2003 論文集一本。

五、其他